19. SITE 229

The Shipboard Scientific Party[1]
With Additional Report From G. Müller, Universität Heidelberg, Germany

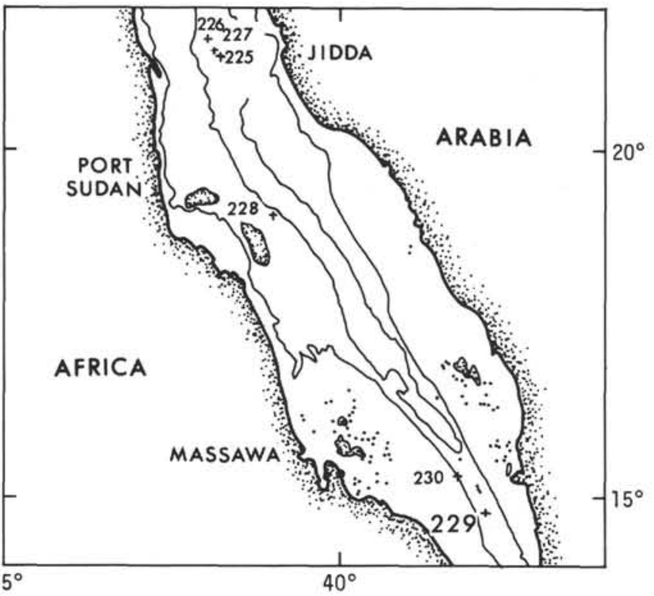

Figure 1. *Position of Site 229 and other Leg 23 sites in the Red Sea. Contours at 200 and 1000 meters, from Laughton (1970).*

SITE DATA

Dates: 0000 27 Apr-1030 28 Apr 72

Time: 35 hours

Position (Figure 1): 14°46.09′N, 42°11.47′E

Holes Drilled: 2

Water Depth by Echo-Sounder: 852 corr. meters

Total Penetration: 212 meters

Total Core Recovered: 148.1 meters from 23 cores

Age of Oldest Sediment: Late Pleistocene

Basement: Not reached

ABSTRACT

A rapidly deposited uniform sequence of clay-rich carbonate nanno ooze has been deposited in the last 350,000 years. The sediment is largely of biogenic origin and probably represents material swept from the shelves of the southern Red Sea into the basin south of Zebayir Island by seasonal currents. There has been intermittent volcanism. Large quantities of gas (including hydrocarbons) in the sediments led to the eventual abandonment of the site. The available evidence is not inconsistent with this site lying over the axial trough of the Red Sea (see Site Summary).

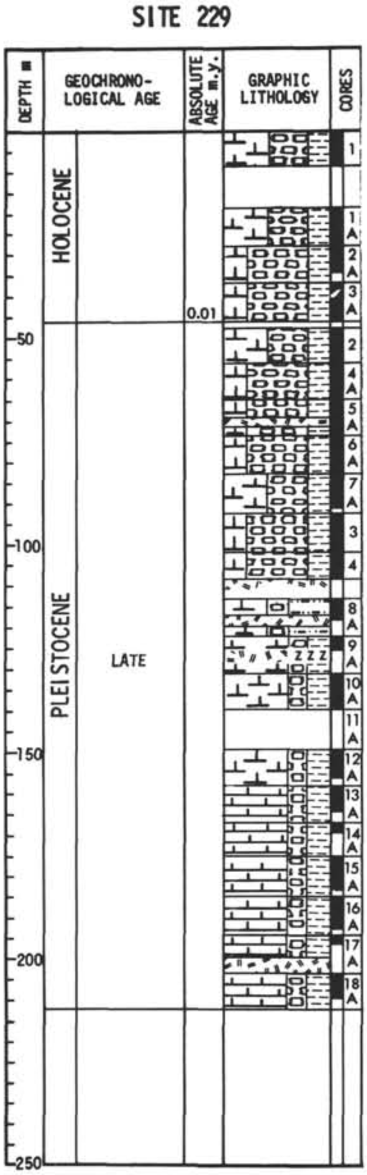

---

[1] Robert B. Whitmarsh, National Institute of Oceanography, Wormley, Godalming, Surrey, United Kingdom; David A. Ross, Woods Hole Oceanographic Institution, Woods Hole, Massachusetts; Syed Ali, State University of New York, Stony Brook, New York; Joseph E. Boudreaux, Texaco, Inc., New Orleans, Louisiana; Robert Coleman, U. S. Geological Survey, Menlo Park, California; Robert L. Fleisher, University of Southern California, Los Angeles, California; Ronald W. Girdler, The University, Newcastle-upon-Tyne, United Kingdom; Frank T. Manheim, U. S. Geological Survey, Woods Hole, Massachusetts; Albert Matter, Geologisches Institut, Universität, Bern, Switzerland; Catherine Nigrini, Lexington, Massachusetts; Peter Stoffers, Laboratorium für Sedimentforschung, Universität Heidelberg, Heidelberg, Germany; Peter R. Supko, Scripps Institution of Oceanography, La Jolla, California

BACKGROUND AND OBJECTIVES

Three rifts marking the boundaries between the Arabian, Nubian and Somalian plates can be found in the region centered on Afar (Figure 2). These rifts are the East African Rift Valley and the axial trough of the Sheba Ridge (Gulf of Aden) and of the Red Sea. All the rifts are marked by seismicity, and sea-floor spreading magnetic anomalies can be found over the two submarine rifts. A fourth rift exists in northern Afar which extends south-southeast from the Gulf of Zula, part of which is below sea-level (Tazieff et al., 1972; Lowell and Genik, 1972). In the Afar region, however, nowhere can one of the four rifts be seen to clearly connect with any other. This is the crux of the problem of Afar. If the strict geometry of plate tectonics can be applied to a problem of this complexity and scale, then the connections of the rifts should be explicable by a network of rifts, transform faults, and possibly trenches.

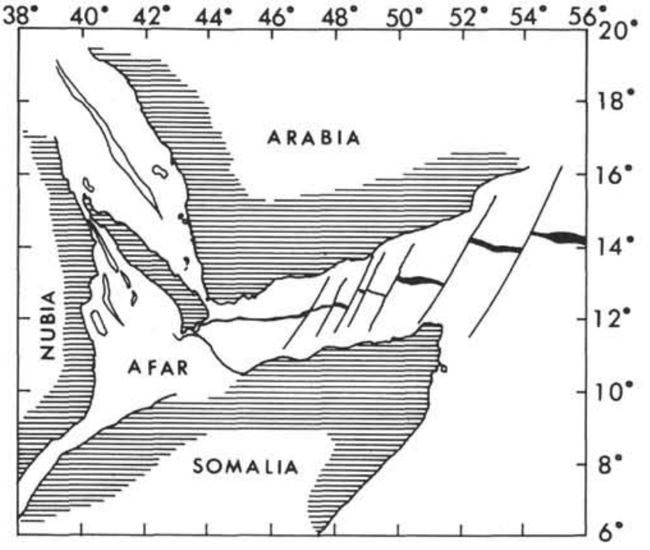

Figure 2. *Location of the Afar region relative to the southern Red Sea, Gulf of Aden, and East African Rift. Oceanic-type rifts are shown in black. (Modified after Tazieff et al., 1972.)*

The edge of the axial trough of the southern Red Sea can be defined by the 500-fathom (914 m) contour (Laughton, 1970). This trough has parallel linear magnetic anomalies (Allan, 1970) which can be explained by continuous sea-floor spreading over about the last 3.5 m.y. (Vine, 1966). South of 15°N, however, the sea is less than 500 fathoms (914 m) deep, and no continuous rift is evident although linear magnetic anomalies parallel to the Red Sea trend can be observed at least as far south as 14°N (Girdler, 1970). Site 229 was proposed to be in an enclosed basin about 850 meters deep[2] between 15° and 14°N just south of Zebayir Island (Figure 3). Although the sea is shallower here, there appears to be at least 500 meters of sediment on seismic reflection profiles (unpublished data of *Chain*-100, *Conrad*-9) so that the acoustic basement lies at least 1350 meters below sea level. This depth is comparable with the depth of the mainly sediment-free axial valley in the rest of the southern Red Sea and suggests that structurally the axial valley continues south of Zebayir Island. The petrological studies of Gass et al. (1973) fit this view, since they found tholeiitic basalts on Jebel at Tair, only slightly alkaline tholeiites on Zebayir Island, and alkaline basalts on the Hanish/Zukur islands. They also found fissures trending 342° on Jebel at Tair and Zebayir Island, but the dominant structural trend in the Hanish/Zukur islands group is 045° (Gass et al., 1965). This latter trend is very close to the 047° trend expected by Girdler and Darracott (1972) for a transform fault about a pole at 31.5°N, 23°E which describes the separation of Arabia from Nubia. Thus the Hanish/Zukur islands differ in petrology and structural trends from the islands to the north and may mark the termination of the axial trough in the Red Sea proper by a transform fault. The gravity data of Allan (1970) are also consistent with the view that the axial trough extends south of 15°N in that a positive Bouguer anomaly, characteristics of the axial trough elsewhere in the Red Sea, is still present between 14° and 15°N (N.B. captions of Allan's figs. 14 and 15 are interchanged). Thus the main objective of Site 229 was to confirm that it lay over oceanic crust formed in the last 3.5 m.y. The site

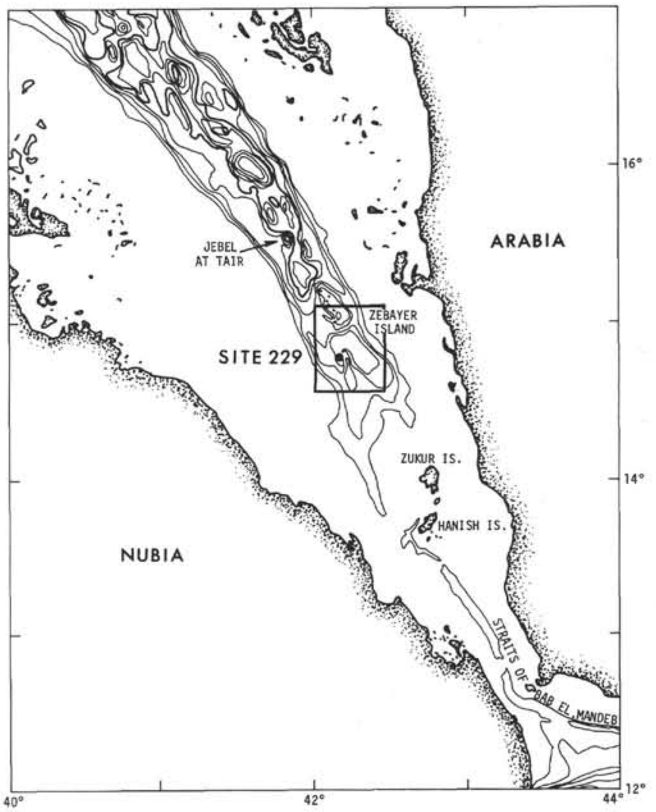

Figure 3. *Bathymetry of the Red Sea around Site 229 (from Laughton, 1970). Contours at 100-fathom intervals; 500 and 1000 fathom contours are bolder.*

---

[2] Although it would have been of considerable interest to drill in even shallower water to the south, this was not possible for technical reasons; 850 meters was at the extreme of *Glomar Challenger's* capabilities in shallow water.

was also unusual in presenting thick sediments within the axial trough (?) and therefore promised a detailed section covering the Quaternary history of the southern Red Sea.

The objectives of drilling at Site 229 were therefore

1) To sample, and to date, igneous basement in order to discover, if it were basalt, if it had been formed during the current phase of spreading.

2) To determine the Quaternary history of the southern Red Sea.

The JOIDES Advisory Panel on Pollution Prevention and Safety made a number of general recommendations for all the Red Sea sites together, among which were the constraints to core continuously and to monitor downhole temperatures.

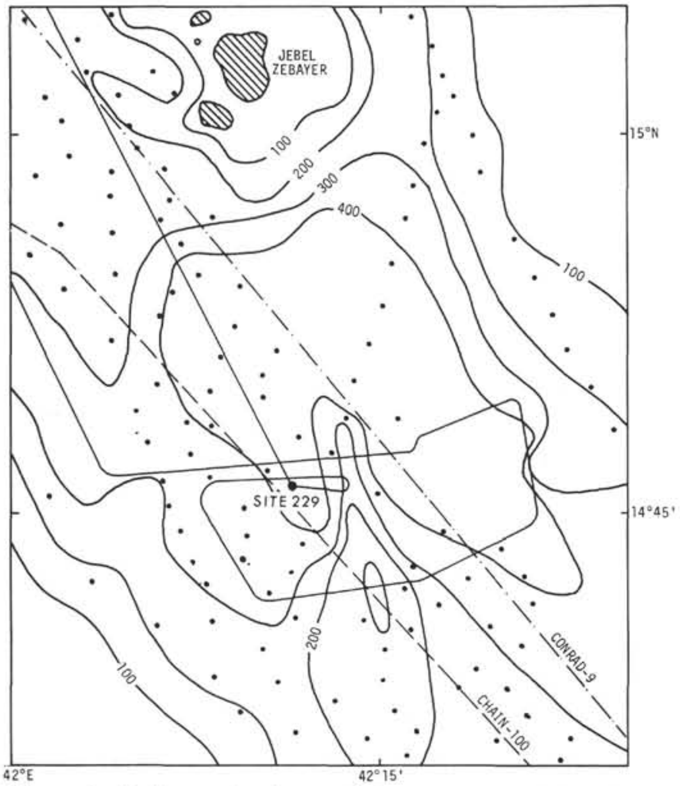

Figure 4. *Bathymetric chart of the area around Site 229 with the approach and departure tracks of* Glomar Challenger, *and the tracks of* Conrad *and* Chain. *Contour interval 100 fathoms, depths in corrected fathoms, dots represent soundings by other vessels (after Laughton, unpublished).* Conrad-9 *soundings provided by Dennis E. Hayes, Lamont-Doherty Geological Observatory.*

OPERATIONS

The general area of Site 229 was approached from the north-northwest on 26 Apr 72 (see Figure 4 for track). The proposed site lay south of Zebayir Island in a shallow basin with the shape of an inverted letter U open to the south-southeast. According to the Admiralty collected soundings (Hydrographic Department, 1972), the only bathymetric data available onboard, the deeper parts of the basin were in the north, but this area lay within the 12-mile territorial limit of Yemeni-owned Centre Island. Outside the 12-mile limit no sounding indicated a depth greater than 850 meters, which was the minimum depth agreed upon with Global Marine Inc. for the site. However, there were areas without soundings in this region, and there was a good chance that a presite survey would discover deep enough water.

Thus, a 5-hour survey was begun at 2045 hours covering both limbs of the U-shaped basin outside territorial limits. Only one suitable site was found, over the western limb, and *Glomar Challenger* returned to this point after the survey. A 16-kHz beacon was dropped underway at 5 knots and the ship returned over the beacon after the towed gear had been recovered.

Drilling at Site 229 was difficult due to poor weather (winds up to 50 mph) and the shallow water depth. Due to these winds and the shallow water depth, drilling had to be halted frequently because the ship moved off the hole. At the first hole (229) the bumper subs sanded up following a heat flow attempt. After the fourth core the hole was abandoned, the pipe pulled, and the bumper subs were cleaned. A second hole (229A) succeeded in penetrating deeper but had to be abandoned because of increasing contents of methane and ethane gas in the cores.

At Hole 229 we took a surface punch core, drilled 38 meters, took another core, drilled 37 meters, took two cores, and tried a heat flow measurement (Table 1). Total penetration was 108 meters before the site was abandoned at 1830 hours on 27 Apr 72. We cored 33 meters and recovered 29.1 meters. The relatively high amount of drilling without coring was done to bury the bottom hole assembly. Gas was detected in the first three cores.

Hole 229A was drilled to a depth of 212 meters. We cored 162 meters, recovering 119 meters of core and drilled 50 meters. Gas was detected in essentially all the cores. Initially, only H_2S was present, but starting with Core 3 (37-46 m) methane was detected. The CH_4/C_2H_6 ratio from gas chromatography was 6000 from Core 6 and generally decreased, reaching a minimum of 830 in Core 17. The decrease in the CH_4/C_2H_6 ratio was mainly due to an increase in ethane. Gas pressure was sufficient to disturb most of the cores. A possible indication of propane was detected in a sample from Core 18 ($CH_4/C_2H_6 = 950$). The above aspects led us to abandon the hole at about 1000 hours on 28 Apr 72.

Glomar Challenger left Site 229 at 1330, 28 Apr 72. A course was immediately set for Site 230. Because the vessel would pass within the territorial waters of Yemen, no gear was streamed and consequently a seismic profile was not obtained over the beacon on departure.

LITHOLOGY

Site 229 was almost continuously cored to a depth of 212 meters. The sediments, ranging in age from Holocene to Late Pleistocene, comprise a single lithologic unit with remarkably little variation.

Description

The sediment type is basically a calcareous ooze, with detrital silt and clay present in relatively minor quantity. The calcareous components are recognizable nannofossils on one hand and silt- and clay-sized carbonate particles on the other. Depending upon relative amounts of these two

TABLE 1
Coring Summary, Site 229

Core	Date/Time Core on Deck (Time Zone -3)	Subbottom Depth (m)	Cored (m)	Recovered (m)
Hole 229				
	27 Apr:			
1	0715	0-9	9.0	1.0
2	0840	47-56	9.0	9.3
3	1015	93-102	9.0	9.4
4	1120	102-108	6.0	9.4
HF[a]	1145	108	0.0	0.0
5	1830	108-108	0.0	CC
		Totals	33.0	29.1
Hole 229A				
	27 Apr:			
1	1925	19-28	9.0	9.0
2	1955	28-37	9.0	6.4
3	2025	37-46	9.0	9.4
4	2110	56-65	9.0	9.4
5	2150	65-74	9.0	9.4
6	2225	74-83	9.0	9.2
7	2300	83-92	9.0	8.0
	28 Apr:			
8	0015	113-122	9.0	4.5
9	0110	122-131	9.0	2.5
10	0145	131-140	9.0	9.4
11	0305	140-149	9.0	0.0
12	0355	149-158	9.0	7.0
13	0515	158-167	9.0	6.3
14	0605	167-176	9.0	3.0
15	0650	176-185	9.0	8.0
16	0730	185-194	9.0	8.0
17	0815	194-203	9.0	2.2
18	0915	203-212	9.0	7.3
		Totals	162.0	119.0

[a]Von Herzen heat flow probe.

components, the sediment is either a clay-rich micarb-rich nanno ooze or a clay-rich nanno-rich micarb ooze (or chalk) according to DSDP nomenclature.

Compositional ranges for the major components are: nannos ~25%-60%, micarb particles 25%-60%, detrital material 10% to an occasional 25% (clay and silt, with clay greatly dominant), and forams Tr-10% (locally higher). The calcium carbonate content of a sample from each core varies between 36% and 84%, and, except for a lower value in 229-1-1, the organic content lies between 0.5% and 1.6%. Pteropods are scattered throughout as well as being locally concentrated in coarser layers and are present to 5%. Otoliths are present up to 2%. A large high-spired gastropod (2 cm) and a large pelecypod (4 cm) were found. Micropelecypods were common in many of the samples. Volcanic glass makes up about 2% of the sediment. The sediment is semilithified chalk below about 150 meters.

Dominant colors for the oozes and chalks are greenish-gray, dusky yellow-green, and olive hues. There is no striking correlation between color and clay content; rather, the olive colors seem to be related to finely dispersed iron.

Occasional layers of greenish-black (hand specimen) palagonite tuff occur, varying in thickness from 5 to some 60-70 cm (see below for a detailed description). With the exception of one layer, they are cemented to a vary hard rock by carbonate and zeolite. A single 90-cm glass bed in Core 9 has been altered to 60% zeolite.

Nearly all cores were gassy, with CO_2, H_2S, methane, and ethane detected. The ratio of ethane/methane increased significantly toward the bottom of the hole. The less consolidated cores showed fragmentation and bubble formation due to gas expansion.

Due to limited space, the tables of grain size, carbon-carbonate, and X-ray mineralogy data are presented with data from other sites in Appendices I, II, and III, respectively, at the end of the volume.

Tuffites[3]

Introduction

The Pleistocene greenish calcareous ooze found at Site 229, which is situated about 15 miles south of the volcanic Zebayir Island in a water depth of 852 meters, contains significant admixtures of volcanic glass and several intervals of tuffites.[4] Tuffites were encountered in the following samples: 229-3, CC, 229-5, CC, 229A-8-1, 2-3, and 229A-17-2 of which Cores 8 and 17 were studied in particular.

Core 8 (113-122 m) contains three different tuffite layers (Figure 5) with thicknesses of about 20, 60, and 60 cm separated from each other by either a soft, silty clay calcareous nanno ooze (between tuffites 2 and 3) or by a lithified silty clay nanno ooze (chalk) between tuffites 1 and 2. Core 17 (196 m) contains a single tuffite layer with a thickness of about 70 cm.

Megascopic Description

Sample 8-1, 20-40 cm: Fine- to medium-grained (0.1-0.3 mm) greenish-gray tuffite with several well-rounded marl pebbles (Figure 5). Carbonate concentration ranges between 15%-20%.

Sample 8-2, 30-87 cm: A medium- to coarse-grained, grayish-black basal layer (Figure 6) (average grain size 0.3 mm) with abundant larger pumice fragments (0.5-1 mm) grades into fine- to medium-grained tuffite (grain size 0.1-0.3 mm), suggesting graded bedding.

A layer of well-rounded marl pebbles (0.2-0.8 cm) is observed at 55 cm (Figure 6). The carbonate content increases from 7% in the basal layer to 15% in the finer grained tuffite portions.

Sample 8-3, 17-76 cm: Fine-grained, grayish-black tuffite (grain size of "matrix" 0.06-0.09 mm) with abundant pumice fragments (1-2 mm) and large marl pebbles (Figure 6). Carbonate concentration ranges 10%-20%.

Sample 17-2, 85-150 cm: Greenish-black, well stratified, fine-grained tuffite (grain size 0.06-0.15 mm) with carbonate concentrations ranging between 5%-10%. At 132 cm a spherical concretion (diameter about 2 cm) is found (Figure 6).

---

[3] P. Stoffers and G. Müller.

[4] The term "tuffite" is used for a sedimentary rock containing more than 50% pyroclastic material.

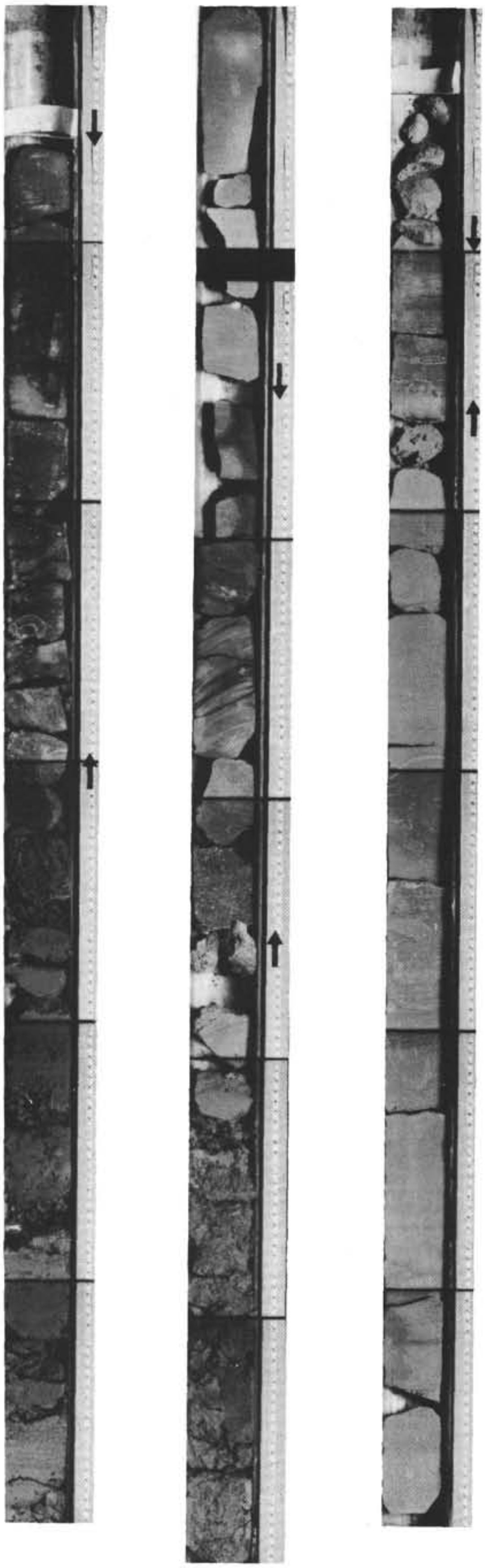

Figure 5. *Photographed Core 8, Sections 1, 2, 3. The tuffites are indicated by arrows.*

Microscopy and Mineralogy

Thin-section studies of the various tuffites indicate the presence of four different groups of components: (1) pyroclastic material, (2) epiclastic material, (3) biogenic constituents, (4) alteration products.

1) Pyroclastic material: In all tuffites studies, this group amounts to more than 80% of the total rock. Small fragments of greenish-yellowish glass (Figures 7, 8) together with larger fragments of light colored pumice (Figure 8) and glass shards derived from pumice are major pyroclastic constituents. Fragments of volcanic rocks and pyroxene are of major importance.

In general, the greenish-yellowish glass particles (together with the biogenic and epiclastic material) form a "matrix" in which larger pumice fragments float.

According to their refractive index, the colored glass fragments have a basaltic composition (n = 1.54-1.58), whereas the refractive index of pumice glass (n = 1.51-1.52) indicates a trachytic-andesitic composition. The volcanic rock fragments (Figure 8) consist of lath-shaped plagioclase (labradorite) in a glassy groundmass. An andesitic-basaltic composition is most probable.

2) Epiclastic (detrital) material: Minor amounts of mica, quartz, and feldspar(?) are interspersed in the pyroclastic material. Large, well-rounded marl pebbles occur in distinct layers. They consist of a mixture of micritic calcite with clay minerals and quartz.

3) Biogenic constituents: A large part of the carbonate content of the tuffites can be attributed to foraminifera and nannofossils (Figure 7) together with very few fragments of echinoderms and fish debris randomly distributed within the rock.

4) Alteration products: A portion of the glassy constituents indicates devitrification (spotty undulation). Alteration products are montmorillonite and analcite. Some pumice fragments have been completely converted into calcite without changing the primary structure (Figure 9). Often the vesicles of pumice fragments are filled either with calcite (Figure 10) or analcite (Figures 11, 12). Their wall structures still consist of unaltered volcanic glass. Pyroxene often shows partial or full replacement by calcite.

Lithification

The tuffites (and the intercalated chalk) are cemented with fine-grained calcite. In Core 17, Section 2, a concretion has formed by completely filling the pore space with calcite without changing the original mineralogy and the structure of the sediment (Figures 13, 14).

Results and Conclusions

The tuffites encountered at Site 229 consist of three primary constituents of different origin: pyroclastic, epiclastic, and biogenic. The presence of two types of volcanic glass indicates different sources of the pyroclastic material.

No palagonitization could be observed in any sample studied. The partial devitrification of the basaltic glass is due to submarine weathering (halmyrolysis) which leads to the formation of montmorillonite plus analcite. Alkalies and alkali earths are liberated and become part of the interstitial solutions. If these solutions are already enriched in Ca^{++} and HCO_3^-, a further supply of Ca^{++}

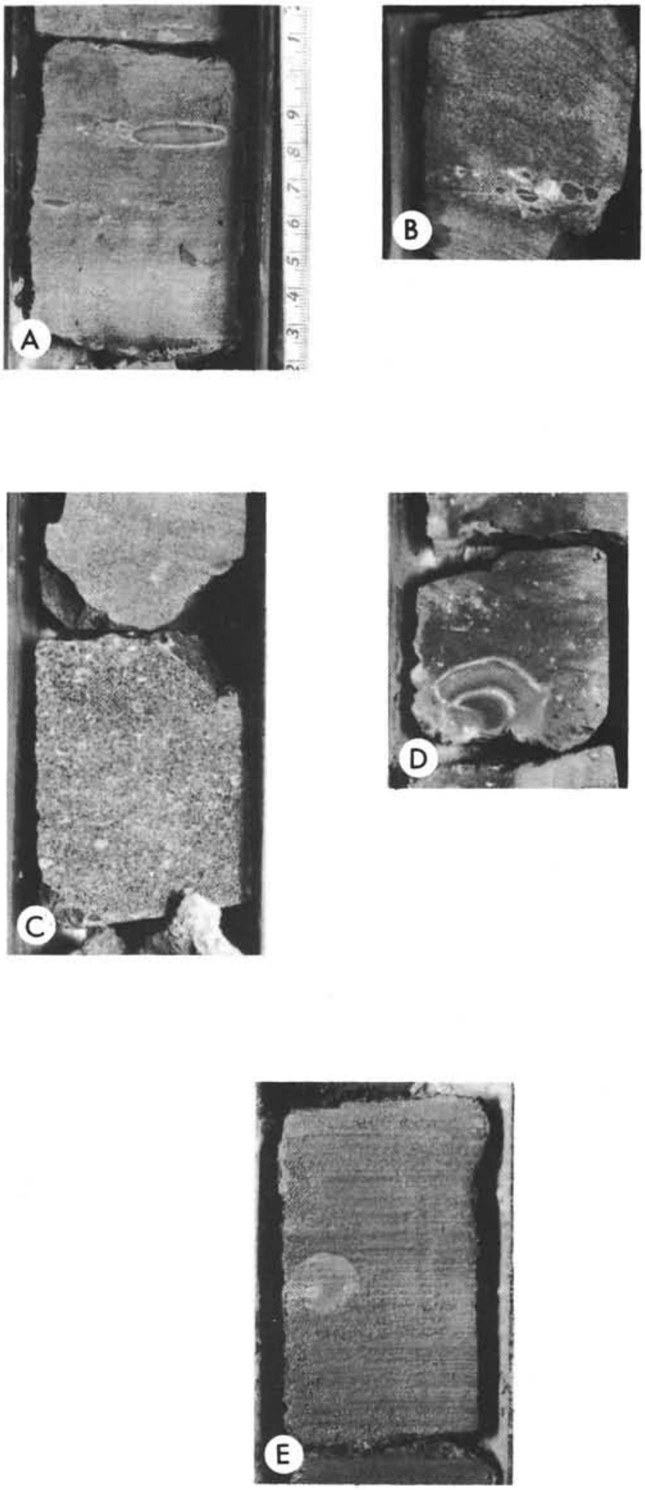

Figure 6. *Tuffites from the various tuffite horizons. (a) 8-1, 20-40 cm; tuffite with well-rounded marl pebbles. (b) 8-2, 30-87 cm; tuffite with layer of well-rounded marl pebbles. (c) 8-2, 30-87 cm; coarse-grained basal part of tuffite. (d) 8-3, 17-76 cm; contorted marl pebbles and pumice fragments in fine-grained tuffite. (e) 17-2, 85-150 cm; calcareous concretion in fine-grained tuffite.*

causes oversaturation and precipitation of calcite. This calcite is found as a micritic cement or as replacement calcite of pumice and pyroxenes. These observations indicate that the pyroclastic material is derived from subaerial rather than from submarine volcanism.

The concretion in Core 17, Section 2 (Figure 6) is assumed to have formed in situ by preferential calcite precipitation, probably due to the decay of a higher concentration of organic matter in this part of the sediment. The process of calcite precipitation within the tuffites may also be responsible for the lithification of the intercalated nanno ooze (chalk) in Core 13.

BIOSTRATIGRAPHY

Foraminifera

One of the more striking aspects of the planktonic foraminiferal faunas at Site 229 is the significantly increased diversity of some samples relative to other Red Sea sites. While these assemblages remain somewhat impoverished by normal deep-sea standards, the occasional presence of such forms as *Globorotalia hirsuta* and *G. crassaformis* indicates the influence of the influx of more normal surface water and plankton populations from the Gulf of Aden.

To the extent that the faunal classifications employed for Sites 225 through 228 are useful at this location, most samples are tentatively assigned to the relatively diverse *Globigerinoides sacculifer* Biofacies. At a number of horizons, the diversity of foraminiferal populations decreases considerably, and some assemblages are strongly dominated by *Turborotalita quinqueloba.* At some levels, particularly within 229A-6-6, 229A-8 through 12 and 229A-14 through 18, significant portions of some samples consist mainly of relatively poorly preserved and filled tests, although the remainder in these samples are empty and not recrystallized. In general, the species compositions of the filled and empty fractions are similar, but in a few samples the differences are significant.

In view of the high sedimentation rate calculated at this site, and the absence of terrigenous detritus, it seems likely that a high proportion of the sediment recovered here was derived from adjacent topographic highs. Hydrodynamic factors may thus account for some of the variations in species assemblages in different samples, particularly in those dominated by small tests. The filled specimens may be reworked as well, although the similarities in species composition with well-preserved populations suggests that the age of the two fractions may not differ greatly. In view of the shallow-water origin of all benthic species observed, it is difficult to verify this assumption.

Pteropods, which are occasionally present in cores at other Red Sea sites, are particularly common, and sometimes completely dominant, at a number of horizons at this locality, especially in Cores 229-1 through 229A-7.

Nannofossils

Hole 229 was drilled in sediments of Late Quaternary age. Hole 229A penetrated sediments ranging in age from

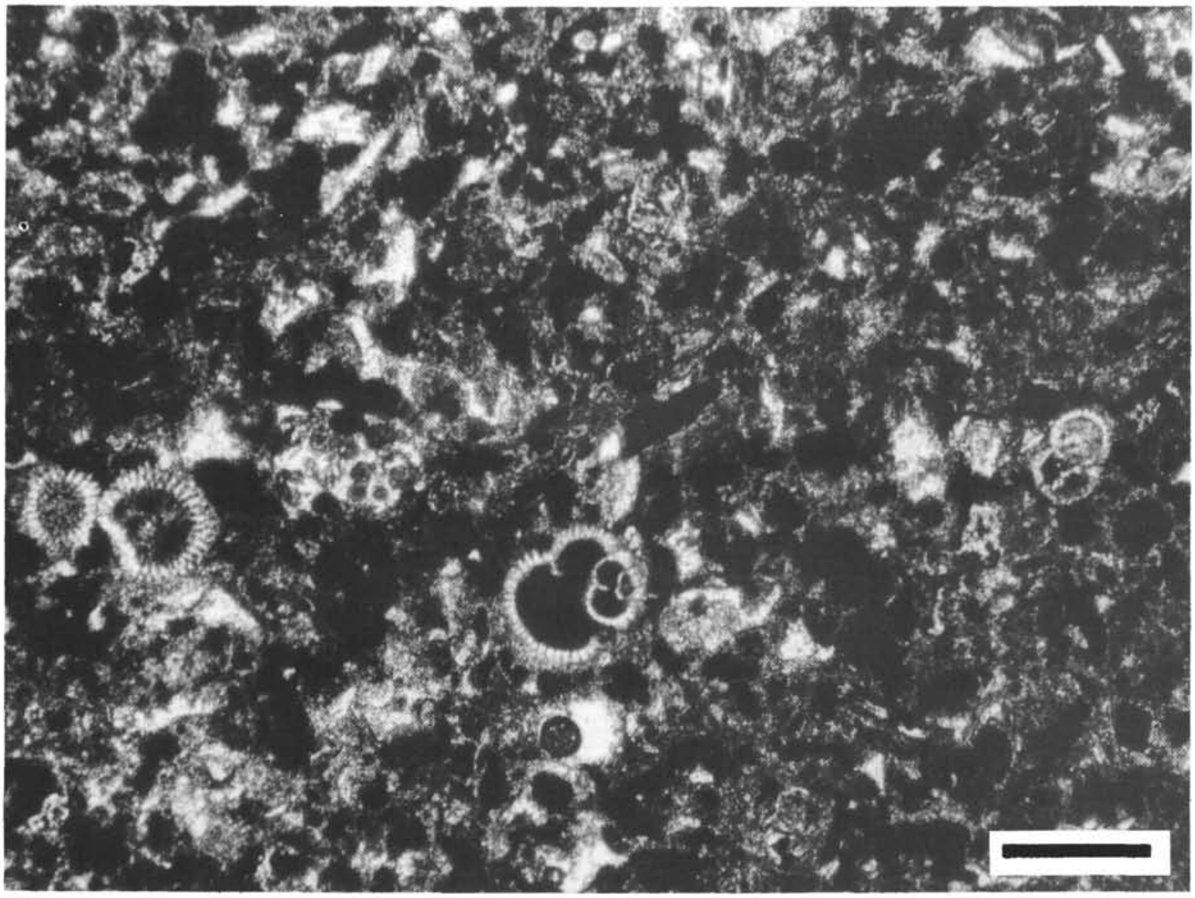

Figure 7. *Tuffite mainly composed of greenish glass fragments and lesser amounts of biogenic components. crossed nicols. Site 229, Core 8A, Section 1, Interval 30-35 cm. Scale bar represents 0.4 mm.*

Holocene to Late Pleistocene. Paleontological evidence suggests that an expanded Late Quaternary sedimentary section is present in this hole.

The *Emiliania huxleyi* Zone (Hay et al., 1967) is present in the Holocene and Pleistocene sections of Core 229A-1 and Sample 229A-2-1, 136-137 cm. Nannofossils present within the zone are listed as follows: *Gephyrocapsa oceanica, Gephyrocapsa protohuxleyi?, Cyclococcolithus leptoporus, Thorocosphaera heimi, Umbilicosphaera mirabilis, Syracosphaera histrica, Helicopontosphaera kamptneri, Emiliania huxleyi.*

The Late Pleistocene section of Hole 229A occurs in Cores 2 to 18. Recognizable nannofossil zones are listed as follows: *Gephyrocapsa oceanica* Zone (Sample 2-3, 79-80 cm to Core 7); *Gephyrocapsa caribbeanica* Subzone (Core 8 and Sample 9-1, 75-76 cm); *Coccolithus doronicoides* Zone (Sample 9, CC to Core 18).

Nannofossils are very abundant throughout the stratigraphic sequence and preservation is excellent.

Radiolaria

In Hole 229 a single radiolarian was found in the sample examined from the core catcher of Core 1. Rare sponge spicules were noted in Samples 2, CC and 4, CC.

In Hole 229A numerous sponge spicules were observed in Cores 1 through 7. A single radiolarian was observed in the material examined from Sample 3, CC.

Biostratigraphic Summary

Nannofossils are particularly abundant in sediments at Site 229 and provide the time-stratigraphic basis for dating the cores. The Pleistocene-Holocene *Emiliania huxleyi* Zone is present as low as Sample 229A-2-1, 136-137 cm (30 m); the remainder of the sediments recovered are of Late Pleistocene age. The earliest samples examined are referred to the *Coccolithus doronicoides* Zone.

Most foraminiferal samples are tentatively referred to the *Globigerinoides sacculifer* Biofacies, although faunas generally are more diverse than those observed at other Red Sea sites. This reflects the influx of more normal marine surface waters and planktonic faunas from the Gulf of Aden. Some of the fluctuations in diversity and preservation can, in all likelihood, be accounted for by downslope transport and reworking from slightly older sediments. Pteropods are common at many horizons, particularly in the upper 80 meters of recovered sediments.

Radiolaria are essentially absent at this site. Sponge spicules are numerous in sediments from Cores 229A-1 through 7.

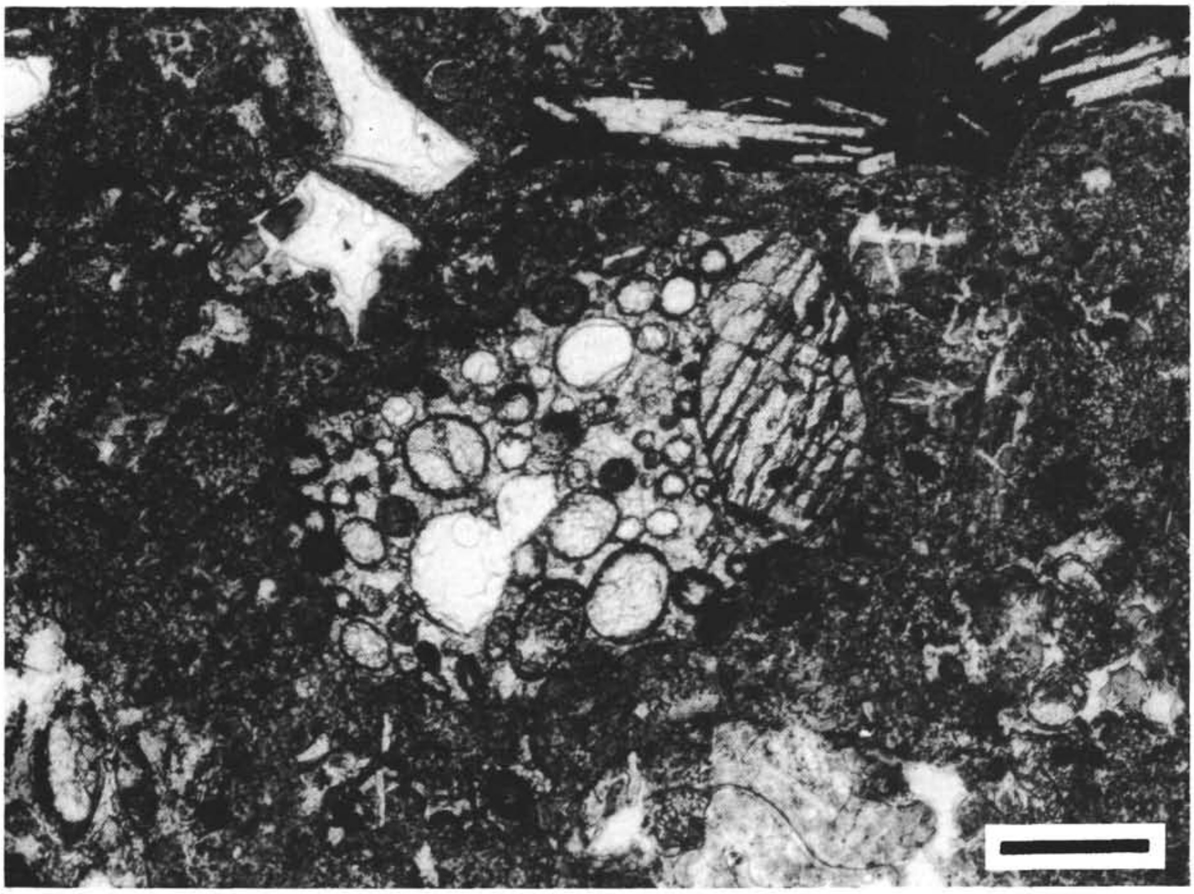

Figure 8. *Tuffite with fragments of pumice (center), glass shards (upper left), volcanic rock (upper right), and greenish glass (lower right) in a fine-grained matrix-rich in glass. Site 229, Core 8A, Section 2, Interval 83-85 cm. Scale bar represents 0.4 mm.*

Sedimentation Rates

The lack of horizons at this site for which reliable absolute ages are available results in considerable uncertainty in interpreting the sedimentation history of the Late Pleistocene. Two alternative explanations are shown graphically on the sedimentation rate chart (Figure 15).

If it is assumed that the lowest occurrence of *Emiliania huxleyi* (47 m) is somewhat younger than the 175,000 year age determined for this horizon elsewhere (Gartner, in preparation), the zone determinations are compatible with a sedimentation rate of at least 580 m/m.y. There is no evidence, however, to support this assumption. The alternative interpretation (dashed line) suggests the very high sedimentation rate of at least 900 m/m.y. for the interval of 47-203 meters, and a considerably lower rate of 270 m/m.y. for the overlying uppermost Pleistocene and Holocene. These values, coupled with the largely biogenous nature of the sediment, the indications of reworked foraminifera, and the topographic location of Site 229, clearly suggest high rates of sediment slumping from adjacent areas.

GEOCHEMISTRY

Solids

The cores consisted largely of calcareous ooze which contained minor amounts of detrital silt and clay and a significant admixture of volcanic ash and its decomposition products. That this ash had a basaltic origin was suggested by significant amounts of Ti, Cr, Ni, Fe, and Mg in the spectrographic analyses (see Table 5, Manheim and Siems, Chapter 29). No significant amounts of heavy metals (Cu, Zn, Pb) or other chalcophilic elements were noted. One dubious sample (21.5 m) showed 100 ppm of Mo.

Some interesting separated phases included a calcite crystal from the welded tuff at around 115 meters, which had strontium and magnesium (200 ppm and 1.5%, respectively) concentrations appropriate to low magnesium calcite, and otoliths of unknown fish species, which contained only 0.05% Mg with 3000 ppm Sr. This might be either low magnesian calcite or aragonite, more probably the latter.

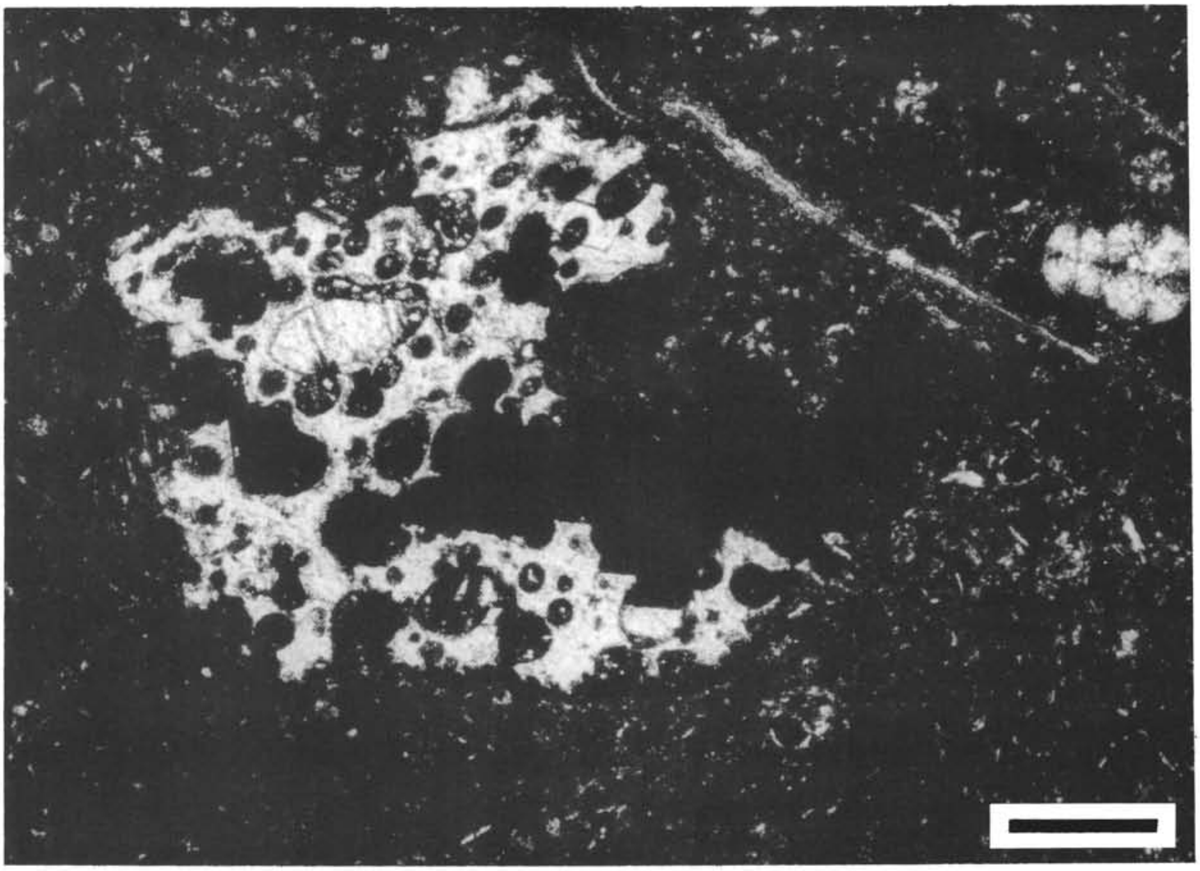

Figure 9. *Pumice replaced by calcite. crossed nicols. Site 229, Core 8A, Section 3, Interval 70-74 cm.*

Interstitial Waters

Holes 229 and 229A were the only holes in the Red Sea drillings which did not show sufficient interstitial salinity gradients with depth to confirm (or deny) the presence of salt or of products of leaching of salt and evaporites. An increase in salinity from 39°/₀₀ at the surface to 42°/₀₀ at depth occurred. The data are summarized in Table 2 and Figure 16. An evaporitic episode in Late Pleistocene time is not reflected in the interstitial salinity, but has possible slight expression in the deuterium data (Friedman and Hardcastle, this volume). See Manheim et al., Chapter 35 for a discussion.

The observed decrease in alkalinity with depth can perhaps be explained by the presence of devitrifying volcanic glass, which liberates alkalies and alkali earths on weathering. Some glasses form clay minerals and zeolites, observed in the hard welded tuffs, whereas others (calcium-rich) form calcium carbonate cements in the sediments. This may be a partial explanation for the failure to find high alkalinities in the very gassy (methane) sediments, especially at depth. Methane production tends to consume CO_2 (Wolfe, 1971).

Water Content

After an initial decrease from over 40% in the uppermost strata, there is little consistent loss of water content with depth down to the lowest strata investigated, in spite of marked increases in consolidation and cementation. At 100-125 meters depth (Figure 17, Table 3) hard, cemented palagonite and zeolitized tuff beds were underlain by very dense, cemented siltstones. Locally, other beds containing abundant volcanic ash also showed appreciable cementation (generally with carbonate). These cementation phenomena appear to account for a part of the water content fluctuations. As usual, disturbance in the upper plastic sediments (flowage, drilling slurry) renders the data uncertain, but reasonable preservation occurred at a shallower depth than elsewhere in Red Sea sites.

One should again emphasize that the fluctuations in water content are probably not artifacts, but are real. The gradual increase in density of sediments which is often implied to be applicable to sedimentary basins simply does not apply to the Red Sea, nor to many other DSDP legs, for which reasonably reliable water content data have been obtained. In the Red Sea samples examined here cementation, rather than consolidation, seems to be the main factor causing decrease in porosity.

Gas

After the second core in Hole 229, abundant gas, shown to be chiefly methane, some CO_2, and a trace of ethane were found (Table 4). Because of the undesirability of

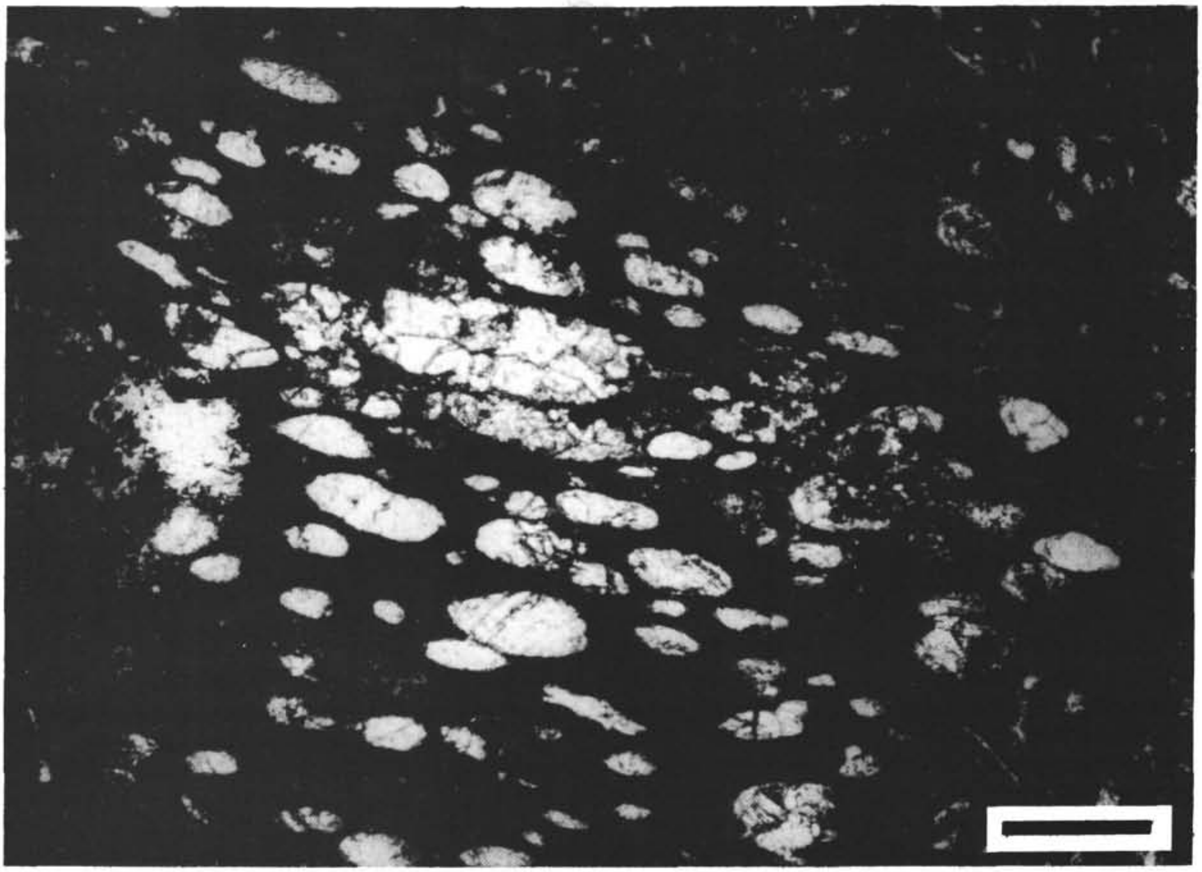

Figure 10. *Pumice vesicles filled with calcite. crossed nicols. Site 229, Core 8A, Section 3, Interval 70-74 cm.*

running the bottom fluid tester (see Geochemical methods, Chapter 2), since there was a tendency to jam the bumper subs when pumping was stopped, there is no way to estimate the total gas present.

More gas is dissolved in pore fluids with increasing pressure, according to Henry's Law. Release of this gas when bringing cores to the surface causes separation of gas pockets in the core liners. By the time liners can be sampled, pressure is close to atmospheric. As seen in Table 4, the CH_4/C_2H_6 ratio dropped consistently with depth in Hole 229A. Although diffusional permeability dropped nearly 10-fold in the hard tuff beds (shown by increase in the formation factor), these beds nevertheless appear leaky enough to maintain something approaching a constant slope trend with depth and do not form a trap for the hydrocarbon gases.

The volume of the gas may be partly explained by the extremely rapid rate of accumulation of the muds; evidently this rate was helpful in reducing loss of organic carbon by decomposition at the sediment-water interface, a favorite concentration point for bacterial attack. Other very rapidly deposited sediments encountered by the DSDP, e.g., on Legs 1, 4, 15 and 23a have also demonstrated enhanced gas accumulation of the "dispersed" type.

CO_2 shows a different pattern. Being much more reactive than methane, it drops in concentration in the vicinity of the tuff beds. This is logical, for the devitrifying glass loses alkalies and alkali earths during weathering, with resulting *p*H increase and opportunity for uptake of CO_2 as calcium carbonate. The cementing of the altered glass shards with carbonate and zeolite testify to this effect. The reactive nature of the CO_2 also helps explain the more erratic fluctuations in its concentration with depth, with respect to methane/ethane ratios.

Emerging from these data is a realization that much more meaningful gas information would be possible if gas could be captured at in situ pressures. Real pressure gradients could then give data of importance for both scientific and safety questions.

Resistivity Measurements

The formation factors in Table 5 show that the hard palogonite tuff layers have much lower but still finite diffusional permeability and do not serve as an effective trap for hydrocarbon gases. This is confirmed by the methane/ethane ratios in Table 4, since approximate continuity in these ratios is maintained through the hard layers.

Isotope Studies

The deuterium/hydrogen ratio of interstitial waters was measured by Friedman and Hardcastle (this volume). The uranium and thorium isotope contents of sediment samples were measured by Ku (this volume).

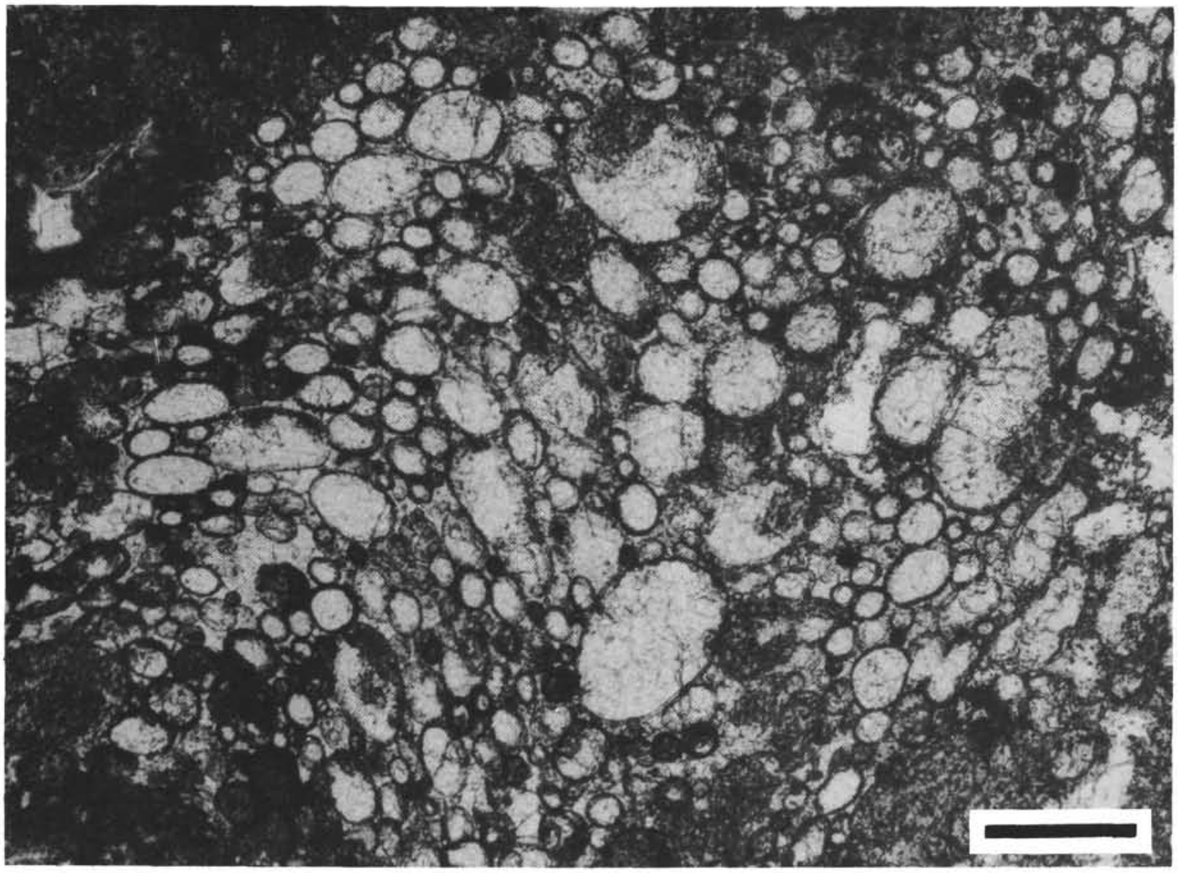

Figure 11. *Pumice vesicles filled with analcite. Site 229, Core 8A, Section 2, Interval 83-85 cm. Scale bar represents 0.4 mm.*

PHYSICAL PROPERTIES

At this site 212 meters of Holocene to late Pleistocene carbonate and nanno oozes containing occasional volcanic tuffs were drilled. Unfortunately, the presence of large quantities of gases, CO_2, H_2S, CH_4, and C_2H_6, made the measurement of physical properties very difficult and the results obtained should be treated with caution.

Water Content, Porosity, and Density

The GRAPE porosity and density as a function of depth are shown in the Site Summary. The large number of breaks and the high frequency "noise" on the plots are due to the presence of voids. The dashed lines are an attempt to salvage some useful information on the assumption that the minimum porosities and maximum densities are the closest to the actual values. Even with this smoothing, the porosities are seen to be very variable ranging from about 50% at 25 meters depth to a maximum of about 75% at 110 meters, while the densities range from a maximum of about 1.9 g/cm^3 at 25 meters depth to a minimum of about 1.4 g/cm^3 at 110 meters. The tendencies for the porosities to increase with depth and the densities to decrease with depth probably reflect the increase in the gas content with depth.

The core plots show surprisingly good agreement between the section weight and GRAPE densities. The section weight densities are sometimes as low as 1.35 g/cm^3 again reflecting the gaseous nature of the sediments. An interesting feature is that even at the core level (e.g., Core 4) a tendency for the density to decrease (rather than increase) with depth can be detected. It is seen that the plots for the deeper cores become more erratic. All these features are a consequence of the gases and voids.

Compressional Wave Velocity

Because of the loose gaseous nature of the sediments, the measurement of sonic velocities was extremely difficult and only two values are shown in the Site Summary. The first is in the Holocene sediments at 27 meters depth giving an approximate value of 1.7 km/sec and the second is a measurement on volcanic tuff interbedded in the upper Pleistocene sediments at 118 meters depth giving a velocity of 3.0 km/sec.

Thermal Conductivity

One attempt was made to measure the thermal conductivity of the soft nanno and carbonate chalk (Sample 229-4, 2 cm). This gave a value of 0.917 Wm^{-1} K^{-1}. A repeat measurement was made leaving the needle probe in the same place, giving 0.854 Wm^{-1} K^{-1}. As the repeatability was poor, no further measurements were made. Furthermore, the mean value obtained (0.885 Wm^{-1} K^{-1}) is about

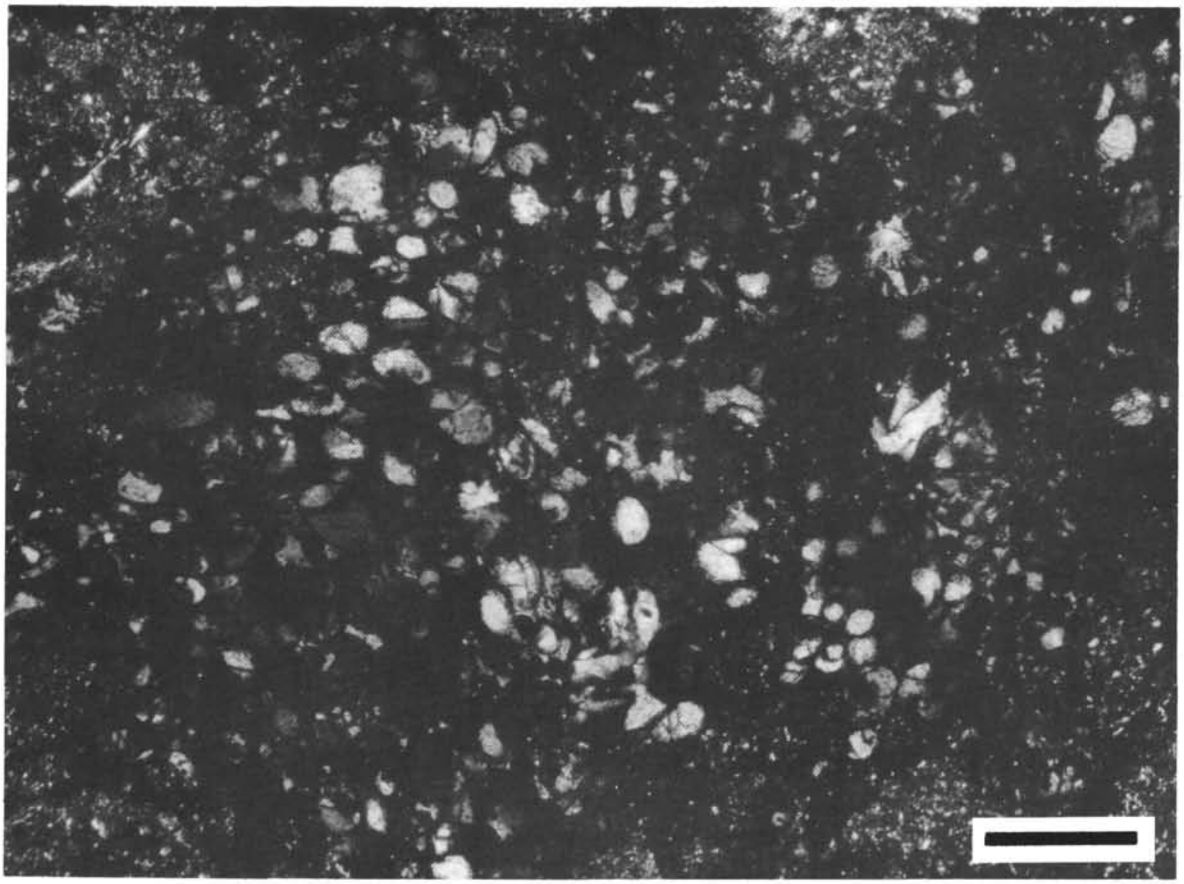

Figure 12. *Pumice vesicles filled with analcite. crossed nicols. Site 229, Core 8A, Section 2, Interval 83-85 cm. Scale bar represents 0.4 mm.*

30% lower than the mean thermal conductivity for Sites 225, 227, and 228, the lower value most probably being due to the presence of gases.

CORRELATION OF REFLECTION PROFILES AND LITHOLOGIES

The site was chosen over a rather flat sediment basin but close to the steep west flank of a north-south-oriented ridge (Figures 4 and 18). No distinctive reflections can be seen except for the steeply dipping (12° slope) group of reflections seen near the bottom of the hole. These beds were probably not sampled since no dipping structures were seen in the bottom cores, but, on the other hand, the dip would be only apparent and not real if the reflections were side echoes from the ridge. The reflections probably mark the top of a folded sequence which is found in the region around the site and which is overlain by subhorizontal beds (Figure 19). The uppermost 0.22 sec beneath the site consists of a large number of subparallel reflections and these are probably due to groups of lithified palagonite tuff beds found in the cores. As was found previously with three other reflection profiles across the basin (unpublished data of *Chain*-100, *Conrad*-9, *Glomar Challenger*-23), and Figure 19, no acoustic basement is visible.

DISCUSSION AND CONCLUSIONS

Southward Extent of the Axial Trough

A major objective of this site was to discover whether oceanic crust, which has been formed in the last 3 m.y. by sea-floor spreading beneath the axial trough north of Zebayir Island, also exists south of the island. The site had to be unexpectedly abandoned due to the large quantities of hydrocarbon gas in the sediments; this prevented our reaching igneous basement. Nevertheless, sufficient evidence was accumulated to resolve the question with some certainty.

Although the whole Red Sea appears to be a region of above-average heat flow, the normal spreading ridge pattern, with the highest values at the spreading axis, is found (see Girdler et al., this volume). Thus, in the southern Red Sea south of 18°N, values of 175 and 180 mWm^{-2} have been found in the axial trough, but outside the trough the heat flow lies between 90 and 140 mWm^{-2}. Because of technical problems, the heat flow at Site 229 can only be estimated to be at least 127 mWm^{-2}, and thus this measurement does not conclusively demonstrate that the site overlay the axial trough.

There is strong evidence, however, for concluding that beds of halite do not underlie the site, based on the

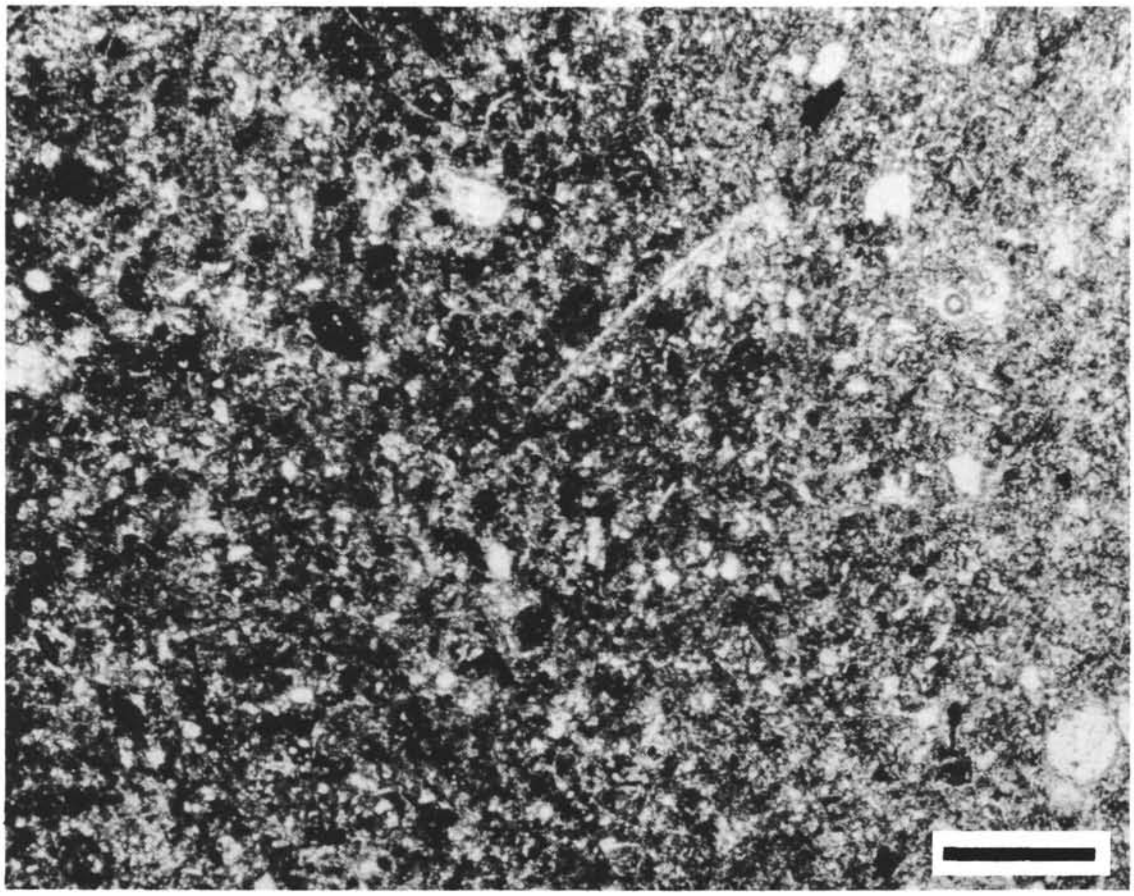

Figure 13. *Calcareous concretion in tuffitic sediments (left side). Site 229, Core 17A, Section 2, Interval 129-139 cm. Scale bar represents 1 mm.*

evidence of the salinity of interstitial pore waters (see Table 2, Figure 16). These measurements show only a slight but systematic increase of salinity with depth from 39.2°/₀₀ at 9 meters to 42.1°/₀₀ at 177 meters. This gradient is in striking contrast with the very much steeper gradients found at Sites 225, 227, and 228 where evaporites were encountered up to 290 meters below the sea bed. At the present day in the Red Sea salinities as high as 42.1°/₀₀ are only met in the uppermost layer of the northern part (Patzert, 1972); however, it is conceivable that the observed values represent paleosalinities. On the other hand, it could also be argued that evaporites underlie the site but at such a depth that diffusion of saline waters has only a small influence on pore water salinities in the topmost 200 meters.

No definite acoustic basement was seen on seismic reflection profiles across the site although "visible" energy was being returned from up to 0.6 sec beneath the sea bed. It is possible to extrapolate the mean sedimentation rate of 580 m/m.y. to this depth to estimate the age of the oldest reflections beneath the site. In this way an estimated age of 1 m.y. is obtained, which lies within the expected age range of the oceanic crust beneath the axial trough.

Thus, it cannot be concluded that the axial trough of the Red Sea definitely extends south of Zebayir Island, but the evidence from this site seems to favor this interpretation.

Explanation of High Sedimentation Rate

The cored sediments from the two holes at Site 229 are unusual in that they were deposited at the high mean rate of over 580 m/m.y. and yet have a very high content (over 70%) of biogenic carbonate, as well as unusually large amounts of hydrocarbon and other gases. Can the high sedimentation rate be explained on the basis of organic productivity alone? For instance, one of the regions of highest sustained surface productivity is probably within the equatorial current system where divergent waters cause upwelling of nutrient-rich bottom waters. Legs 5 and 8 of the Deep Sea Drilling Project drilled a series of seven holes along a 140°W section across the Pacific equatorial belt, but the highest sedimentation rate was 33 m/m.y. in a Middle Miocene rad nanno ooze at Site 71 (Tracey, Sutton, et al., 1971). The water depth, however, exceeded 4400 meters here, and a proportion of the biogenic carbonate may have been lost by solution. On the other hand, Arrhenius (1963) quotes accumulation rates of calcium carbonate of 5-10 $gm/cm^2/1000$ yr, presumably based on Quaternary cores, for the Equatorial Pacific which, assuming sediment with a water content of 50% by weight, is equivalent to 68-137 m/m.y. Ryther (1959) quotes a theoretical potential net organic production figure for the ocean of 27 $g/m^2/day$ (990 $g/cm^2/1000$ yr) but the mean annual rate in the

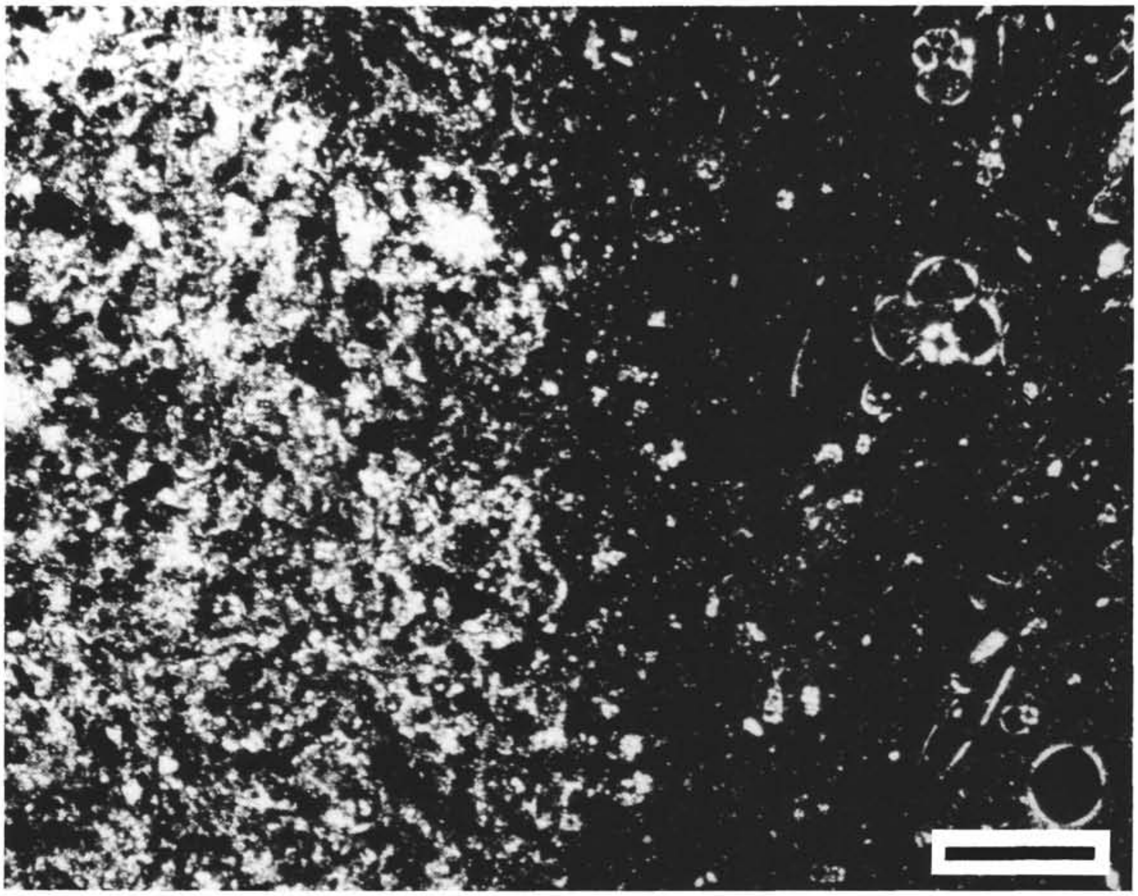

Figure 14. *Same as Figure 12 but under crossed nicols.*

oceans is probably almost two orders of magnitude less. Ryther's figure encompasses only the productivity within the euphotic zone and does not take account of scavenging or solution outside this zone. Thus, it is clear from the above that even given favorable circumstances accumulation rates of 580 m/m.y. would be exceptional.

It should therefore be considered in what other way the circumstances at Site 229 favor such a high rate of accumulation of biogenic carbonate. Firstly, the shallow depth (852-1064 m) of the recovered sediments and the raised temperature of the Red Sea bottom water (21.5°C) would inhibit carbonate solution and encourage preservation of organisms in the sediment. Secondly, the general situation of the site in the southern Red Sea is probably conducive to a high sedimentation rate. The site lies in the deepest part of a small fairly smooth floored basin surrounded on almost all sides by much greater areas of shelf less than 200 meters deep. Patzert (1972) has demonstrated that seasonal winds are the dominant force in determining the surface circulation of the Red Sea. In winter there is a strong northward surface flow in the southernmost Red Sea, and in summer there is a strong southward flow at the surface with a weak counterflow between 30 and 80 meters depth. Although the details of these currents in the southernmost Red Sea are not known in plan view clearly, the stirring action of the wind, the strong currents, and seasonal changes of direction will have the effect of sweeping the shelves of all sediment. The most likely spot for all of this sediment to accumulate would seem to be the deepest part of the sea floor, i.e., the basin south of Zebayir Island. The sand-size material was presumably carried downslope by a near-bottom transport mechanism, as were the otoliths, pteropods, gastropods, pelecypods, echinoids, and filled foraminiferal tests. No certain graded beds were seen in the cores, however, and slumping of some of this coarse material from the ridge to the east and southeast of the site cannot be ruled out. The more abundant finer material is likely to have been carried in suspension. Little appears to be known about the productivity of the waters of the Red Sea shelf beyond the fact that algal blooms have been occasionally reported from this area (Currie, 1955), but for this hypothesis to work these areas must be unusually productive.

Friedman (1972) has suggested a mechanism whereby organisms swept into the southern Red Sea from the Gulf of Aden were killed by the hypersaline conditions and accumulated to form the dark layers found in cores from this part of the Red Sea. This hypothesis was considered as an explanation for the high sedimentation rate at Site 229 but was found wanting. The main reason is that the cores at Site 229 are largely composed of coccoliths or their diagenetic derivatives. There is no evidence, however, that the nannofossil assemblages at this site are any more diverse than those found in the three main sites further north. Such a difference in diversity of species would be expected if only a few of the nannofossil species were able to tolerate

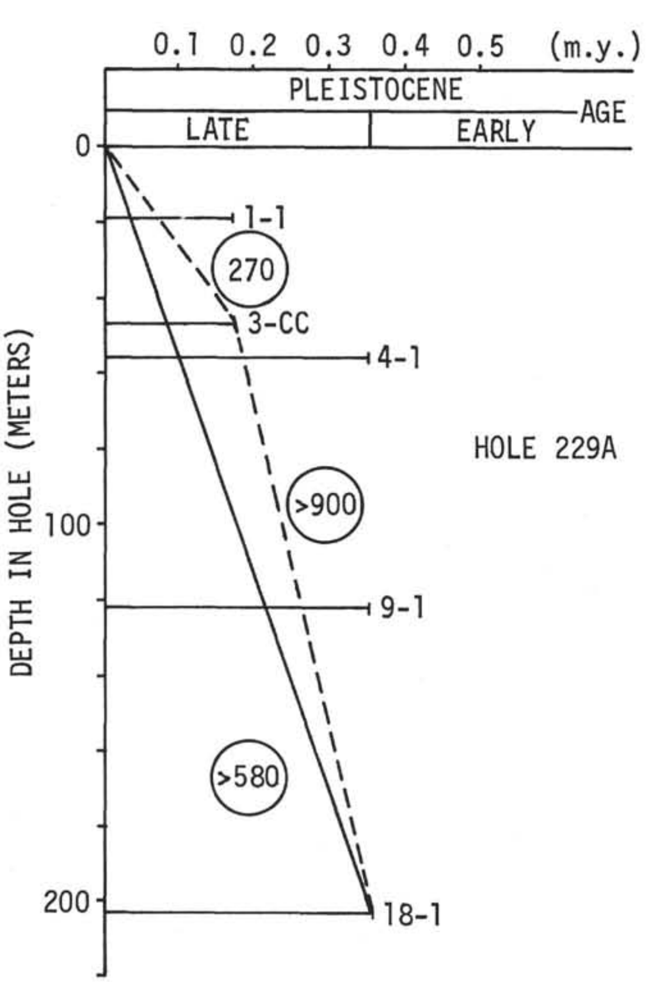

Figure 15. *Sedimentation rate curve, Site 229. Plotted bars are those sufficient to control slopes of lines.*

the Red Sea pelagic environment and the remainder were being killed by the high salinity or temperature. The remote possibility remains that individuals of a species which are swept into the Red Sea do die in large numbers in the new environment even though the species itself can adapt to the Red Sea environment.

Source of Hydrocarbon Gases

Lastly, some explanation of the relatively large quantities of methane, ethane, carbon dioxide, and hydrogen sulfide gases in the cores is appropriate. The methane/ethane ratio decreased with depth, carbon dioxide occurred in variable amounts, and hydrogen sulfide was noted in cores from the top 46 meters. Hydrocarbons were not noted in the top 47 meters, and in no core was a trace of liquid hydrocarbon seen under ultraviolet light. Hunt (1967) has discussed the origin of petroleum in carbonate rocks and has pointed out that since hydrocarbons lighter than C_9 are not synthesized by living organisms, they therefore must be generated within the sediments. Anaerobic bacteria decompose organic matter into the gases CO_2, H_2S, H_2, and CH_4. In carbonate rocks, due to a lack of iron needed to form pyrite, H_2S gas may build up and slow down or even stop the bacterial action, but such levels of H_2S do not seem to have been present at this site. Alternatively, bacterial action may continue even 50 meters or more below the sea bed. The rapid sedimentation rate at this site has probably prevented the complete breakdown at the sea bed of organic carbon by bacterial action so that appreciable quantities remain in the sediments. At greater depths it is too hot for bacterial action and thermal alteration takes over in the production of hydrocarbons but possibly not until the temperature exceed 150°C. Philippi (1968) has shown that in the Los Angeles and Ventura basins the bulk of the petroleum has been generated from a late Miocene source rock at temperatures above 115°C. At

TABLE 2
Interstitial Water Determinations, Holes 229 and 229A

Core, Section, Interval (cm)	Subbottom Depth (m)	H_2O Recovered (ml)	pH	Pore Water Lab. Temp. (°C)	ΔN	Salinity (Corr) (°/₀₀)	Alkalinity (meg/kg)	
Surface Water			8.35	23.2	67.8	37.3	–	
Hole 229								
1-6, 0-10	9	27	7.44	23.6	70.2	39.2	9.3	strong H_2S
2-6, 0-10	56	24	7.50	24.3	73.8	40.6	4.9	
3, CC	102	–	(7.49)	24.6	(71.2)	(39.2)	1.6[a]	
Hole 229A								
2-1, 140-150	29	15	7.43	23.8	72.0	40.2	6.8	
5-6, 0-10	74	17	(7.02)	23.8	73.3	40.8	2.7	
7-2, 140-150	85	22	7.27	23.6	75.5	42.1	2.6	
12-4, 140-150	156	22	6.93	23.8	76.2	42.0	1.6	
15-1, 140-150	177	12	7.34	23.8	76.5	42.1	1.5	
18-5, 70-75	211	8	–	25.3	(77.9)	(43.3)	b	

Note: Analysts: F. T. Manheim and D. Marsee.

[a] Sample apparently contaminated with drilling fluid.

[b] Sample probably slightly evaporated (salinity too high) because of storage of core overnight before sampling.

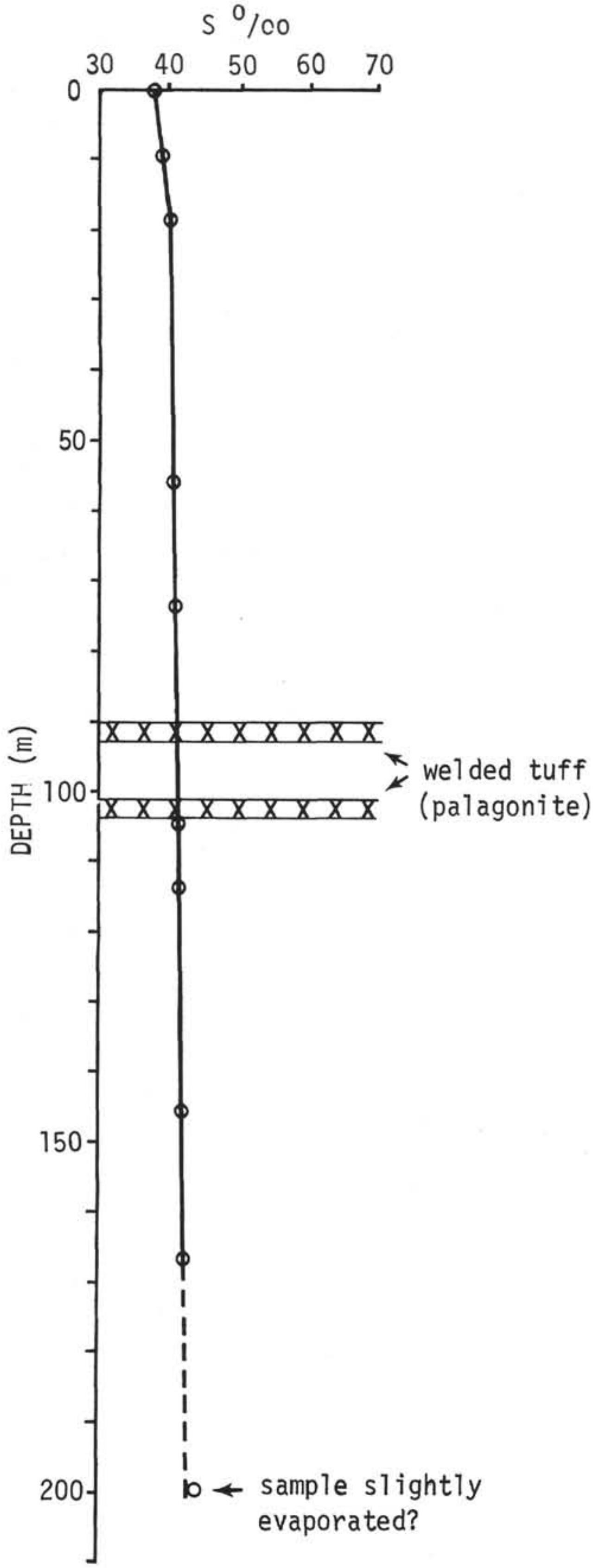

Figure 16. *Salinity of interstitial fluids from Site 229. Salinity is determined by index of refraction, calibrated for seawater solutions.*

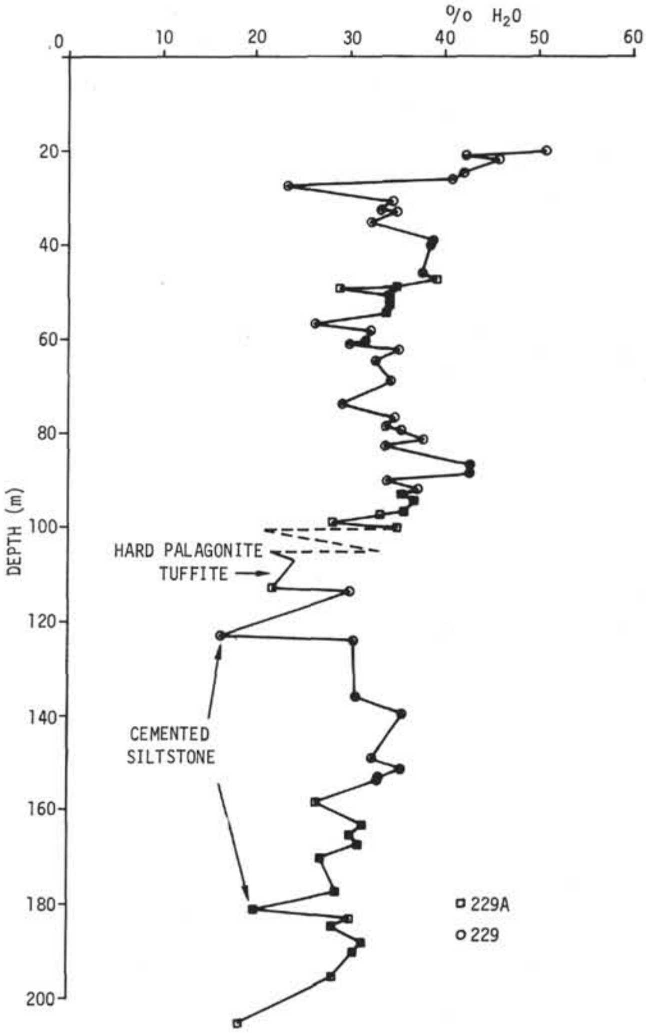

Figure 17. *Water content (weight loss on heating at 110-120° C) in percent wet weight.*

Site 229, provided the sediments are thick enough, such a temperature will exist at depths less than 1000 meters and there would seem to by a strong possibility that at least some of the hydrocarbon gas met in the cores may have been produced by thermal alteration, provided that free upward migration is possible. The low formation factor of the drilled sediments and the steady decrease with depth of the C_2H_6/CH_4 ratio suggest that occasional tuff layers present no serious barrier to hydrocarbon migration. However, if this were the case, then heavier hydrocarbon gases should have been detected on the gas chromatograms. The low alkalinities in the sediments also suggest that the main source of gas is in situ bacterial action. Nevertheless, the results of Vityok (1970) do suggest that hydrocarbons might be escaping into the sea, possibly from the region around Site 229. He reports a line of hydrographic stations from the north end of the Red Sea to the east end of the Gulf of Aden at which analyses of the benzene fraction were made. The highest values, 1180 and 580 μg/l, were found in the Straits of Bab el Mandeb at depths of 50 and 190 meters, respectively. Since the observations were made in October-November, outflowing Red Sea water would have been sampled (Patzert, 1972).

TABLE 3
Water Content, Site 229

Core, Section, Interval (cm)	Subbottom Depth (m)	H_2O (%)
Hole 229		
2-1, 95	47.9	39.1
2-2, 99	49.5	29.0
2-2, 105	49.6	34.3
2-3, 110	51.1	34.7
2-4, 125	52.7	34.3
2-6, 50	55	34.2
3-1, 10	93.1	34.9
3-2, 85	95.3	36.7
3-3, 100	97	35.6
3-4, 990	98.4	33.6
3-5, 25	99.2	28.6
3-6, 70	101.2	34.6
Hole 229A		
1-1, 110	20.1	51.2
1-2, 94	21.4	41.8
1-3, 20	22.2	45.6
1-4, 120	24.7	41.7
1-5, 80	25.8	41.0
1-6, 42	26.9	23.4
2-2, 110	30.6	34.3
2-3, 110	32.1	33.2
2-4, 80	33.3	35.2
2-5, 73	34.7	32.2
3-2, –		39.8
3-2, 52	39	39.0
3-2, 135	39.8	38.9
3-6, 140	45.9	37.6
4-1, 40	56.4	25.9
4-2, 145	58.9	32.2
4-3, 120	60.2	31.6
4-4, 50	61	30.2
4-5, 25	62.2	35.3
4-6, 105	64.5	32.5
5-3, 101	69	34.5
5-6, 111	73.6	28.9
6-2, 140	76.9	34.9
6-3, 100	78	33.9
6-4, 100	79.5	35.5
6-5, 140	81.4	38.2
6-6, 100	82.5	33.7
7-3, 80	86.8	42.8
7-4, 110	88.6	42.7
7-5, 116	90.2	33.9
7-6, 140	91.9	37.1
8-1, 80	113.8	30.7
8-3, 20-30	117	22.1
9-1, 69	122.7	15.7
9-2, 57	124.1	30.6
10-4, 120	136.7	30.6
10-6, 135	139.8	36.0
12-1, 140	150.4	32.3
12-2, 120	151.7	35.4
12-3, 100	153	32.1
12-4, 100	154.5	32.5
12-5, 135	158	26.0
13-3, 60	163	31.4
13-5, 170	165	29.8
13-6, 70	167	30.7
14-2, 105	170	26.7
15-1, 120	177	29.0
15-3, 125	181	19.9
15-6, 85	185	27.6
16-2, 130	188	31.3
16-4, 130	191	30.4
16-6, 102	194	28.2
18-2, 140	205	18.4

Depositional History

In summary, the history of this site is believed to have been as follows. During the last 3 m.y. new oceanic crust was formed in this part of the Red Sea by sea-floor spreading in a narrow axial trough just as was happening further north in the Red Sea. The sedimentation history is only known with certainty for the last 350,000 years although it is possible that in the preceding 0.65 m.y., at least, the same conditions applied. Since 0.35 m.y. ago, a rather uniform clay-rich carbonate nanno ooze has been accumulating rapidly at a mean rate of over 580 m/m.y. This sediment is largely composed of calcareous nannoplankton, or their diagenetic derivatives, which have been swept from the shelf of the southernmost Red Sea by currents into the basin south of Zebayir Island. Otoliths and pteropods are scattered throughout the sediments and rarely echinoids, pelecypods, and a gastropod were found. Detrital material is fine grained and never exceeds 25% of the sediment.

There was intermittent subaerial and subaqueous local volcanism from at least two sources, judging by the presence of both clear and green glass. There is about 2% glass in the sediments which also contain occasional, mostly lithified, layers of palagonite tuff. Likely sources are the Zebayir Islands or the other young volcanic islands of the southern Red Sea.

The rapid sedimentation rate prevented the complete breakdown of organic carbon by bacterial action at the sea bed and anaerobic bacteria have given rise to considerable quantities of gas (carbon dioxide, methane, and ethane). Hydrogen sulfide is found in the upper 46 meters.

REFERENCES

Allan, T. D., 1970. Magnetics and gravity field over the Red Sea: Phil. Trans. Roy. Soc. London, Series A, v. 267, p. 153-180.

Arrhenius, G., 1963. Pelagic sediments. *In* The sea, Hill, M. N. (Ed.), New York (Pergamon) p. 655-727.

Currie, R. I., 1955. The "Red" Sea?: Port of Aden Annual, 1954-55.

Friedman, G. M., 1972. Significance of Red Sea in problem of evaporites and basinal limestones: Am. Assoc. Petrol. Geol. Bull., v. 56, p. 1072-1086.

Gartner, S., in preparation. Absolute chronology of the Late Neogene calcareous nannofossil succession in the equatorial Pacific.

TABLE 4
Gas Chromatography, Hole 229A

Core, Section	Subbottom Depth (m)	Air Peak Area[a]	CO_2 Peak Height (Obs)	CO_2 Peak Height (Corr)[b]	CH_4 Peak Area	CH_4/C_2H_6 (Approx)
2-5	35	360	8.5	1.5	[c]	
4-6	64	290	~14	8	385	7000
5-3	70	135	120	117	428	5700
6-5	81	95	170	168	438	6020
7-5	91	55	110	109	450	4000
8-3	120	290	55	49	385	2650
9	~126	185	–	–	428	1600
9	~126	228	79	75	408	2300
9	~126	232	81	77	418	2300
10-5	138	77.5	104	103	435	2000
12-5	156	87.5	65	64	448	1800
13	162	132	108	106	432	1550
14-3	172	128	75	72	430	1800
15-5	183	130	118	115	422	1500
16-6	193	168	218	214	420	1200
17-1	198	202	215	211	415	830
18-5	209	148	110	107	425	950

Note: Analyst: D. Marsee.

[a] 600 represents 100% air.

[b] Correction made for CO_2 presumed to be present as a result of air contamination, taking 600 × 10^2 area as 100% of sample volume. Hydrocarbons and air represent peak areas, CO_2 is peak height. All units are arbitrary, but may be considered very very roughly proportional to relative volumes of gas present. Volume tested in each case is 200μl.

[c] No hydrocarbons detected.

TABLE 5
Resistivity Measurements, Holes 229 and 229A

Core, Section, Interval (cm)	Subbottom Depth (m)	R_s(app)	T°C	R_w(app)	T°C	R_{pw}	T°C	$S(^{\circ}/_{\circ\circ})$	R_s	C	F
Hole 229											
1, CC	9	0.120	23.1	0.048	23.1	0.167	25.8	39.2	0.49	4.1	2.8
2-6, 0-10	56	0.100	23	0.036	23.1	0.159	25.8	40.6	0.50	5.5	3.1
3-2,	96	0.0913	23	0.036	23.1	(0.163)[a]	25	41.0	0.50	5.5	3.0
3 CC	100	0.869	23	0.036	23.1	(0.163)	23.6	41.0	4.77	5.5	29[b]
Hole 229A											
2-1, 140-50	29	0.0781	24.6	0.0298	23.3	0.165	24.0	40.2	0.52	6.7	3.1
5-6, 0-10	74	0.118	25.0	0.0298	23.3	0.160	23.2	40.8	0.79	6.7	4.9
8-2, 35	114	0.664	23.5	0.0410	23.0	0.161	23.0	41.4	3.20	4.8	20[b]
8-2, 96	115	0.408	23.0	0.0410	23.0	0.161	23.0	41.4	1.97	4.8	12.2[c]
9-2, 140-50	124	0.100	28.0	0.0298	23.3	0.154	23.0	42.1	0.67	6.7	4.6
12-4, 140-50	156	0.109	23.8	0.0298	23.3	0.157	23.0	42.0	0.73	6.7	4.7
15-1, 140-50	177	0.178	23.5	0.0298	23.3	0.160	23.0	42.1	1.19	6.7	7.4
18-5, 75	210	0.100	25.5	0.0298	23.3	0.148[d]	24.5	43.3[d]	0.67	6.7	4.8

Note: Data as in Tables 2 to 4. All measurements are in ohm-m. Measurements on sediments are on end of 10-cm liner section where not otherwise noted. Reference fluid was $S = 35.4^{\circ}/_{\circ\circ}$, R_w, = 0.196 at 25°C. R_s is resistivity of sediment, R_{pw} is resistivity of pore water, and R_w is resistivity of reference water. C is cell constant and F is formation factor.

[a] Original squeezed water probably contaminated: R_{pw} 0.196 @ 25°.

[b] Carbonate-cemented palagonite tuff; appeared like dark basalt to the eye, except for lightness and porous, cemented character with light crystal inclusions.

[c] Very hard, green to gray cemented siltstone.

[d] Probable slight evaporation due to overnight storage of core in warm core laboratory.

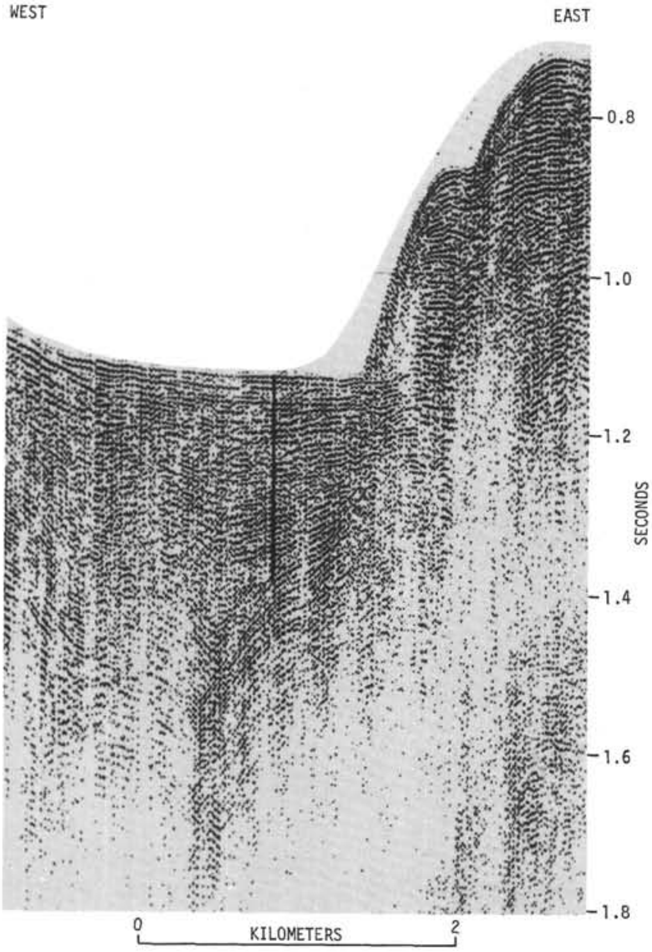

Figure 18. *Seismic reflection profile obtained on the final approach to the site. The vertical line marks the approximate position of the drilled hole.*

Gass, I. G., Mallick, D. I. J., and Cox, K. G., 1965. Royal Society expedition to the south Arabian federation and the Red Sea: Nature, v. 205, p. 952-955.

______, 1973. Volcanic islands of the Red Sea: J. Geol. Soc., v. 129, p. 275-310.

Girdler, R. W., 1970. An aeromagnetic survey of the junction of the Red Sea, Gulf of Aden and Ethiopian rifts (a preliminary report): Phil. Trans. Roy. Soc. London, Series A, v. 267, p. 359-368.

Girdler, R. W. and Darracott, B. W., 1972. African poles of rotation. Comments on earth sciences: Geophysics, v. 2, p. 131-138.

Hay, W. W., Mohler, H., Roth, P. H., Schmidt, R. R., and Boudreaux, J. E., 1967. Calcareous nannoplankton zonation of the Cenozoic of the Gulf Coast and Caribbean-Antillean Area, and Transoceanic Correlation: Trans. Gulf Coast Assoc. Geol. Soc., v. 17, p. 438-480.

Hunt, J. M., 1967. The origin of petroleum in carbonate rocks. *In* Chilingar, V. G. et al. (Eds.), Carbonate Rocks: New York (Elsevier), p. 225-251.

Hydrographic Department of the Admiralty, 1972. Collected soundings, sheet 157.

Laughton, A. S., 1970. A new bathymetric chart of the Red Sea: Phil. Trans. Roy. Soc. London, Series A, v. 267, p. 21-22.

Lowell, J. D. and Genik, G. J., 1972. Sea-floor spreading and structural evolution of the southern Red Sea: Am. Assoc. Petrol. Geol. Bull., v. 56, p. 247-259.

Patzert, W. C., 1972. Seasonal variations in structure and circulation in the Red Sea: Hawaii Inst. Geophys., Rept. 72-13.

Philippi, G. T., 1968. Essentials of the petroleum formation process are organic source material and a subsurface temperature controlled checmical reaction mechanism. *In* Schenk, P. A. and Havenaar, I, Advances in organic geochemistry: Oxford (Pergamon Press), p. 25-46.

Ryther, J. H., 1959. Potential productivity of the sea: Science, v. 130, p. 602-608.

Tazieff, H., Varet, J., Barberi, F., and Giglia, G., 1972. Tectonic significance of the Afar (or Danakil) Depression: Nature, v. 235, p. 144-147.

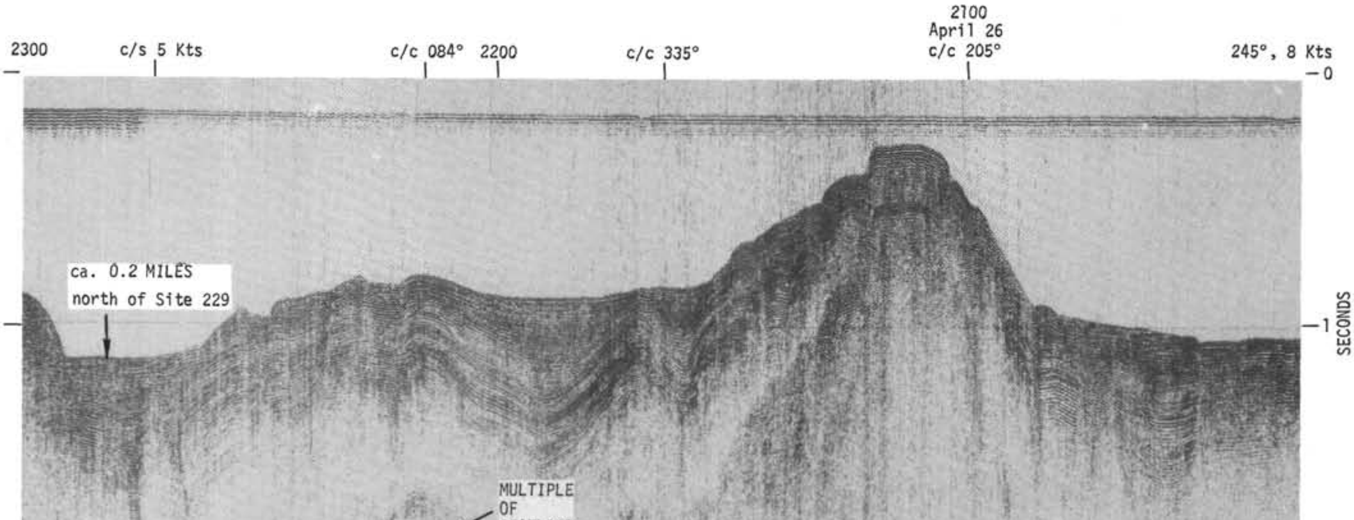

Figure 19. *Seismic reflection profile obtained by* Glomar Challenger *while carrying out the site survey (see Figure 5 for track). The figure shows a folded stratified sequence overlain by a subhorizontal stratified sequence. The eastern arm of the U-shaped basin appears at the extreme right of the figure, the western arm at the left.*

Tracey, J. I., Sutton, G. H., Nesteroff, W. D., Galehouse, J., von der Borch, C. C., Moore, T., Lipps, J., Ul Haq, U. Z. B., and Beckmann, J. P. 1971. Initial Reports of the Deep Sea Drilling Project, Volume 8: Washington (U.S. Government Printing Office).

Vine, F. J., 1966. Spreading of the ocean floor: new evidence: Science, v. 154, p. 1405-1415.

Vityok, D. C., 1970. Soderjaniye benzolnoi fraktsii organicheskovo veshchestva v voda krasnovo morya i adenskovo zaliva, Kimicheskiya rezyrci moray i okianov, red: C. V. Bruyevich, izdatyelstvo "Nauka", Moskva, p. 175-179.

Wolfe, R., 1971. Microbial formation of methane. *In* Rose, A. H. and Wilkinson, J. F. (Eds.), Advances in microbial physiology: v. 6, p. 107-146.

SITE 229

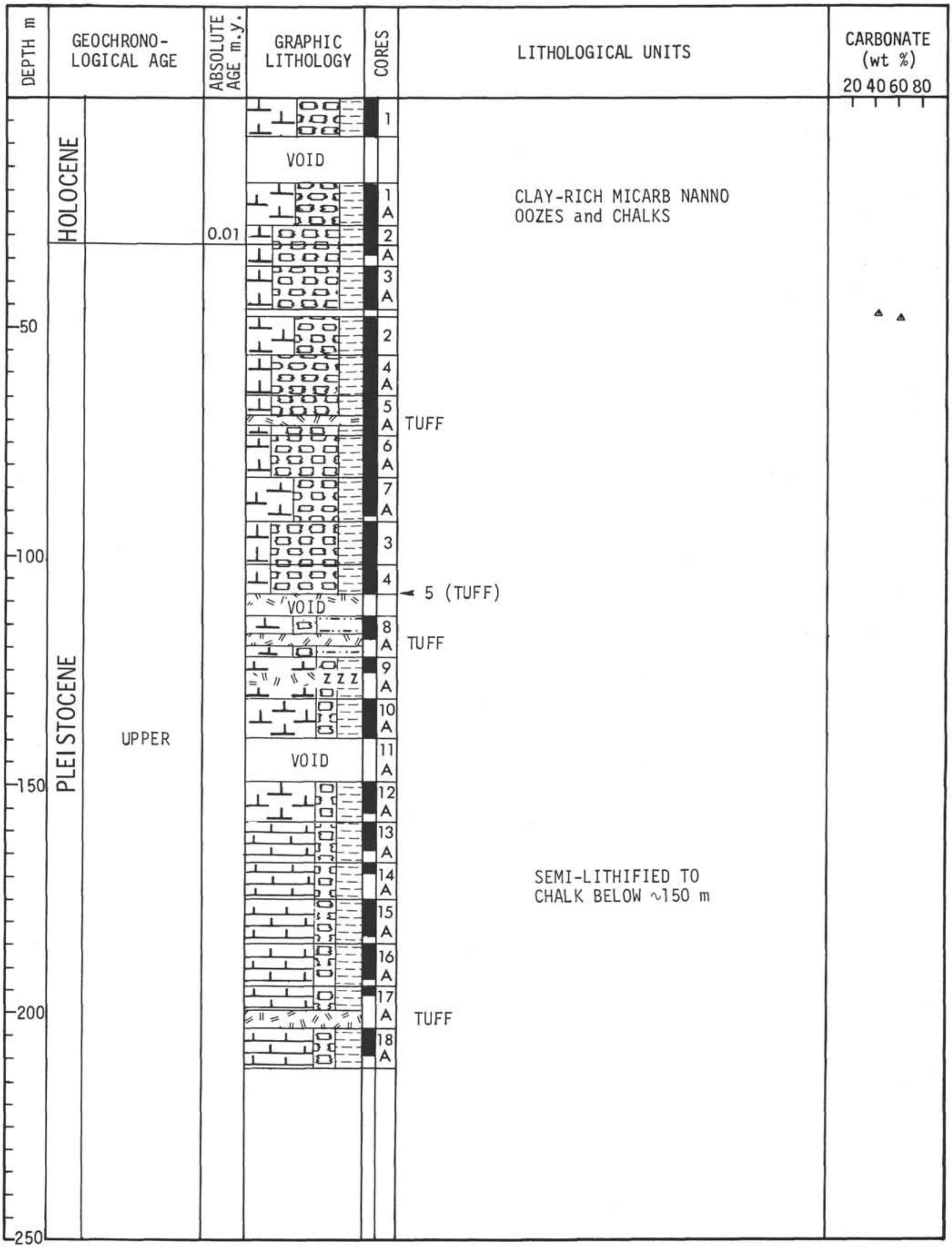
DEPTH m
GEOCHRONO-LOGICAL AGE
ABSOLUTE AGE m.y.
GRAPHIC LITHOLOGY
CORES
LITHOLOGICAL UNITS
CARBONATE (wt %)
20 40 60 80
HOLOCENE
0.01
PLEISTOCENE
UPPER
50
100
150
200
250
VOID
VOID
VOID
1
1 A
2 A
3 A
2
4 A
5 A
6 A
7 A
3
4
8 A
9 A
10 A
11 A
12 A
13 A
14 A
15 A
16 A
17 A
18 A
CLAY-RICH MICARB NANNO OOZES and CHALKS
TUFF
5 (TUFF)
TUFF
SEMI-LITHIFIED TO CHALK BELOW ~150 m
TUFF

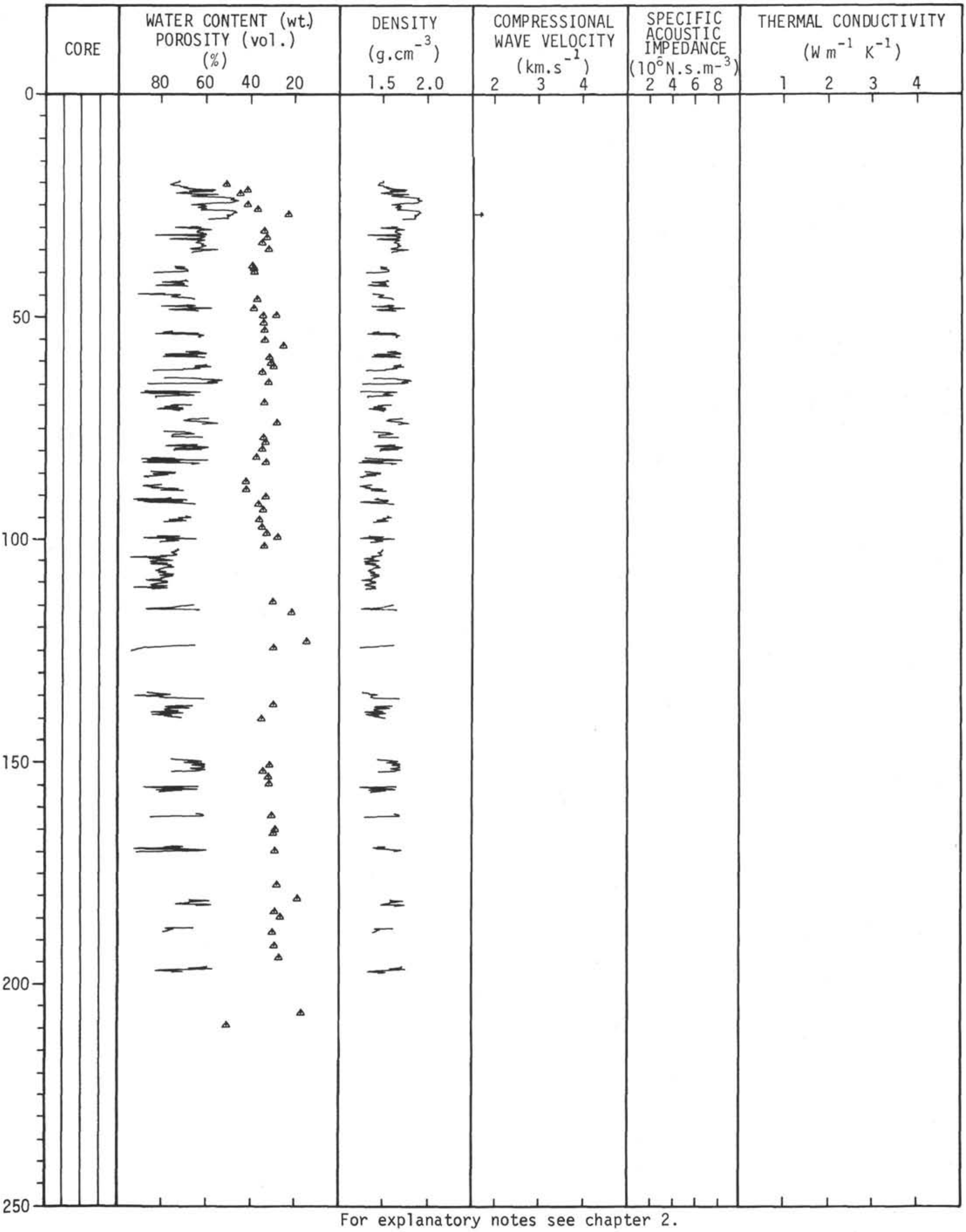

For explanatory notes see chapter 2.

Site 229 Hole Core 1 Cored Interval: 0-9 m

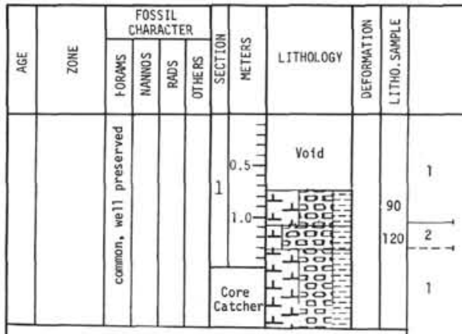

LITHOLOGIC DESCRIPTION

NANNO MICARB OOZE

Gassy core, broken by gas expansion (mostly CO_2). Pteropods abundant.

CLAY-RICH MICARB OOZE

Lithology SS: Section 1-90 cm.
Composition:

Micarb	55%
Nannos	30%
Clay	15%

Lithology SS: Section 1-120 cm.
Composition:

Micarb	65%
Clay	20%
Nannos	15%

Color legend:

1 = olive	5Y 4/3
2 = gray	5Y 5/1

<u>Shore-based laboratory results</u>

	Organic Carbon	Carbonate
Section 1-115 cm =	.3%	44%

Explanatory notes in chapter 2

Site 229 Hole Core 2 Cored Interval: 47-56 m

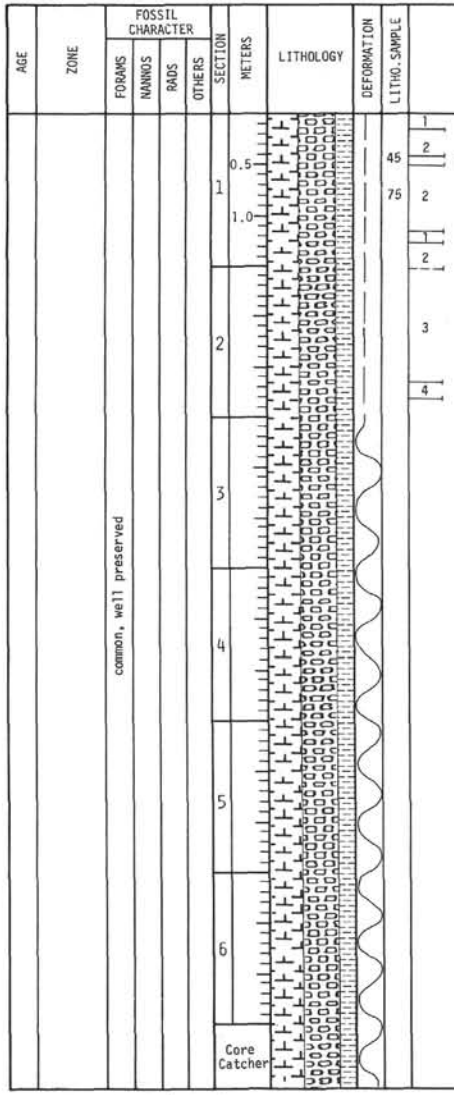

LITHOLOGIC DESCRIPTION

CLAY-RICH NANNO MICARB OOZE

Slight variations in nanno per cent and clay. Pteropods scattered throughout entire core. Numerous otoliths in coarse fraction.

Lithology SS: Section 1-45 cm.
Composition:

Micarb	45%
Nannos	40%
Clay	15%
Glass, rads, spicules	Trace

Lithology SS: Section 1-75 cm.
Composition:

Micarb	55%
Nannos	25%
Clay	20%

Sections 3 to 6, basic color is olive (5Y 5/3), with local pods of olive gray (5Y 4/2, 5/2), light olive gray (5Y 6/2) and gray (5Y 5/1).

Color legend:

1 = olive gray	5Y 4/2
2 = light olive gray	5Y 6/2
3 = olive gray	5Y 5/2
4 = gray	5Y 5/1

<u>Shore-based laboratory results</u>

	Organic Carbon	Carbonate
Section 1- 5 cm =	1.4%	42%
Section 1-100 cm =	.6%	61%
Section 2- 16 cm =	.5%	84%

Explanatory notes in chapter 2

Site 229 Hole Core 3 Cored Interval: 93-102 m

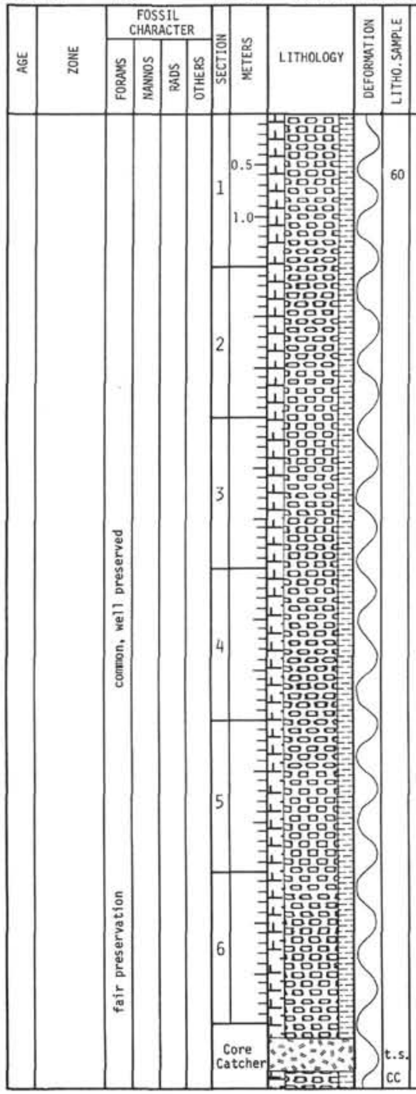

LITHOLOGIC DESCRIPTION

CLAY- AND NANNO-RICH MICARB OOZE

Dusky yellow green (5GY 5/2). 'Biscuit and Paste' deformation throughout, biscuits ~5 cm. Core separated into segments by gas expansion, gaps are 5-15 cm. Pteropods scattered throughout (~5%).

Lithology SS: Section 1-60 cm.
Composition:

Micarb	65%
Nannos	15%
Clay	15%
Pteropods	5%
Forams	Trace
Glass	Trace

Shore-based laboratory results

	Organic Carbon	Carbonate
Section 1-40 cm =	1.5%	61%

2 Pieces (5 cm, 10 cm) CALCITE-CEMENTED PALAGONITE TUFF

Explanatory notes in chapter 2

Site 229 Hole Core 4 Cored Interval: 102-108 m

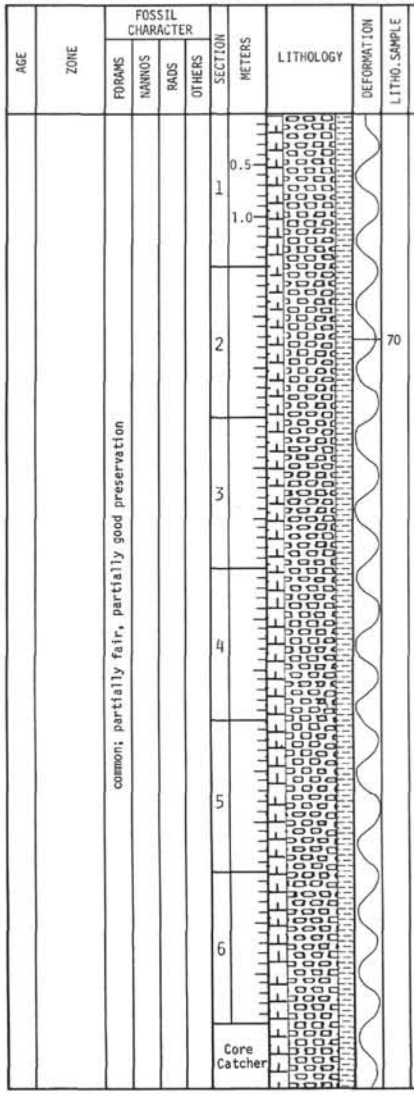

LITHOLOGIC DESCRIPTION

CLAY- AND NANNO-RICH MICARB OOZE

Dusky yellow green (5GY 5/2). Entirely churned by coring. Bubbles due to gas expansion.

Lithology SS: Section 2-70 cm.
Composition:

Micarb	65%
Nannos	15%
Clay	15%
Pteropods	5%
Forams, glass	Trace

Shore-based laboratory results

	Organic Carbon	Carbonate
Section 1-130 cm =	1.1%	56%

Explanatory notes in chapter 2

Site 229 Hole Core 5 Cored Interval: 108 m

AGE	ZONE	FOSSIL CHARACTER				SECTION	METERS	LITHOLOGY	DEFORMATION	LITHO. SAMPLE	LITHOLOGIC DESCRIPTION
		FORAMS	NANNOS	RADS	OTHERS						
						Core Catcher		Not to Scale 			(CC only) PALAGONITE TUFF, CARBONATE CEMENTED

Explanatory notes in chapter 2

Site 229 Hole A Core 1 Cored Interval: 19-28 m

AGE	ZONE	FOSSIL CHARACTER				SECTION	METERS	LITHOLOGY	DEFORMATION	LITHO. SAMPLE
		FORAMS	NANNOS	RADS	OTHERS					
		abundant, well preserved				1 2 3 4 5 6 Core Catcher	0.5 1.0	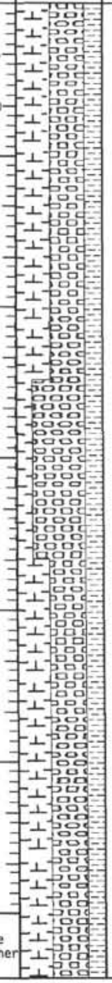		80 100 130

LITHOLOGIC DESCRIPTION

2 3 2 3 1 2 1 2 3 1 2 3 1 2 3 1 3 2 1

Gray CLAY- AND NANNO-RICH MICARB OOZE

Olive colors due to finely dispersed iron, not clay. Pteropods scattered throughout, locally abundant in coarse graded(?) layers. Numerous otoliths in coarse fraction. Strong H_2S odor.

Light olive MICARB-NANNO OOZE

Graded? (More Pteropods)

Lithology SS: Sections 1-80 cm, 2-100 cm.

Composition:

Nannos	50%
Micarb	40%
Clay	10%

Lithology SS: Section 3-130 cm.

Composition:

Carbonate	60%
Nannos	20%
Clay	20%
Glass	Trace

Color legend:

1 = light olive gray 5Y 6/1
2 = light olive 10Y 5/4
3 = olive 5Y 4/3

Colors locally interbedded on 1-3 cm scale, not shown.

<u>Shore-based laboratory results</u>

	Organic Carbon	Carbonate
Section 1-130 cm =	1.6%	68%

X-ray mineralogy:	Section 3-30 cm
Calcite	26%
Dolomite	2%
Aragonite	13%
Mg-Calcite	14%
Quartz	14%
K-feldspar	3%
Plagioclase	14%
Mica	6%
Chlorite	1%
Palygorskite	5%
Pyrite	1%
Amphibole	2%

Explanatory notes in chapter 2

Site 229 Hole A Core 2 Cored Interval: 28-37 m

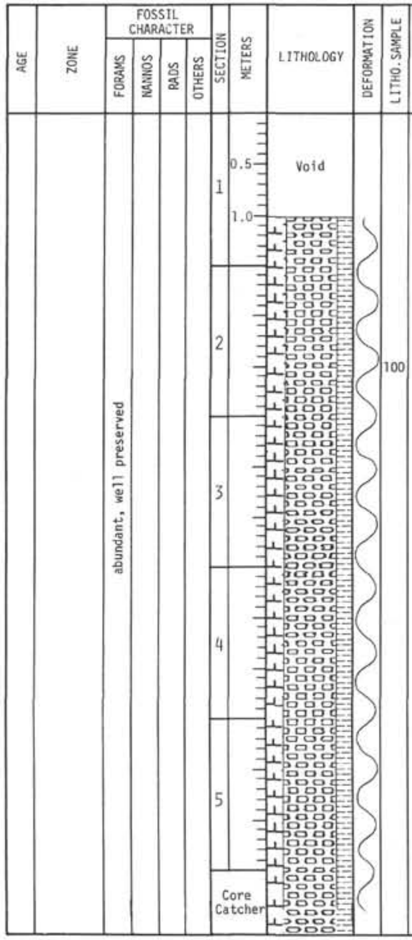

LITHOLOGIC DESCRIPTION

CLAY- AND NANNO-RICH MICARB OOZE

Light olive (10Y 5/4). Numerous otoliths in coarse fraction. Strong H_2S odor, gas expansion cracks.

Lithology SS: Section 2-100 cm.
Composition:

Coarser, more pteropods	Micarb	50%
	Clay	25%
	Nannos	20%
	Pteropods	5%
	Volcanic glass	<2%

Large (2 cm) high-spired gastropod and several small echinoids, Sec. 3.

Local 1-2 cm bands of gray, (5Y 6/1), same lithology.

Shore-based laboratory results

	Organic Carbon	Carbonate
Section 2-120 cm =	1.3%	70%

Explanatory notes in chapter 2

Site 229 Hole A Core 3 Cored Interval: 37-46 m

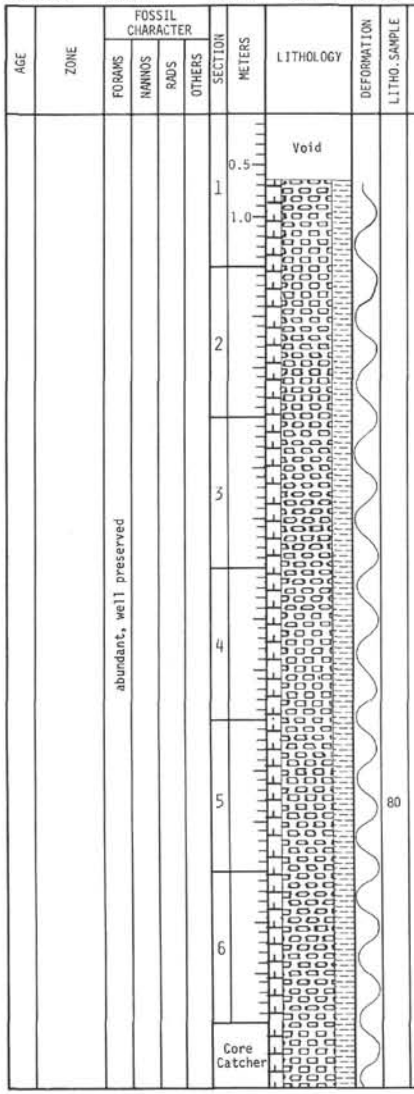

LITHOLOGIC DESCRIPTION

CLAY- AND NANNO-RICH MICARB OOZE

Light olive (10Y 5/4). Strong H_2S odor, gas expansion cracks. Numerous otoliths in coarse fraction. Rare pelecypod fragments.

Lithology SS: Section 5-80 cm.
Composition:

Micarb	55%
Clay and silt	20%
Nannos	20%
Pteropods	5%
Volcanic glass	<2%

Shore-based laboratory results

	Organic Carbon	Carbonate
Section 2-35 cm =	1.4%	64%

Explanatory notes in chapter 2

Site 229 Hole A Core 4 Cored Interval: 56-65 m

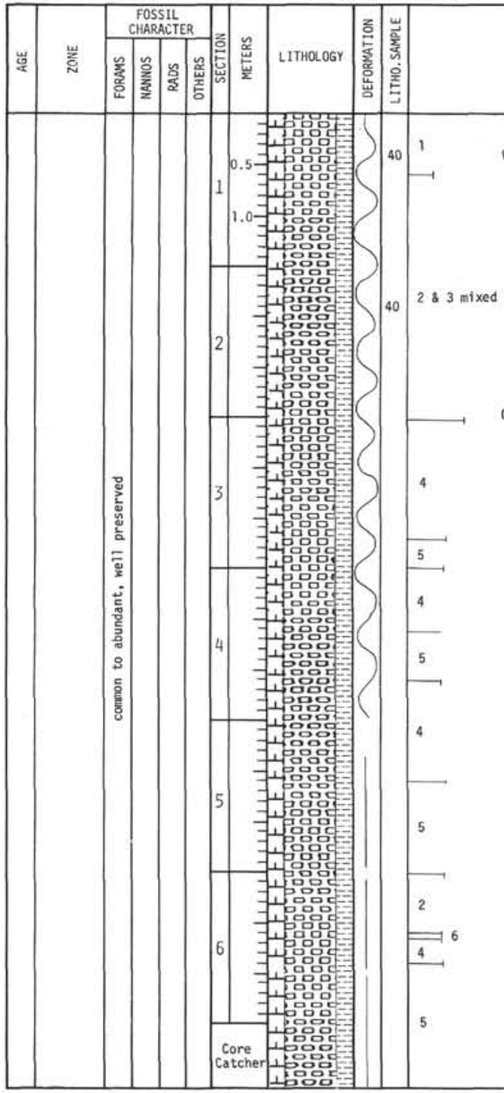

LITHOLOGIC DESCRIPTION

CLAY- AND NANNO-RICH MICARB OOZE

Numerous otoliths in coarse fraction.

Lithology SS: Section 1-40 cm.
Composition:

Micarb	65%
Nannos	20%
Clay	15%

Lithology SS: Section 2-40 cm.
Composition:

Micarb	50%
Nannos	30%
Clay	15%
Pteropods	5%
Glass	Trace

Color legend:

1 =	light olive gray	5Y 6/1
2 =	gray olive	10Y 4/2
3 =	light olive	10Y 5/4
4 =	greenish gray	5G 6/1
5 =	dusky yellowish green	5GY 5/2
6 =	dark greenish gray	5G 4/1

Shore-based laboratory results

	Organic Carbon	Carbonate
Section 1-70 cm =	.7%	51%

Explanatory notes in chapter 2

Site 229 Hole A Core 5 Cored Interval: 55-74 m

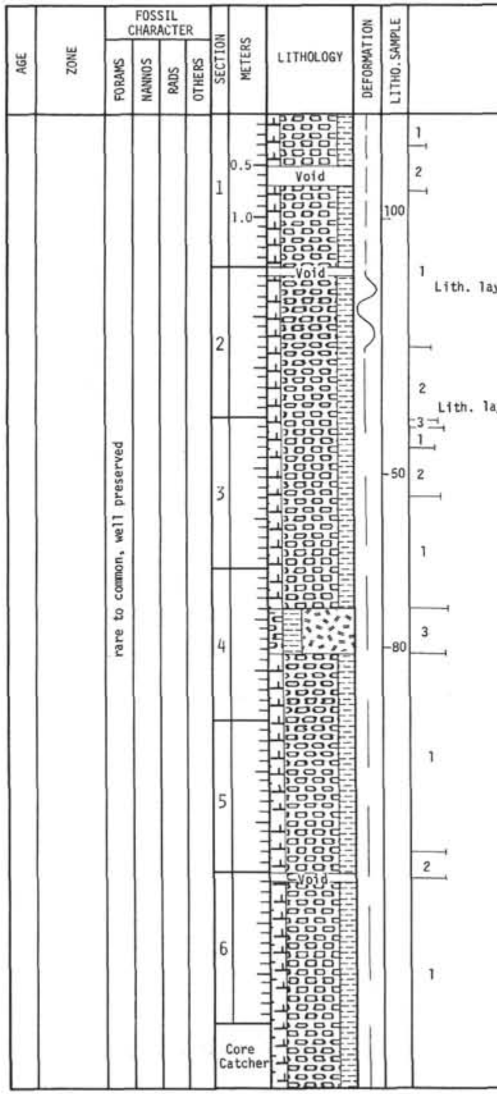

LITHOLOGIC DESCRIPTION

CLAY- AND NANNO-RICH MICARB OOZE

Lithology SS: Section 1-100 cm.
Composition:

Micarb	50%
Clay	20%
Nannos	20%
Glass	10%
Pteropods	~2%

Lithology SS: Section 3-50 cm.
Composition:

Micarb	60%
Clay	15%
Nannos	15%
Glass	10%

Color legend:

1 =	dusky yellowish green	5GY 5/2
2 =	greenish gray	5G 6/1
3 =	dark greenish gray	5GY 4/1

CLAY- AND CARBONATE-RICH VOLCANIC ASH

Shore-based laboratory results

	Organic Carbon	Carbonate
Section 2-30 cm =	.6%	47%

X-ray mineralogy:	Section 4-60 cm
Calcite	34%
Dolomite	3%
Aragonite	5%
Quartz	16%
K-feldspar	5%
Plagioclase	14%
Mica	7%
Chlorite	2%
Palygorskite	9%
Pyrite	4%

Explanatory notes in chapter 2

Site 229 Hole A Core 6 Cored Interval: 74-83 m

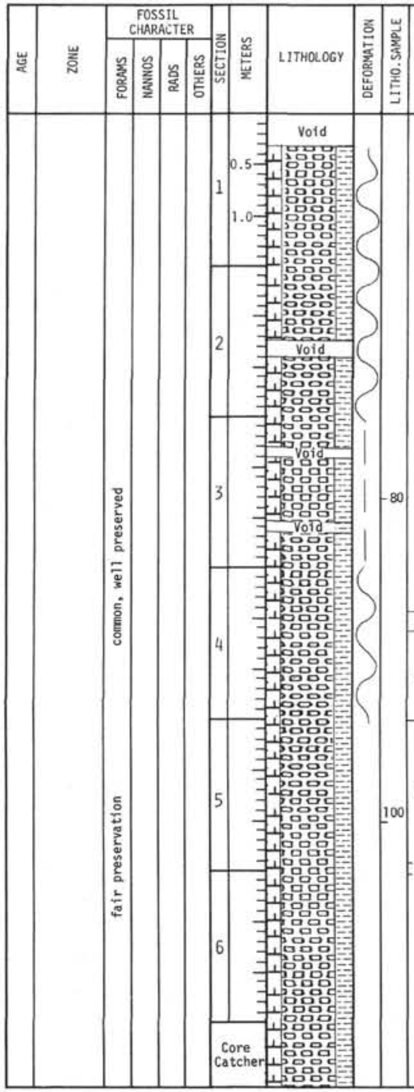

Lith. Yellow green SILTY CLAY-NANNO-RICH MICARB OOZE

Dusky yellow green (5GY 5/2) except as otherwise noted.

Lithology SS: Section 5-100 cm.
Composition:

Micarb	50%
Detrital	20%
Nannos	15%
Rads	5%
Glass	5%
Pteropods	5%
Forams	Trace

Color legend:

1 =	dusky yellow green	5GY 5/2
2 =	greenish gray	5G 4/1
3 =	greenish gray	5G 6/1
4 =	pale olive	10Y 6/2

1 mottled with 2

3

4

3

Shore-based laboratory results

	Organic Carbon	Carbonate
Section 1-105 cm =	.5%	36%

Grain size: Sections

	5-85 cm,	5-114 cm,	5-120 cm
Sand	28%	39%	28%
Silt	42%	41%	44%
Clay	30%	20%	28%

Explanatory notes in chapter 2

Site 229 Hole A Core 7 Cored Interval: 83-92 m

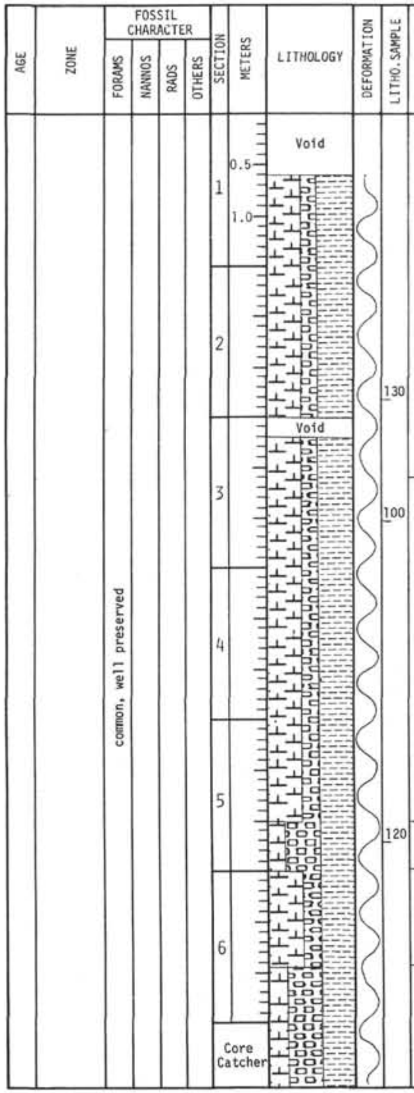

MICARB-RICH CLAY NANNO OOZE

Lithology SS: Section 2-130 cm.
Composition:

Nannos	40%
Micarb	20%
Detrital	20%
Glass	5%
Rads	Trace

Lithology SS: Section 3-100 cm.
Composition:

Nannos	40%
Micarb	30%
Detrital	25%
Glass	5%

Lithology SS: Section 5-120 cm
Composition:

Micarb	55%
Nannos	20%
Detrital	20%
Glass	5%

Color legend:

1 =	dusky yellow green	5GY 5/2
2 =	gray olive	10Y 4/2
3 =	greenish gray	5GY 6/1

1

2

3

2

3

Shore-based laboratory results

	Organic Carbon	Carbonate
Section 1-41 cm =	1.2%	61%

Explanatory notes in chapter 2

Site 229 Hole A Core 8 Cored Interval: 113-122 m

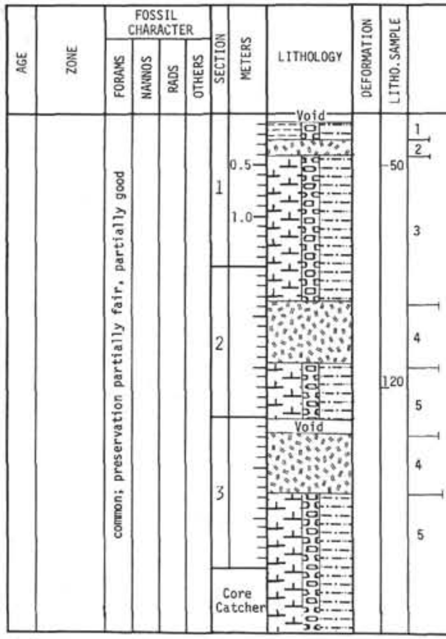

LITHOLOGIC DESCRIPTION

MICARB-RICH SILTY CLAY-NANNO OOZE AND CHALK and PALAGONITE TUFF.

Carbonate cemented.

chalk with zeolite and glass, slump folded

Lithology SS: Average.

Composition:

Nannos	40-50%
Micarb	20-30%
Detrital	20-30%
Zeolite	5-10%
Glass	Trace- 5%

Color legend:

1 = greenish gray 5GY 6/1
2 = dark greensih gray 5GY 4/1
3 = dark greenish gray 5G 4/1
4 = gray black N2
5 = gray olive 10Y 4/2

Shore-based laboratory results

	Organic Carbon	Carbonate
Section 1-64 cm =	.8%	45%

Explanatory notes in chapter 2

Site 229 Hole A Core 9 Cored Interval: 122-131 m

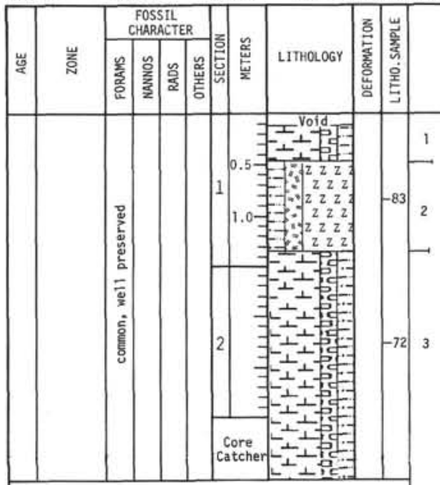

LITHOLOGIC DESCRIPTION

SILTY CLAY- AND GLASS-RICH ZEOLITE SEDIMENT

Medium bluish gray (5B 5/1). Voids due to gas expansion.

Lithology SS: Section 1-83 cm.

Composition:

Zeolite	~60%
Glass	20%
Silty clay	15%
Forams	5-10%
Nannos	<2%

SILTY CLAY- AND MICARB-RICH NANNO OOZE

Lithology SS: Section 2-72 cm.

Composition:

Nannos	60%
Micarb	20%
Silt and clay	15%
Glass	~5%

Color legend:

1 = dusky yellow green 5GY 5/2
2 = medium bluish gray 5B 5/1
3 = light olive 10Y 5/4

Shore-based laboratory results

	Organic Carbon	Carbonate
Section 2-15 cm =	1.2%	70%

Explanatory notes in chapter 2

Site 229 Hole A Core 10 Cored Interval: 131-140 m

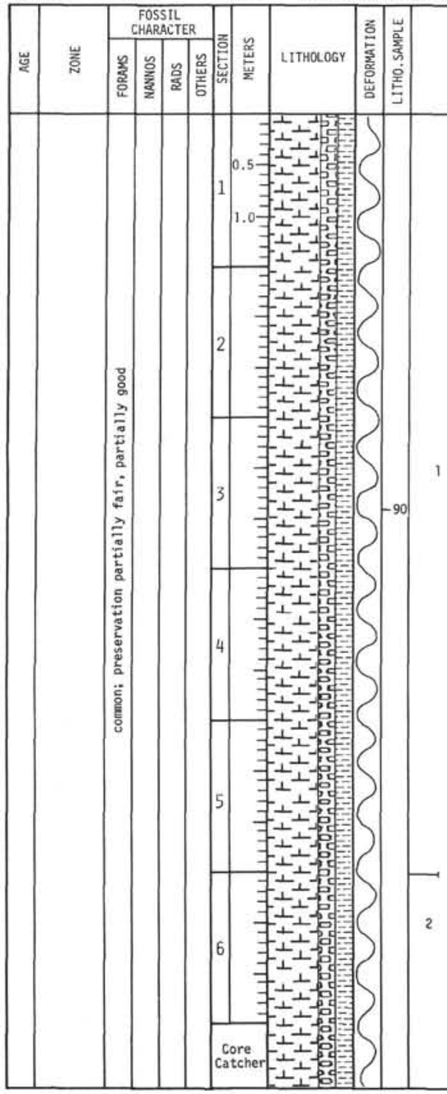

LITHOLOGIC DESCRIPTION

Pale olive MICARB RICH NANNO OOZE

Very disturbed bv drilling and by explanding gas.

Lithology SS: Section 3-90 cm.
Composition:

Nannos	60%
Micarb	20%
Clay	10%
Zeolite	5%
Forams	5%

Color legend:

1 = pale olive 10Y 6/2
2 = dusky yellow green 5GY 5/2

1

2

Sulfide rich layers at 105 cm.

Shore-based laboratory results

	Organic Carbon	Carbonate
Section 1-90 cm =	1.2%	67%

Explanatory notes in chapter 2

Site 229 Hole A Core 12 Cored Interval: 149-158 m

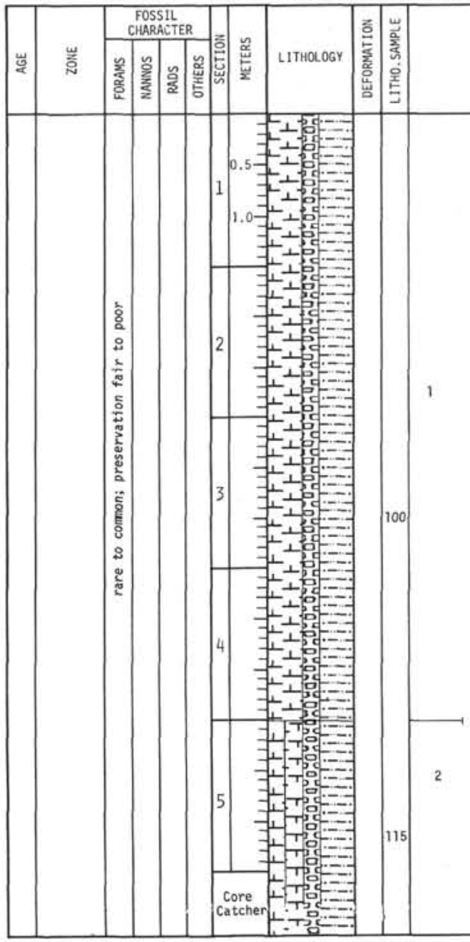

LITHOLOGIC DESCRIPTION

Olive SILTY CLAY-MICARB-RICH NANNO OOZE AND CHALK

Homogeneous and stiff, with semilithified layers.

Lithology SS: Section 3-100 cm.
Composition:

Nannos	40%
Detrital	40%
Micarb	15%
Forams	5%
Zeolite	<2%

Lithology SS: Section 5-115 cm.
Composition:

Detrital	40%
Nannos	20%
Micarb	20%
Forams	15%
Zeolite	5%
Glass	1- 2%

Color legend:

1 = pale olive 10Y 6/2
2 = dark greenish gray 5GY 4/1

1

2

FORAM NANNO MICARB RICH DETRITAL CLAYEY SILT

Shore-based laboratory results

	Organic Carbon	Carbonate
Section 1-12 cm =	1.0%	53%

Explanatory notes in chapter 2

Site 229 Hole A Core 13 Cored Interval: 158-167 m

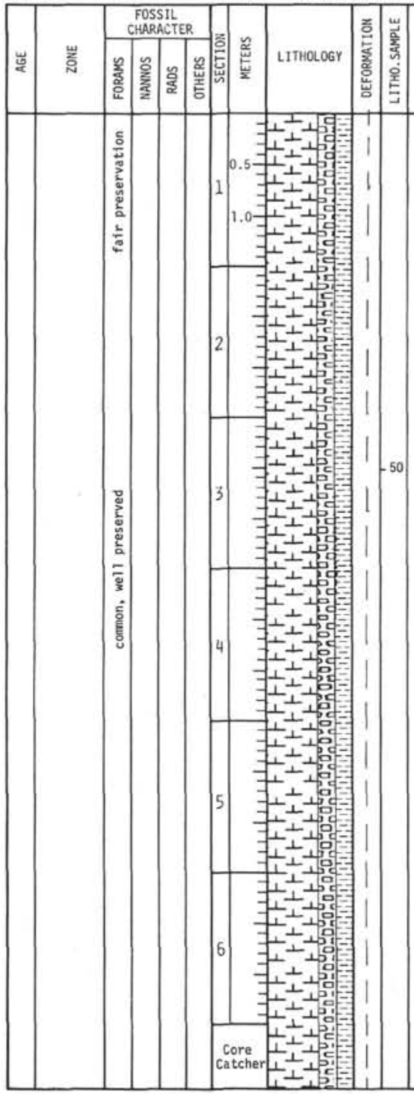

LITHOLOGIC DESCRIPTION

CLAY-MICARB-RICH NANNO OOZE AND CHALK

Dusky yellow green (5GY 5/2). Homogeneous and stiff, with local semilithified layers. Pteropods and otoliths rare.

Lithology SS: Section 3-50 cm.
Composition:

Nannos	60%
Micarb	15%
Silt and clay	15%
Zeolite	5%
Glass	5%

Shore-based laboratory results

	Organic Carbon	Carbonate
Section 1-110 cm =	.8%	73%

Explanatory notes in chapter 2

Site 229 Hole A Core 14 Cored Interval: 167-176 m

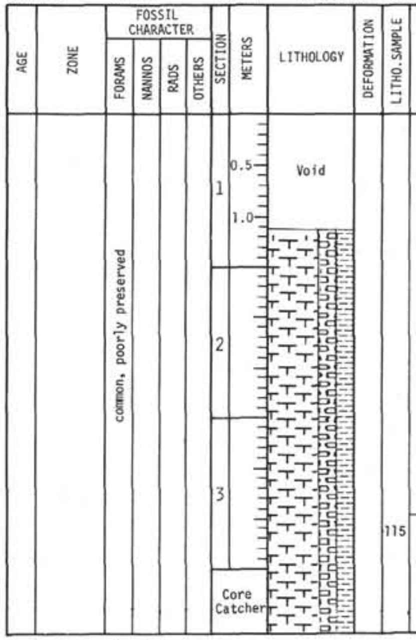

LITHOLOGIC DESCRIPTION

SILTY CLAY-MICARB-RICH NANNO OOZE

Zeolite no longer present.

Lithology SS: Section 3-115 cm.
Composition:

Nannos	60%
Micarb	20%
Detrital	20%

1

Color legend:
1 = dusky yellow green 5GY 5/2
2 = pale blue green 5BG 7/2

Lithified to Chalk

2

Explanatory notes in chapter 2

Site 229 Hole A Core 15 Cored Interval: 176-185 m

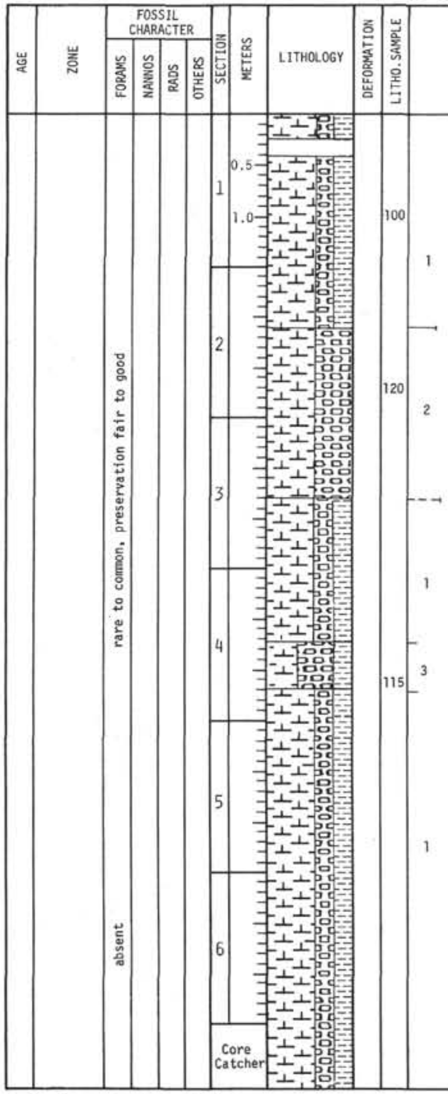

LITHOLOGIC DESCRIPTION

Two slightly differing lithologies, by color:

Yellow green SILTY CLAY-MICARB RICH NANNO CHALK

Lithology SS: Section 1-100 cm.
Composition:

Nannos	60%
Micarb	25%
Detrital	15%
Forams and rads	Trace

Pale olive MICARB NANNO CHALK

Lithology SS: Section 2-120 cm.
Composition:

Nannos	50%
Micarb	40%
Detrital	10%

Lithology SS: Section 4-115 cm.
Composition:

Nannos	40%
Micarb	30%
Detrital	25%
Forams	5%

Color legend:
1 = dusky yellow green 5GY 5/2
2 = pale olive 10Y 6/2
3 = dark greenish gray 5G 4/1

Shore-based laboratory results

	Organic Carbon	Carbonate
Section 2-90 cm =	.5%	77%

Explanatory notes in chapter 2

Site 229 Hole A Core 16 Cored Interval: 185-194 m

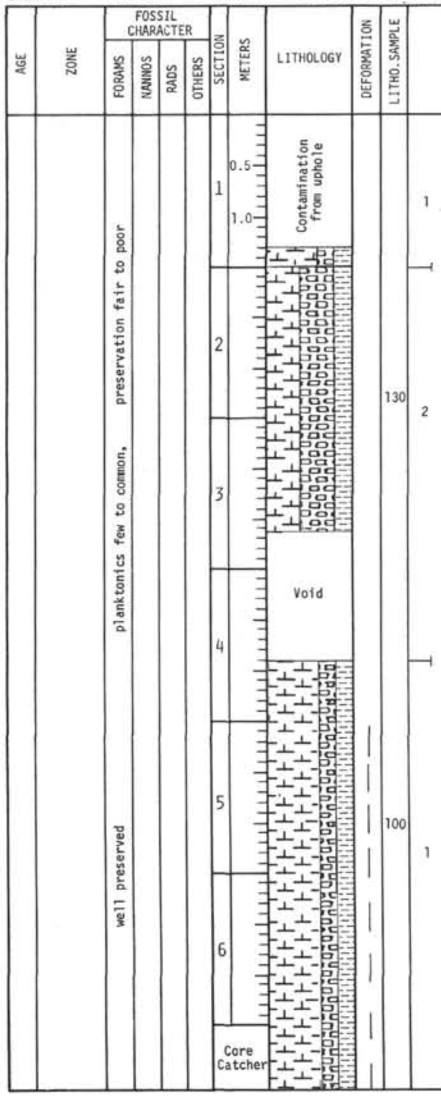

LITHOLOGIC DESCRIPTION

Two slightly differing lithologies, by color:

Yellowish green SILTY CLAY-MICARB RICH NANNO CHALK

Lithology SS: Section 5-100 cm.
Composition:

Nannos	45%
Detrital	20%
Micarb	15%
Pteropods	10%
Fish debris	5%
Forams	5%

Light olive SILTY CLAY-RICH MICARB NANNO CHALK

Lightology SS: Section 2-130 cm.
Composition:

Nannos	50%
Micarb	30%
Detrital	20%

Color legend:
1 = dusky yellowish green 5GY 5/2
2 = light olive 10Y 5/4

Shore-based laboratory results

	Organic Carbon	Carbonate
Section 2-75 cm =	1.2%	61%

Explanatory notes in chapter 2

Site 229 Hole A Core 17 Cored Interval: 194-203 m

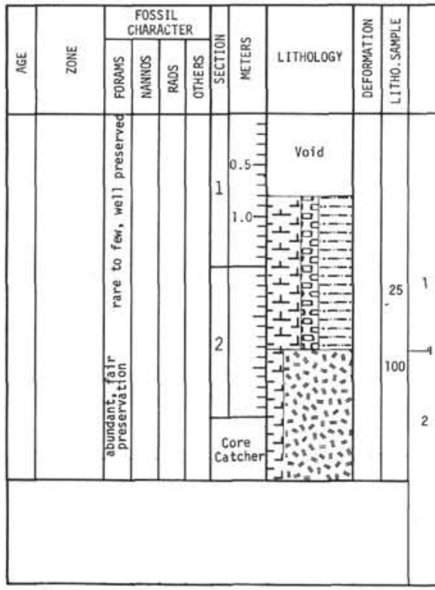

LITHOLOGIC DESCRIPTION

Greenish SILTY CLAY MICARB NANNO CHALK

VOLCANIC GLASS AND PALAGONITE TUFF

Color legend:

1 =	dusky yellow green	5GY 5/2
2 =	greenish black	5G 2/1

Shore-based laboratory results

	Organic Carbon	Carbonate
Section 1-142 cm =	1.2%	50%

Explanatory notes in chapter 2

Site 229 Hole A Core 18 Cored Interval: 203-212 m

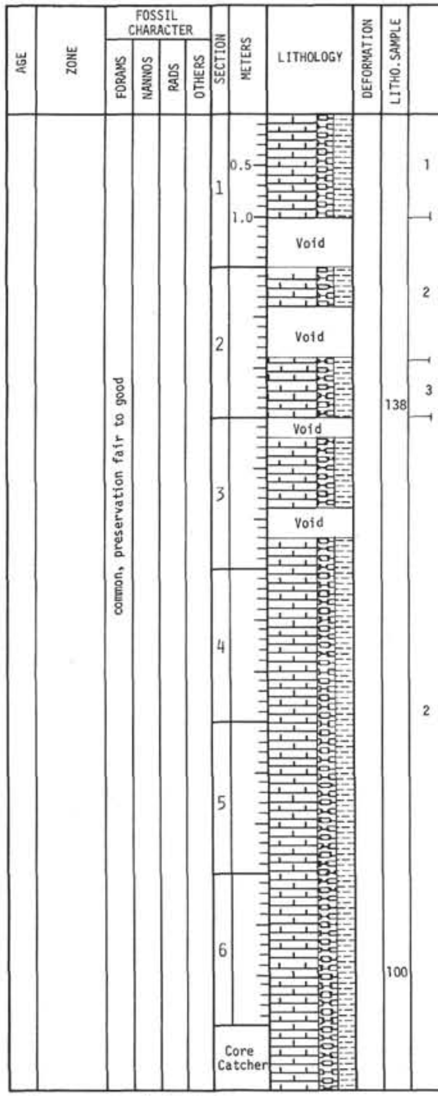

LITHOLOGIC DESCRIPTION

SILTY CLAY-MICARB-RICH NANNO CHALK

Pale olive (10Y 6/2) except where noted.

Lithology SS: Section 6-100 cm.

Composition:

Nannos	50%
Micarb	25%
Detrital	20%
Pteropods	~5%
Otoliths	~2%

Color legend:

1 =	dusky yellow green with gray	5GY 5/2 N3
2 =	pale olive	10Y 6/2
3 =	greenish gray	5GY 6/1

Shore-based laboratory results

	Organic Carbon	Carbonate
Section 1-67 cm =	.6%	58%

Explanatory notes in chapter 2

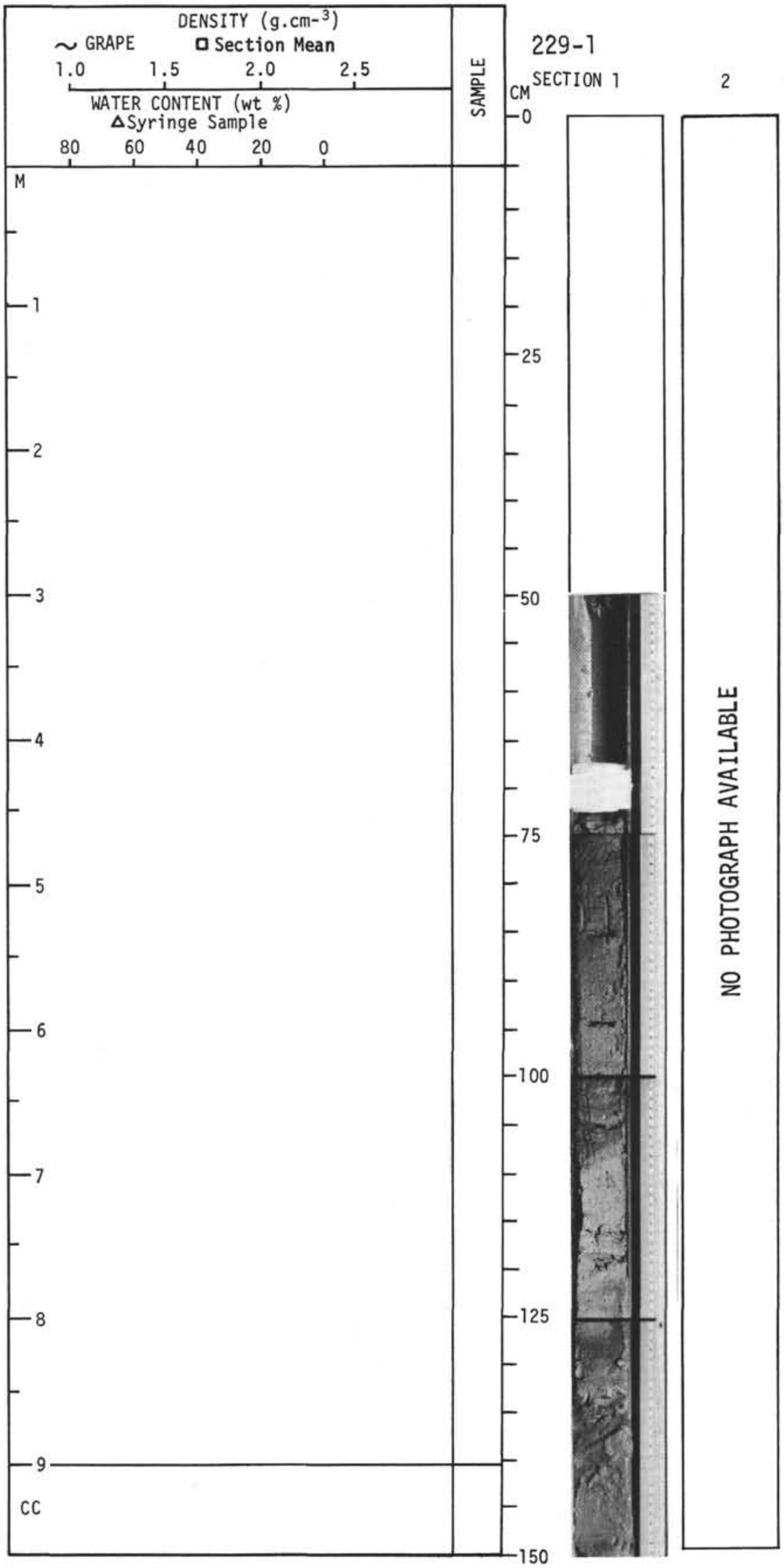

For Explanatory Notes, see Chapter 2

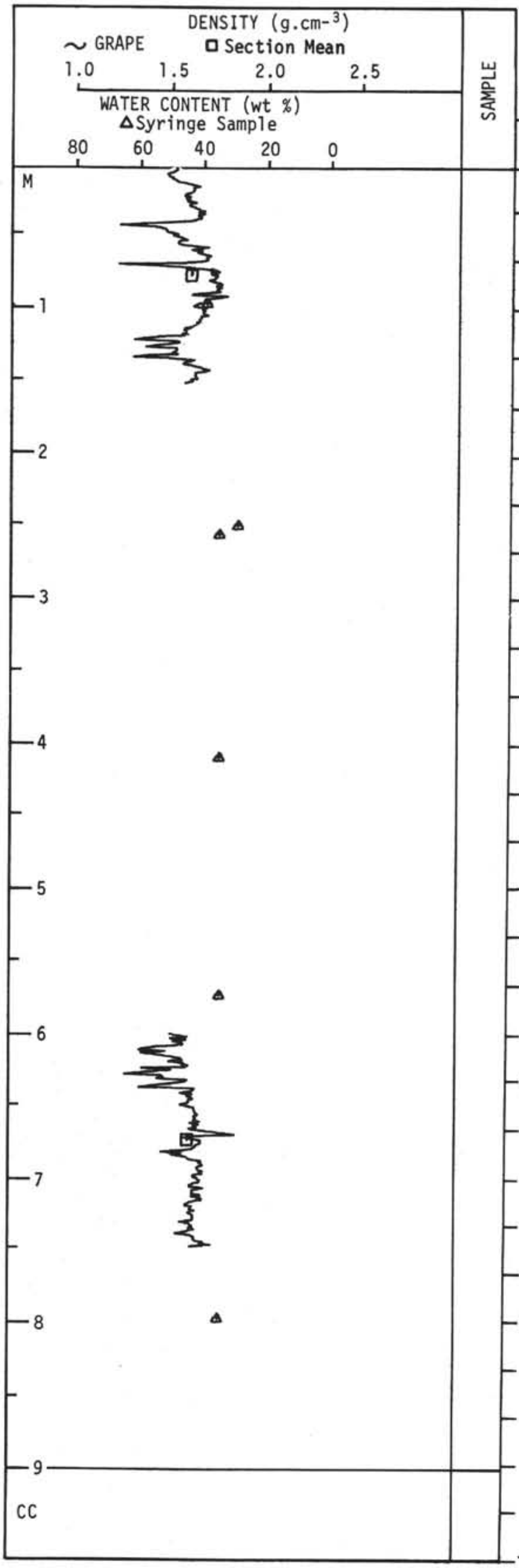

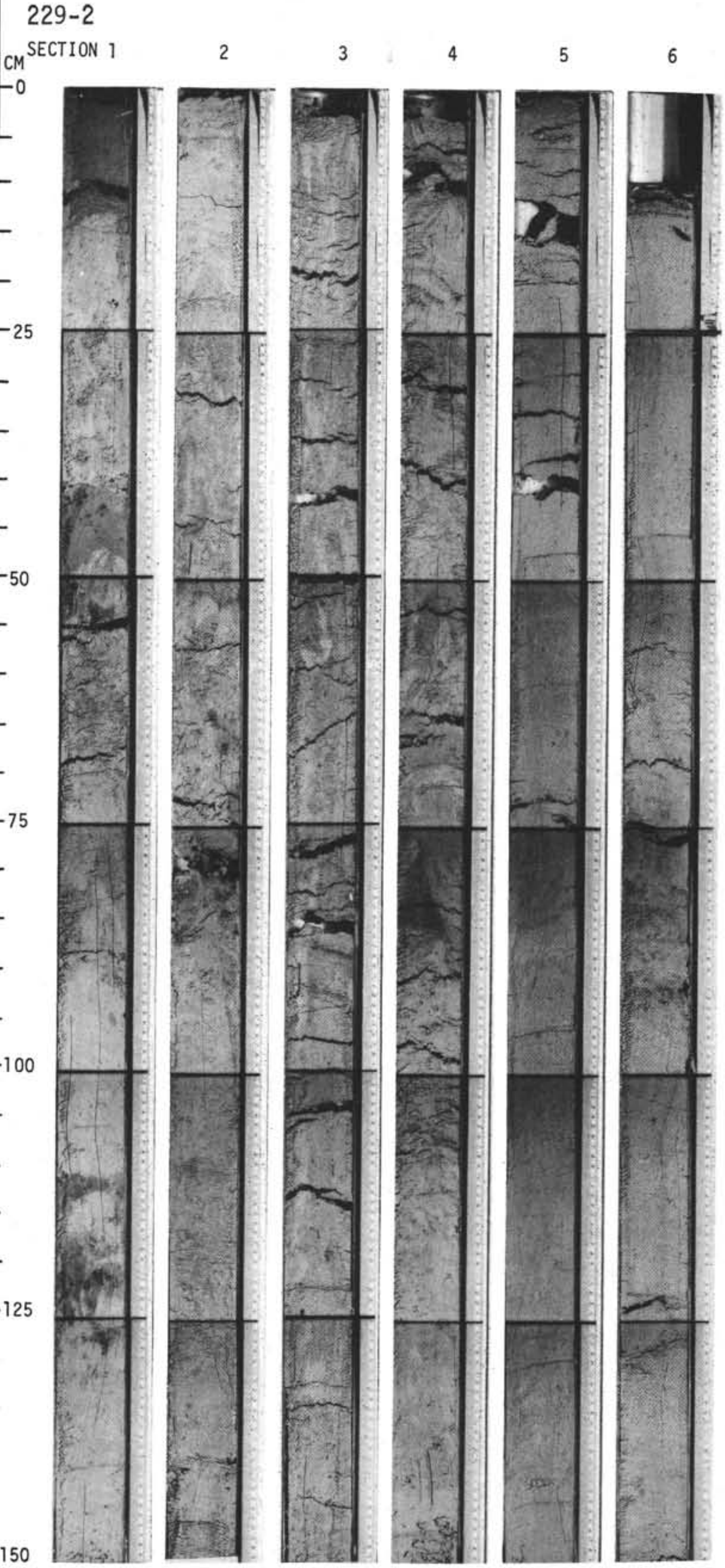

For Explanatory Notes, see Chapter 2

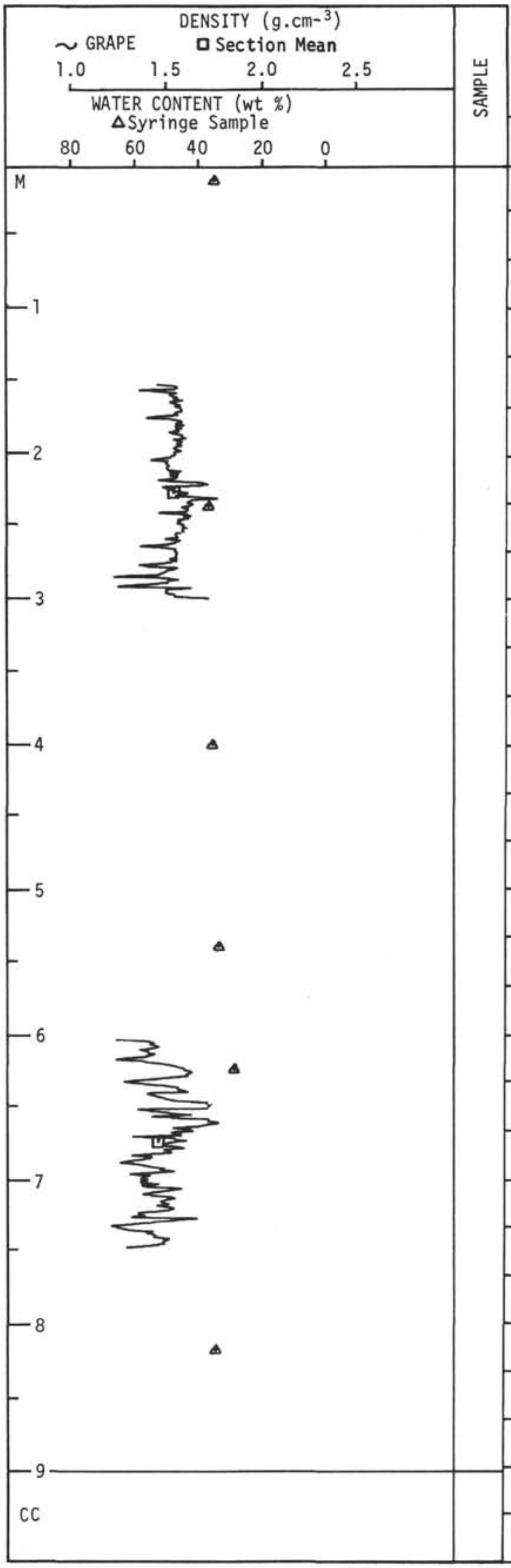

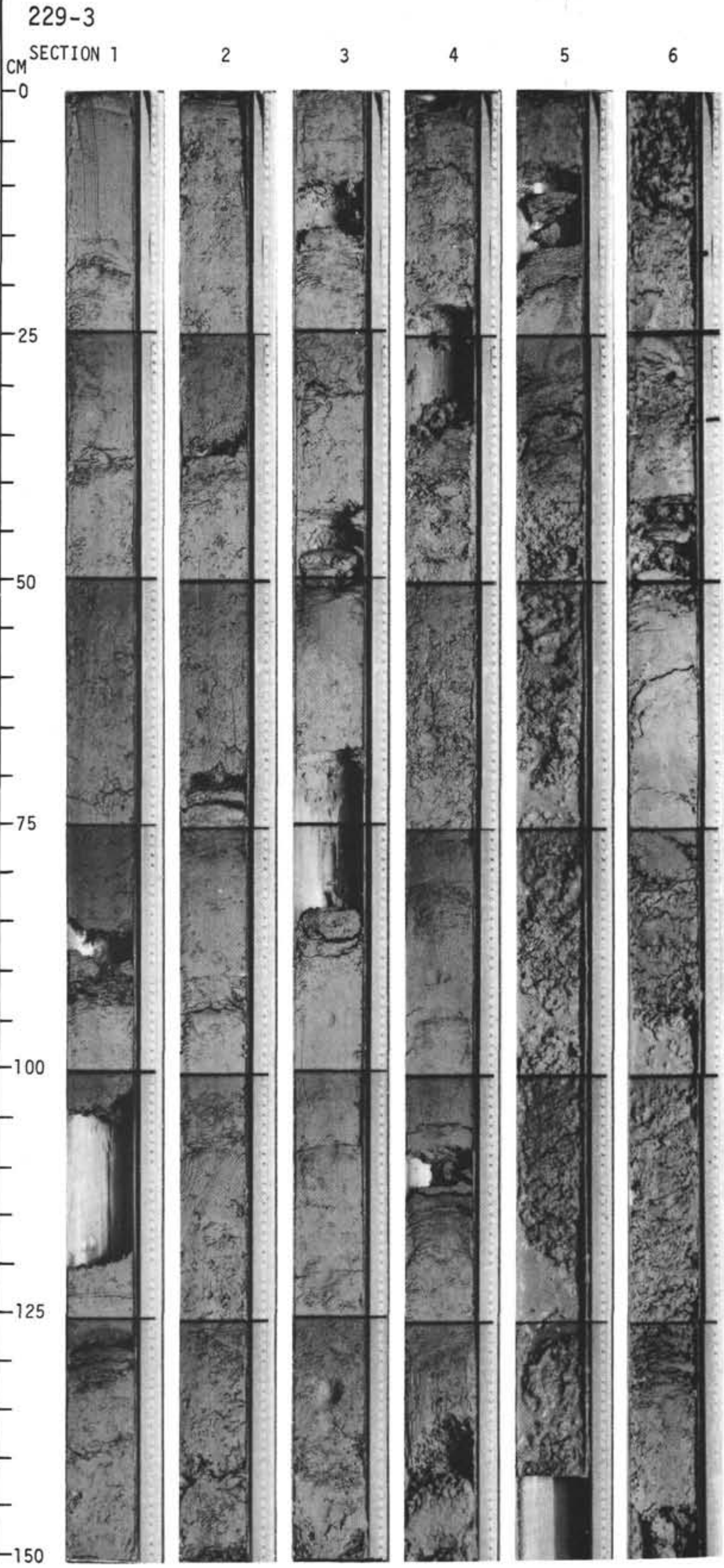

For Explanatory Notes, see Chapter 2

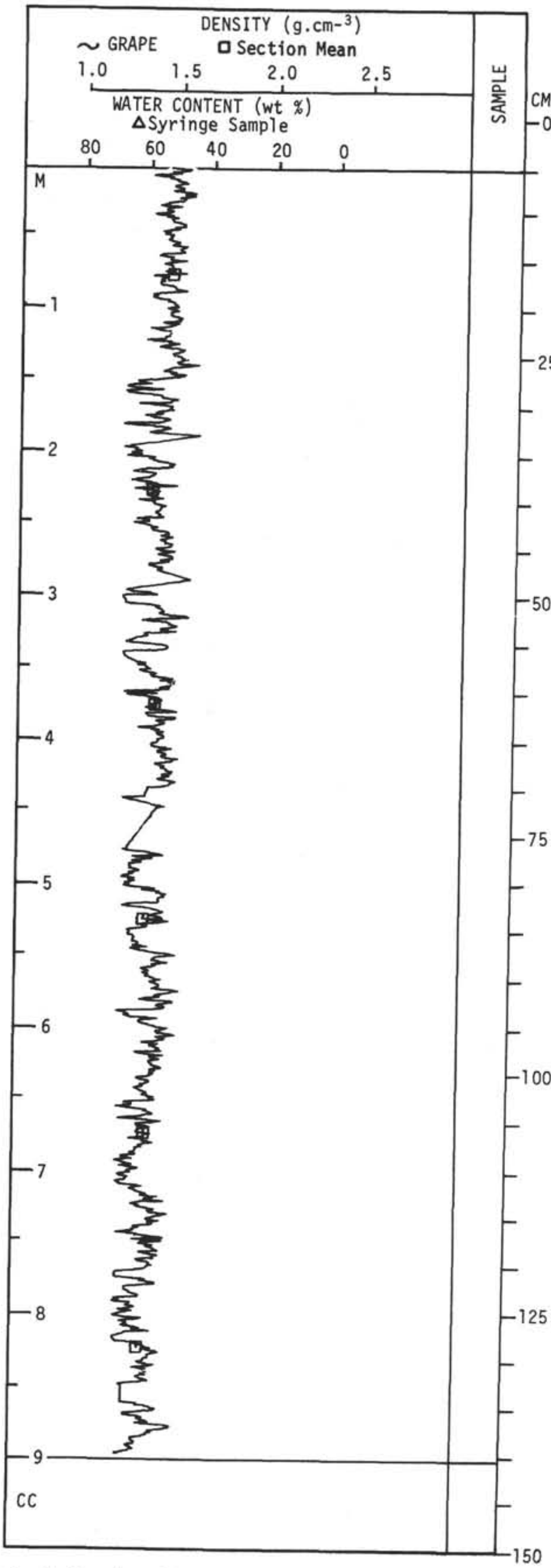

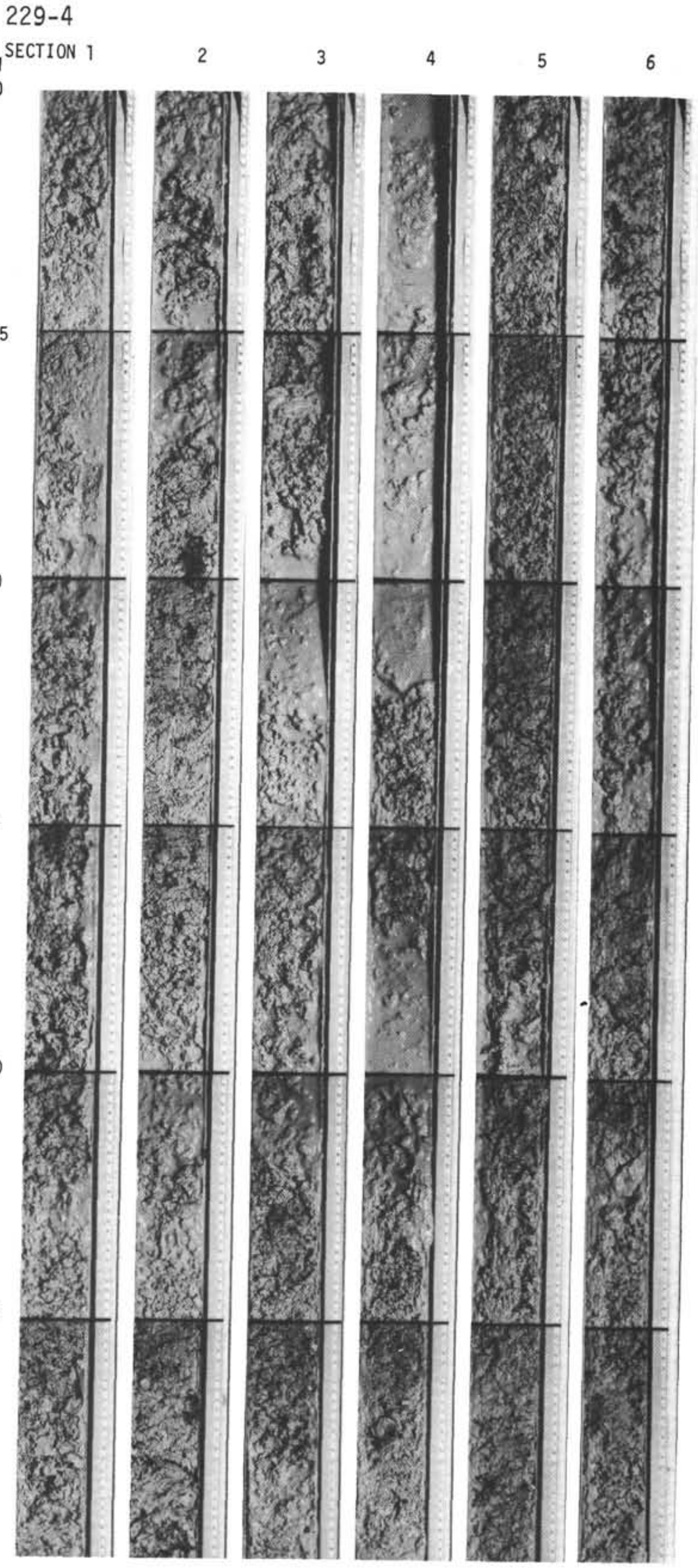

For Explanatory Notes, see Chapter 2

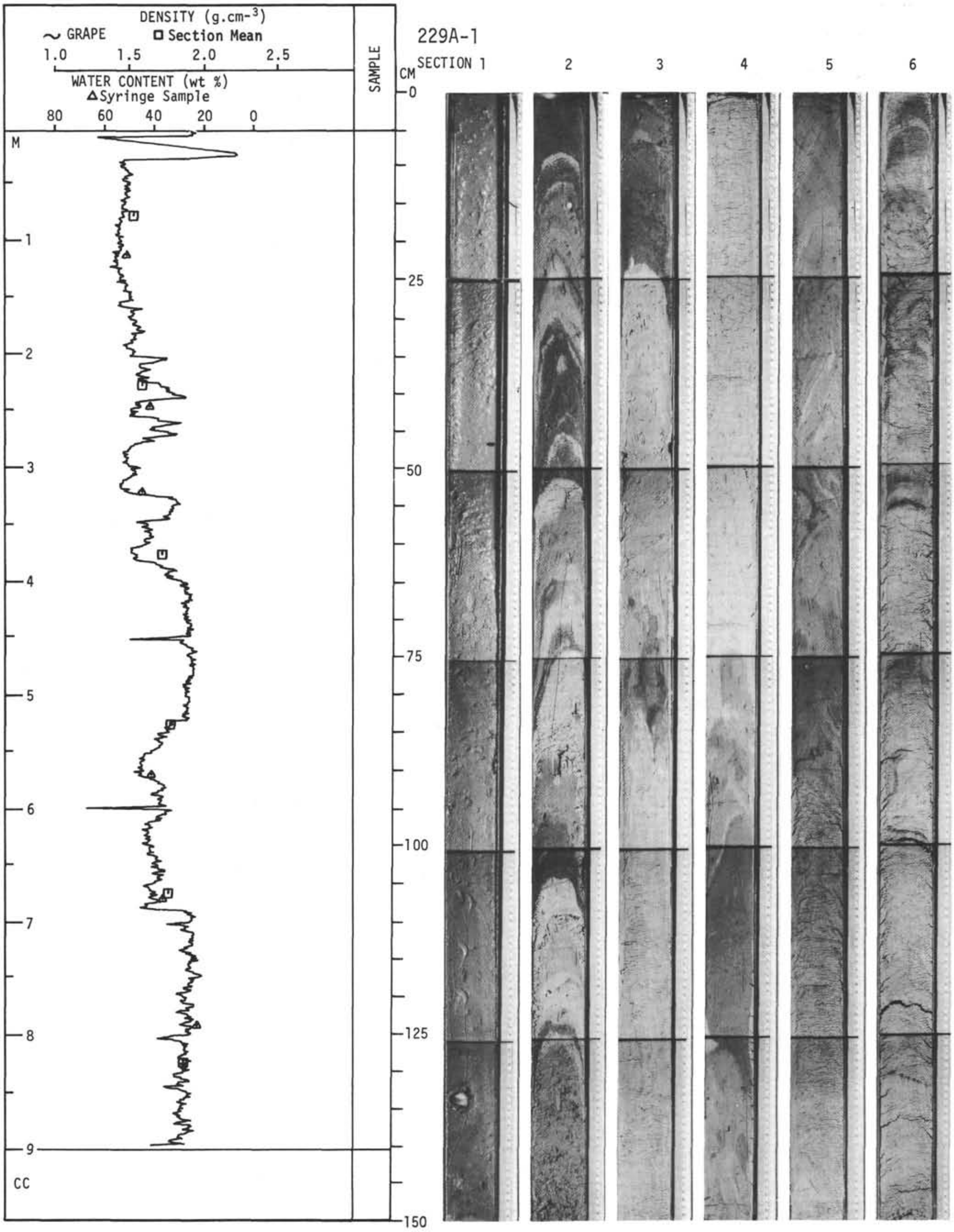

For Explanatory Notes, see Chapter 2

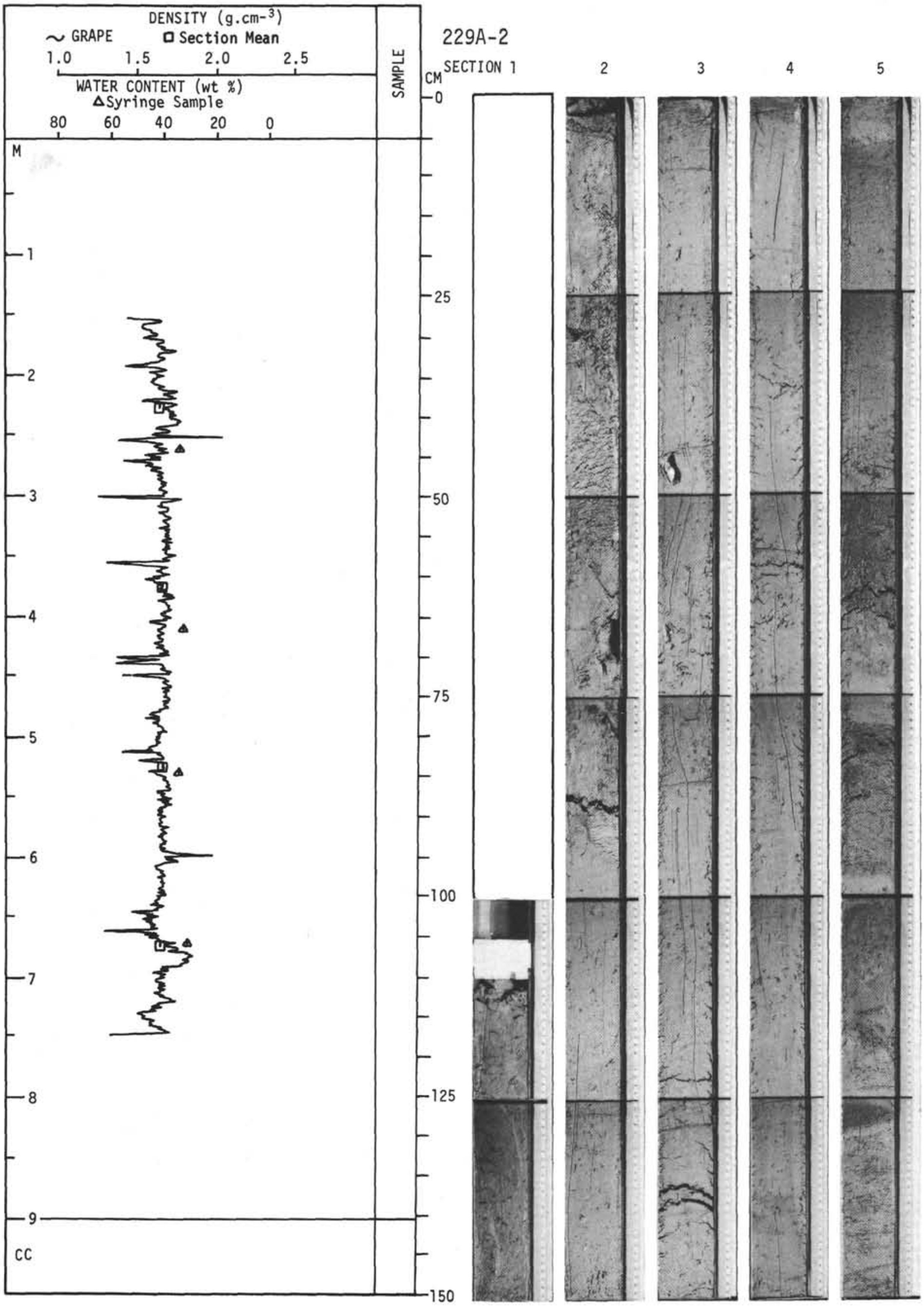

For Explanatory Notes, see Chapter 2

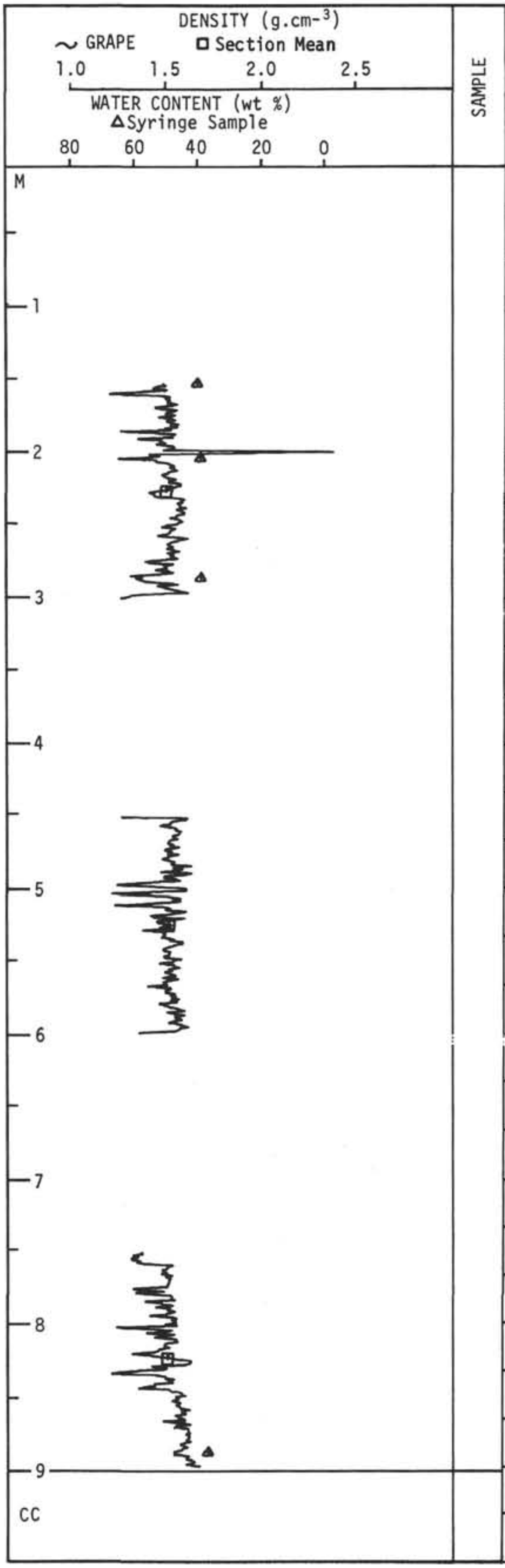

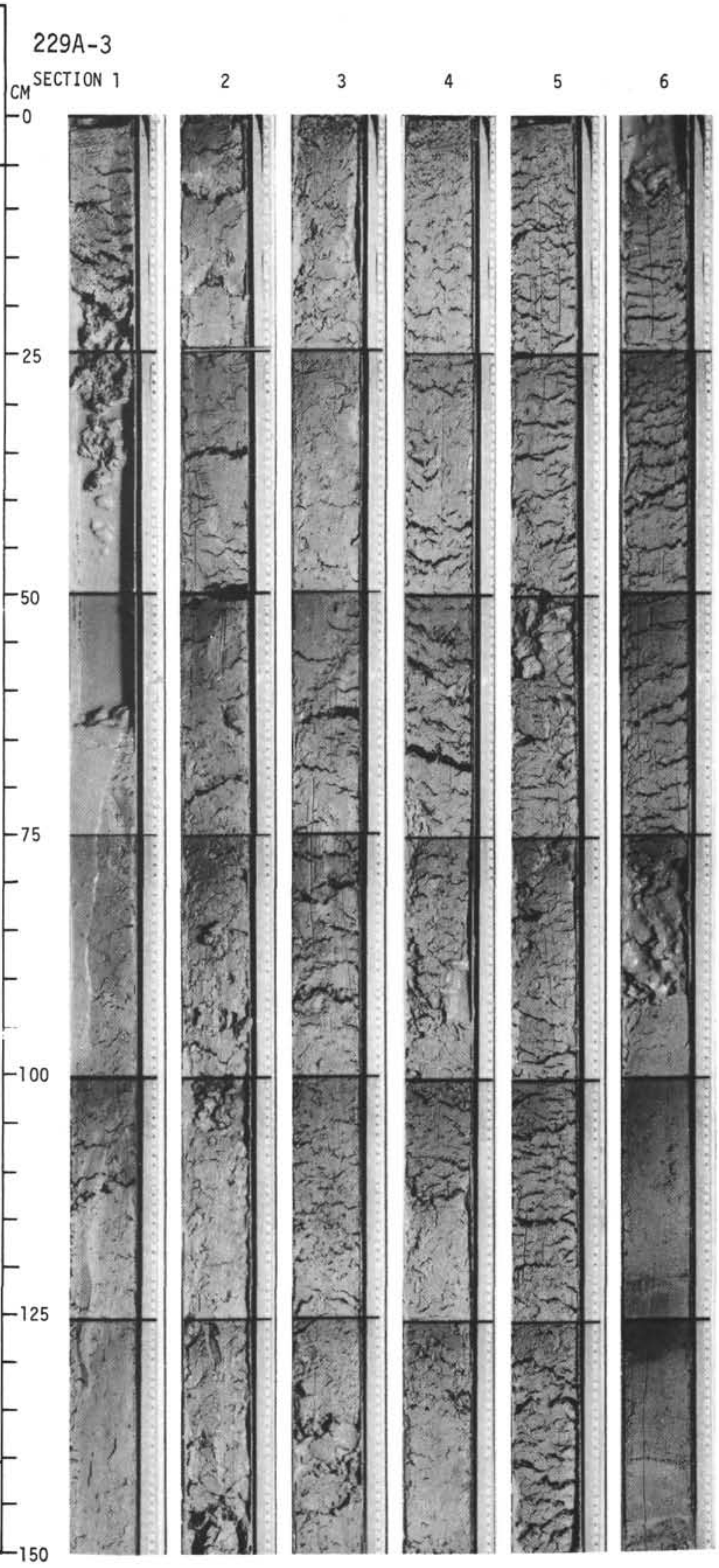

For Explanatory Notes, see Chapter 2

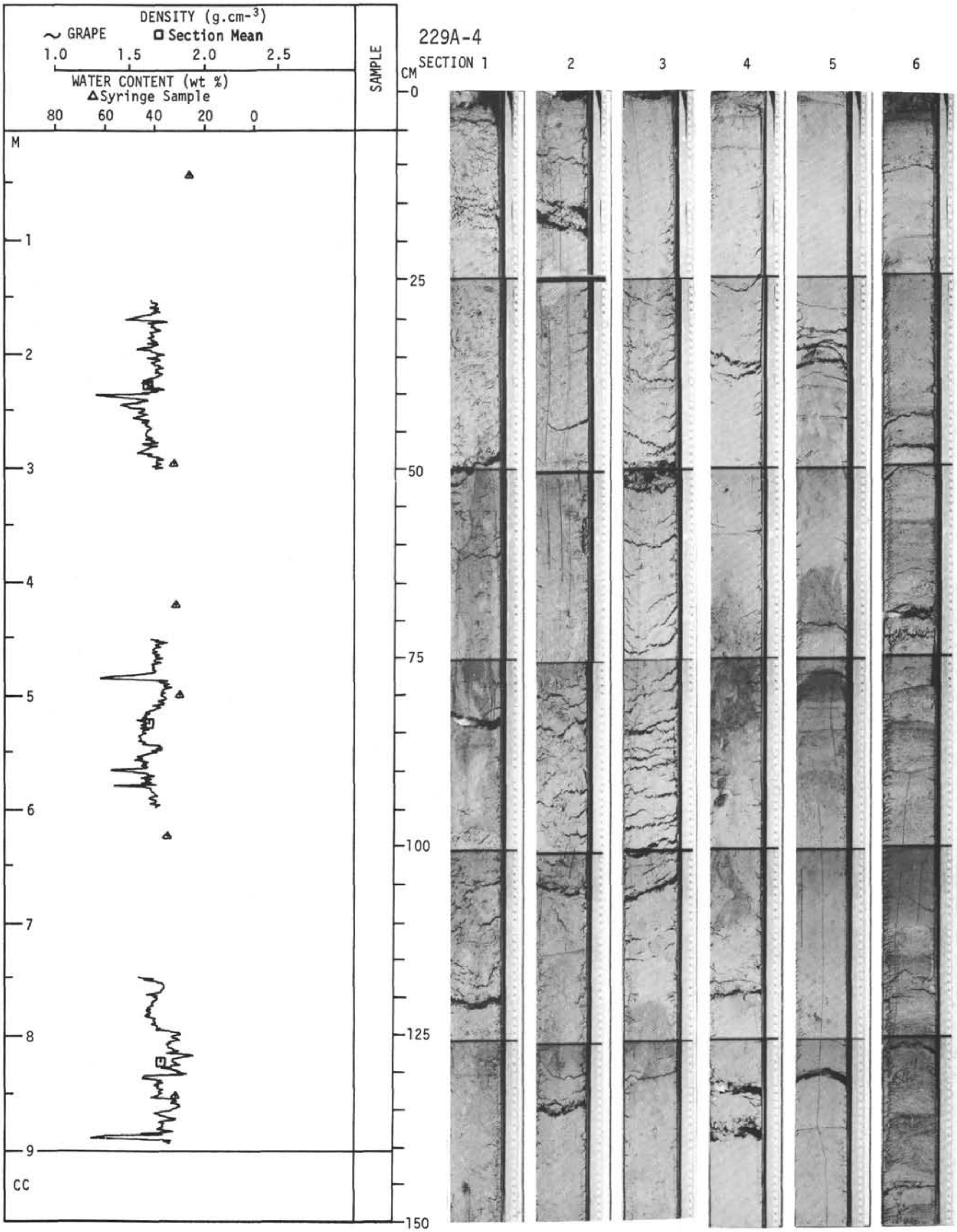

For Explanatory Notes, see Chapter 2

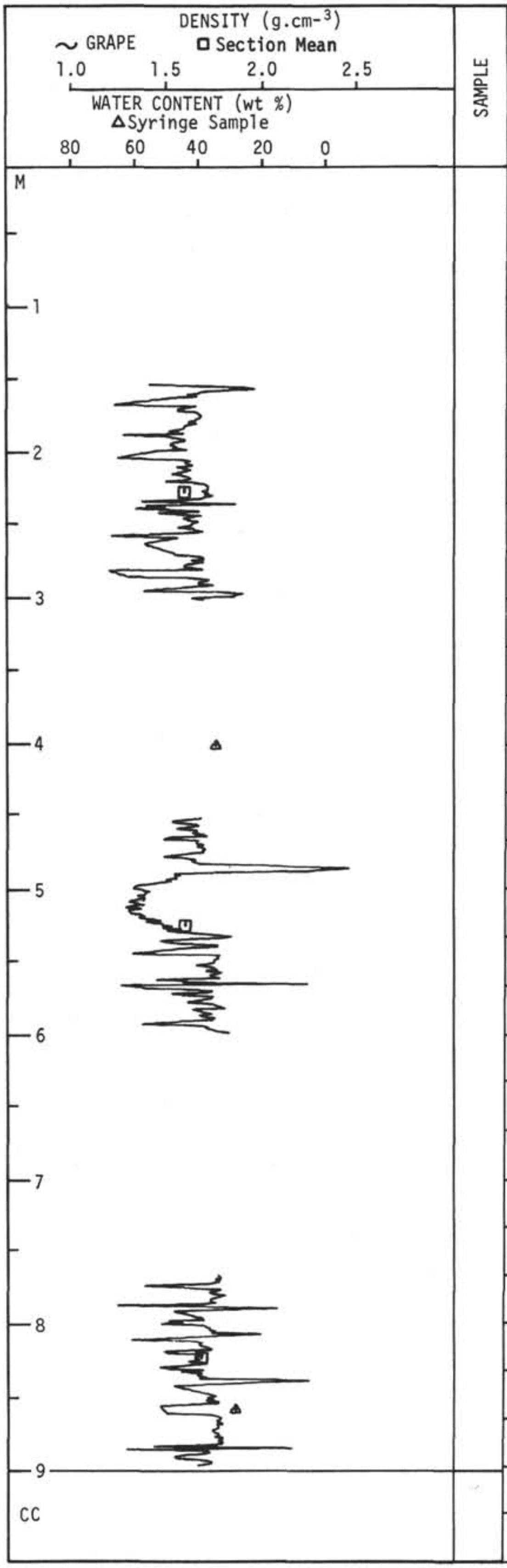

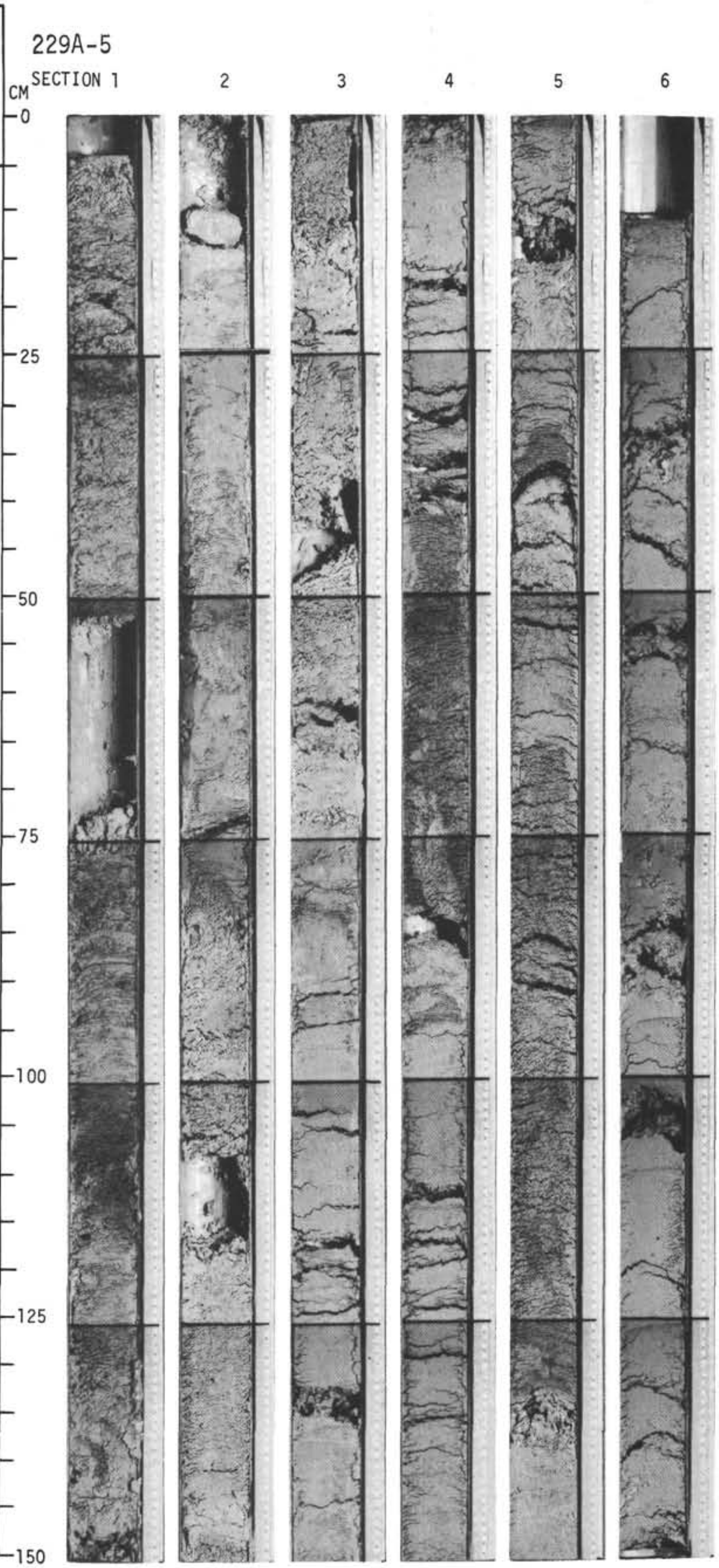

For Explanatory Notes, see Chapter 2

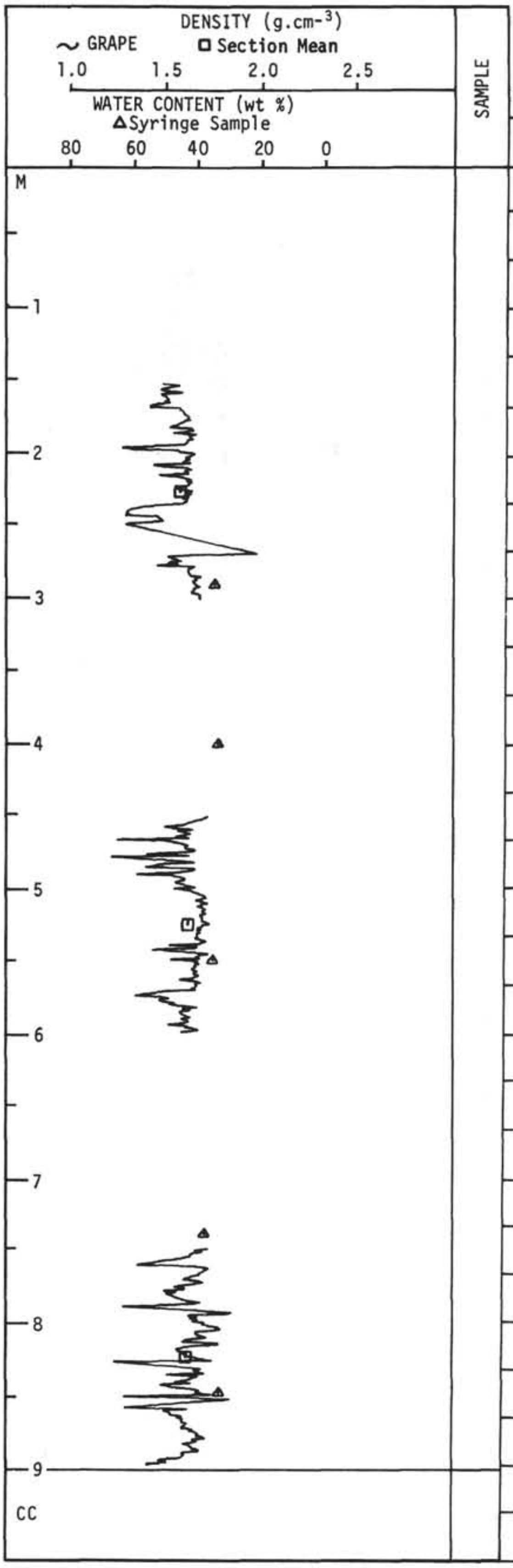

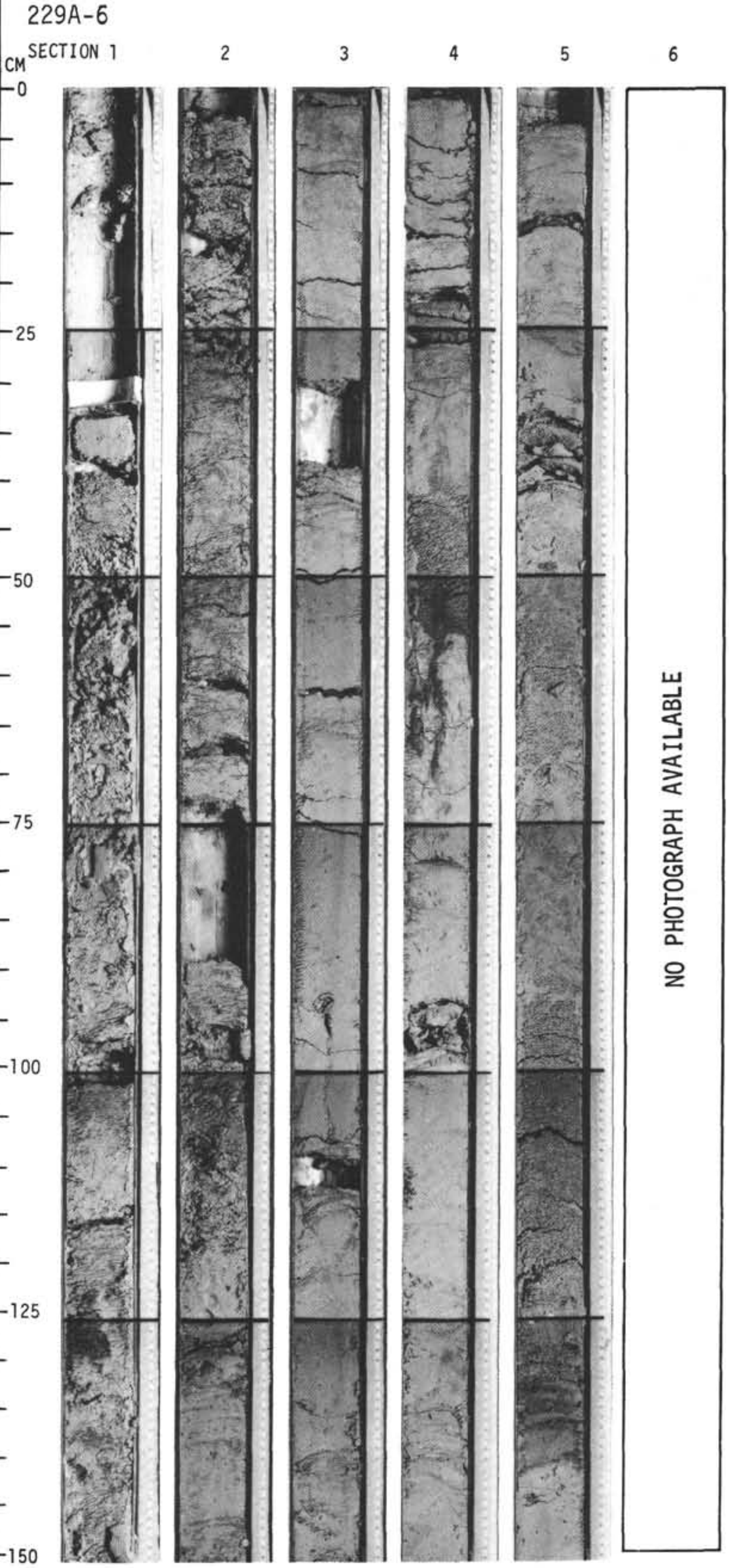

For Explanatory Notes, see Chapter 2

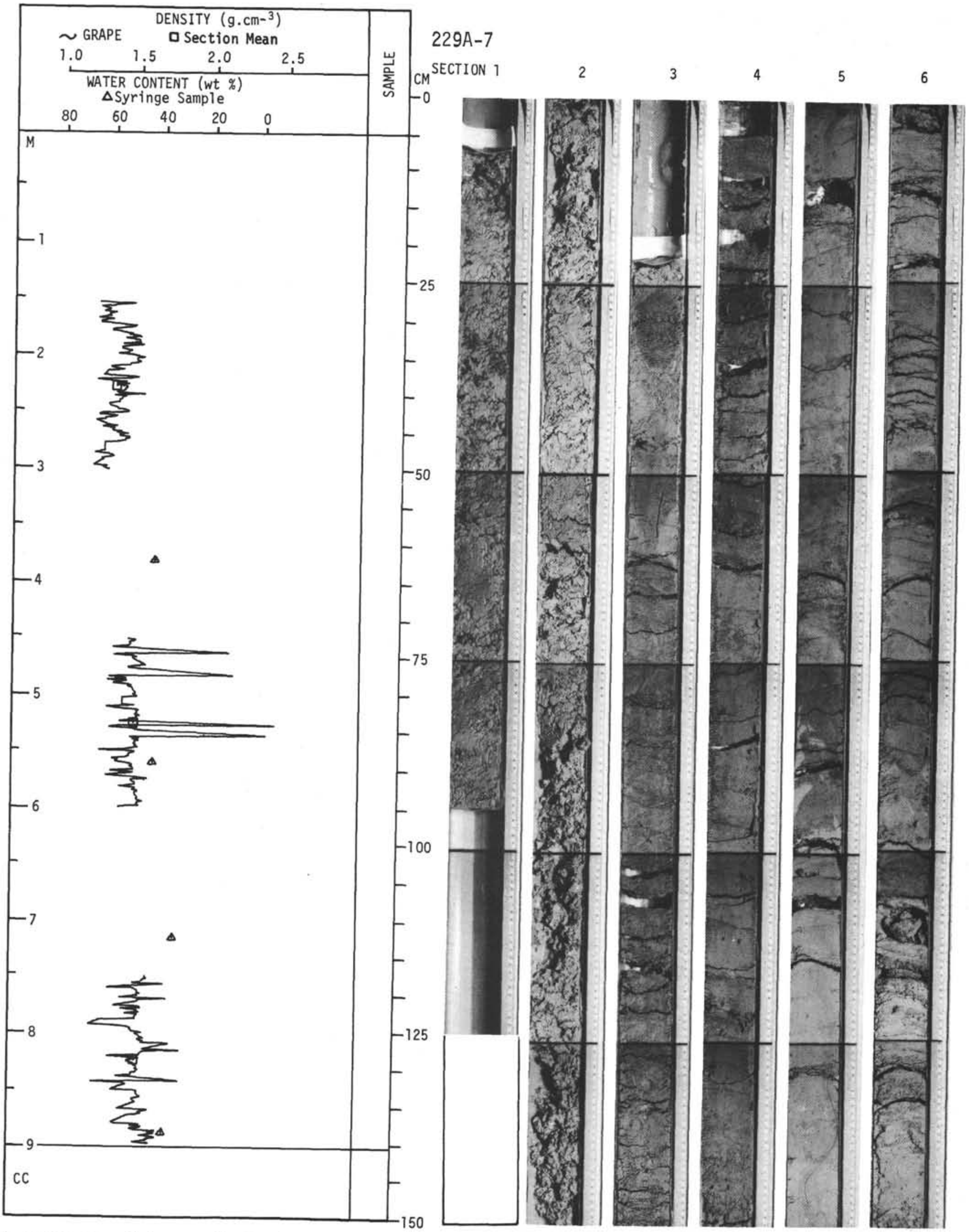

For Explanatory Notes, see Chapter 2

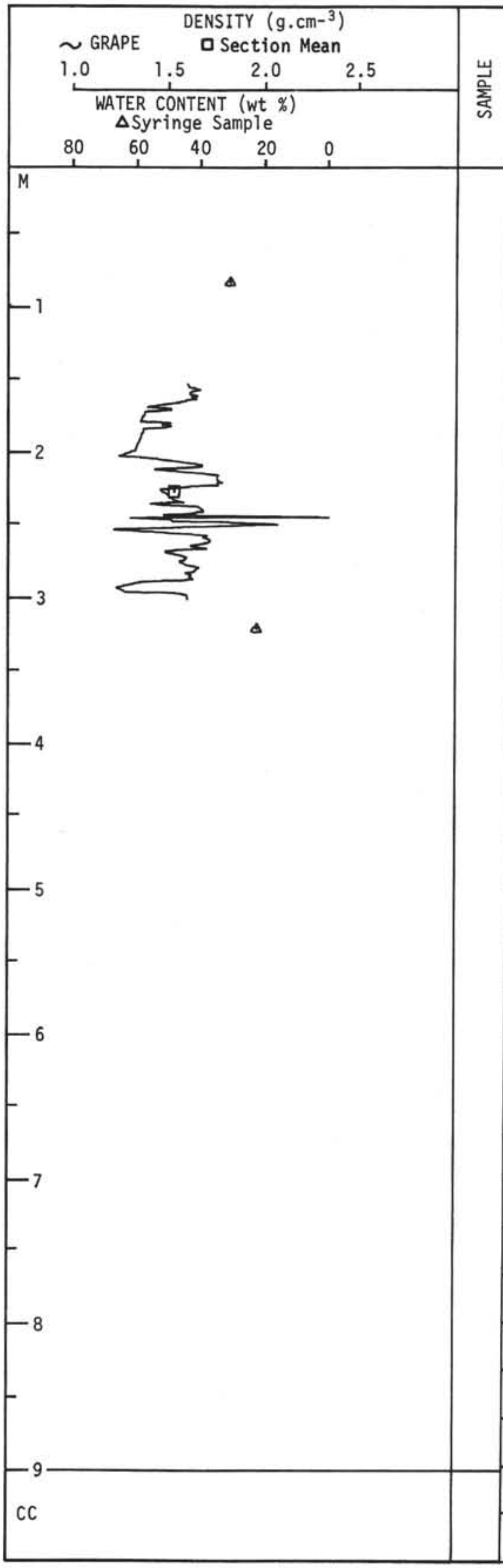

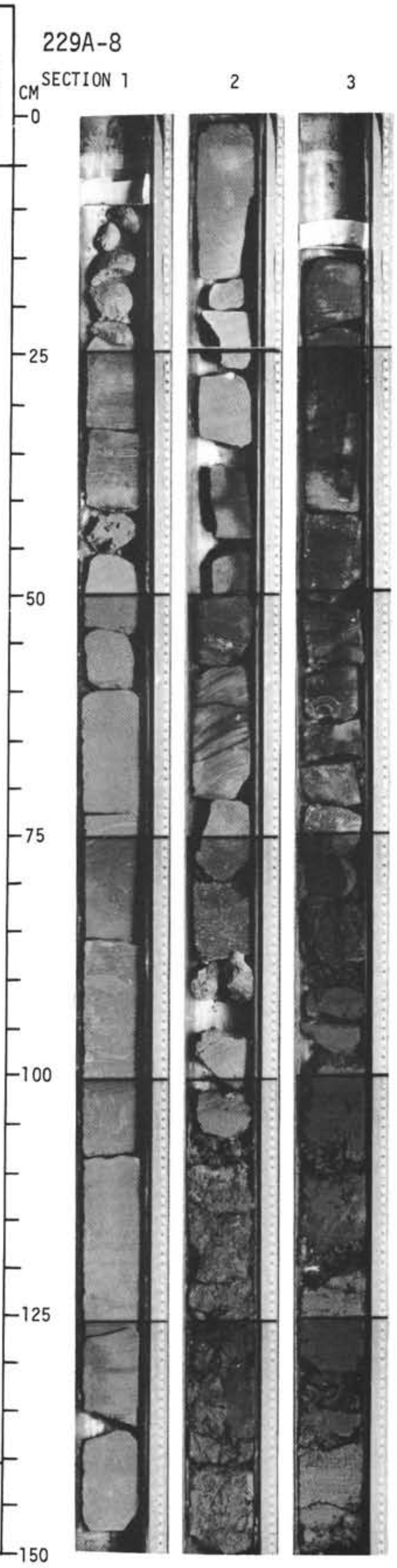

For Explanatory Notes, see Chapter 2

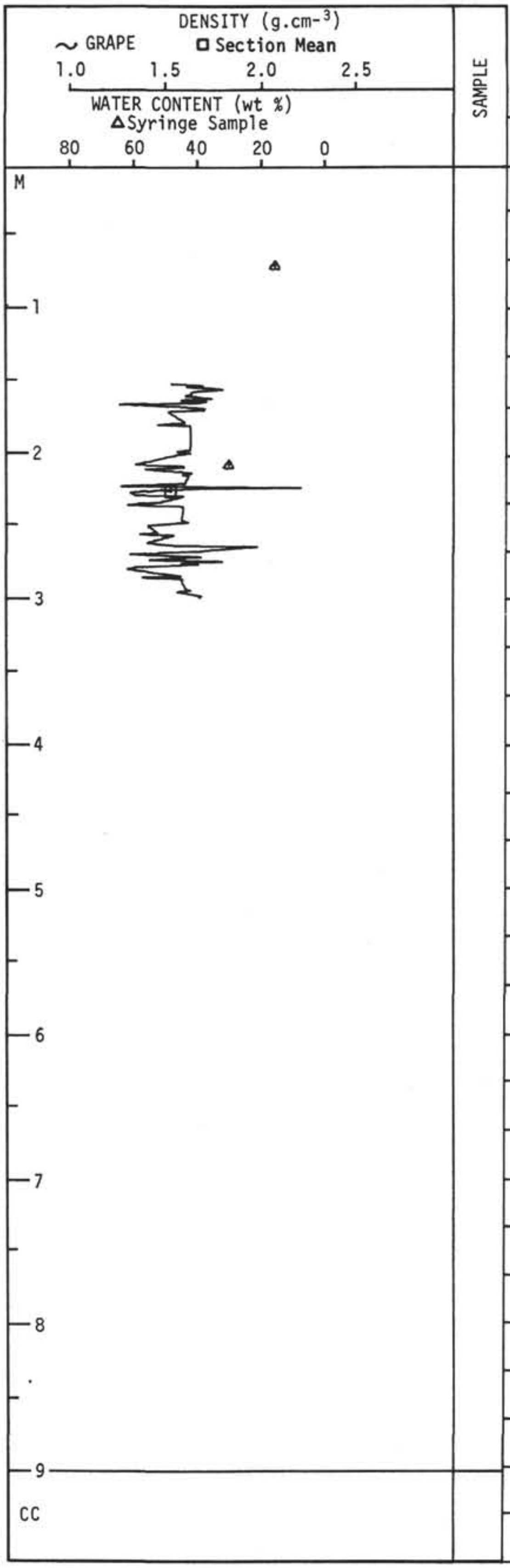

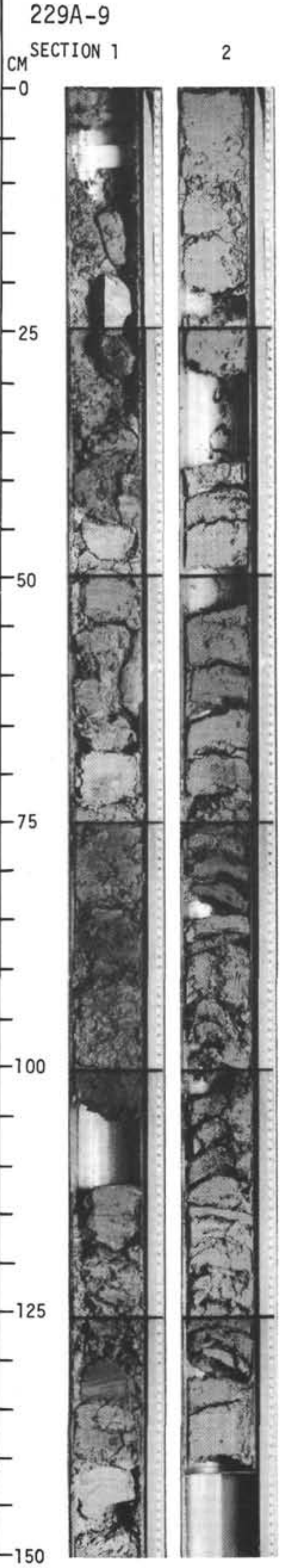

For Explanatory Notes, see Chapter 2

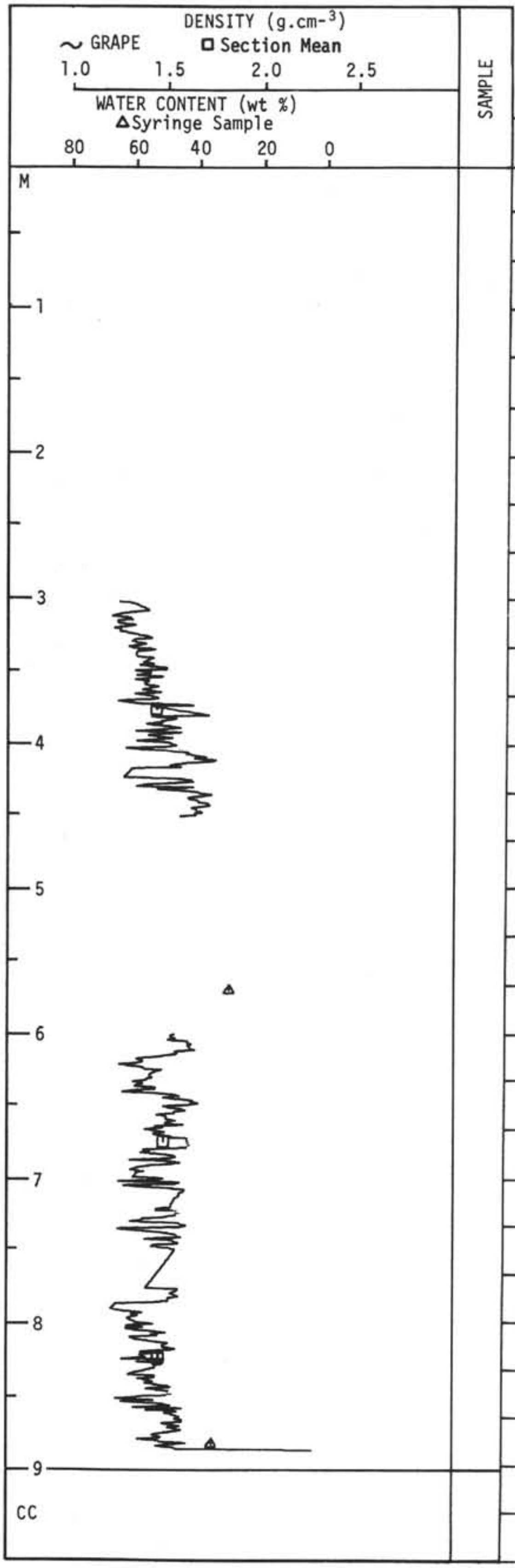

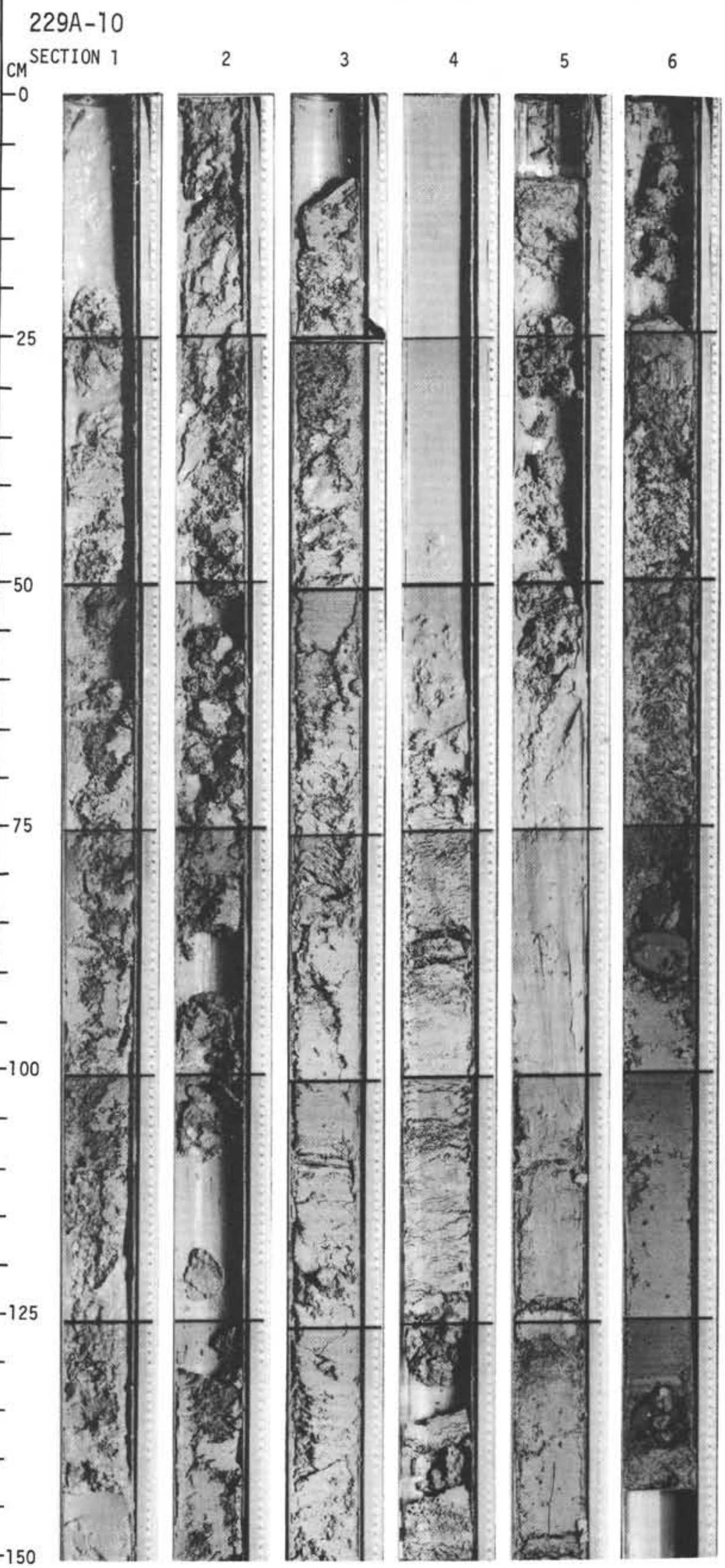

For Explanatory Notes, see Chapter 2

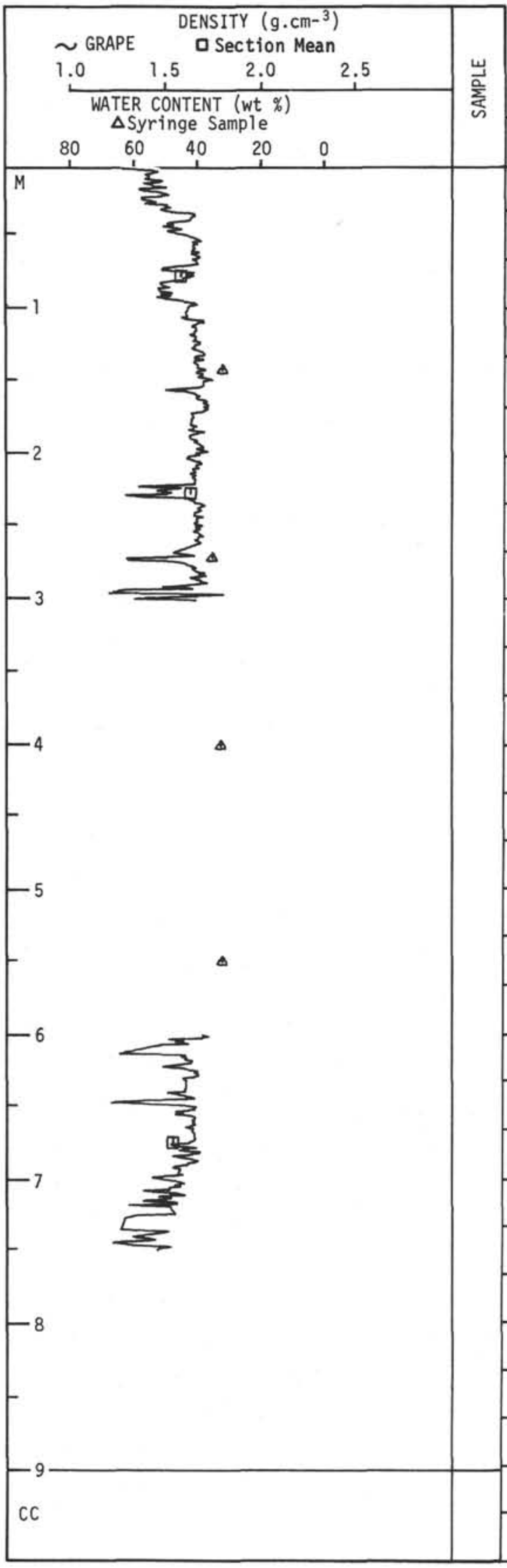

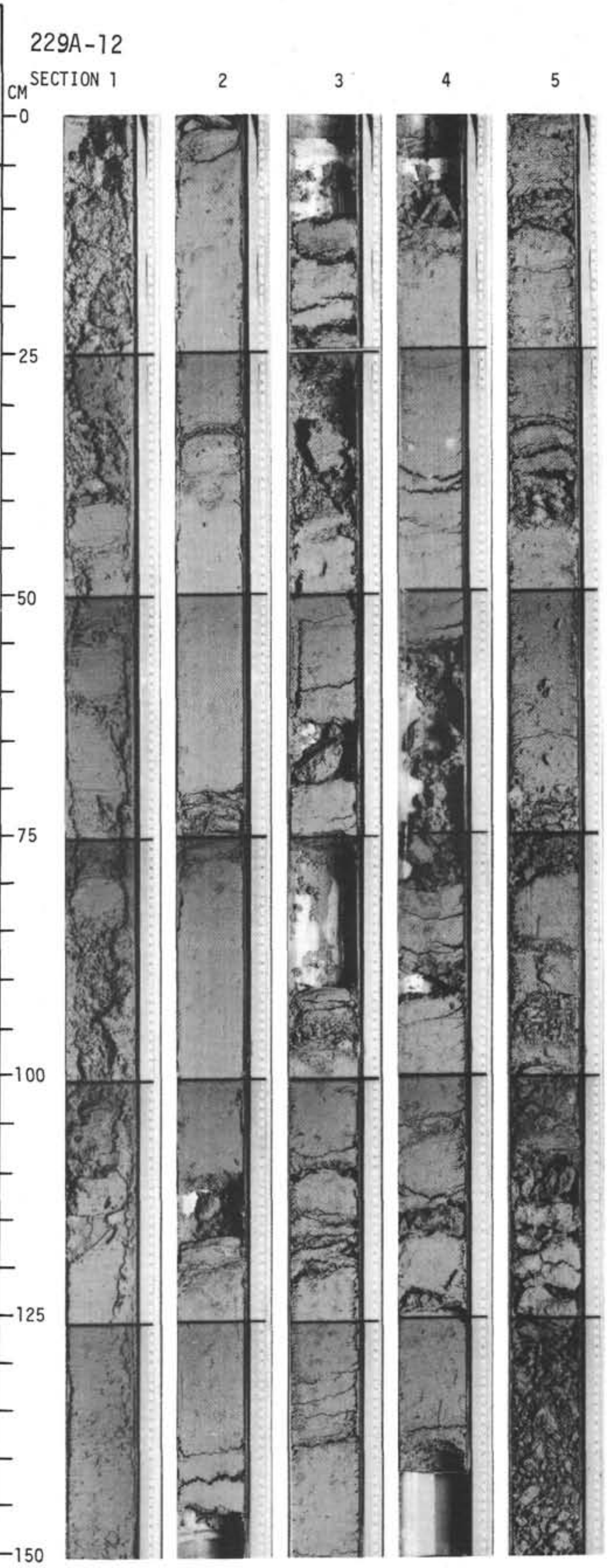

For Explanatory Notes, see Chapter 2

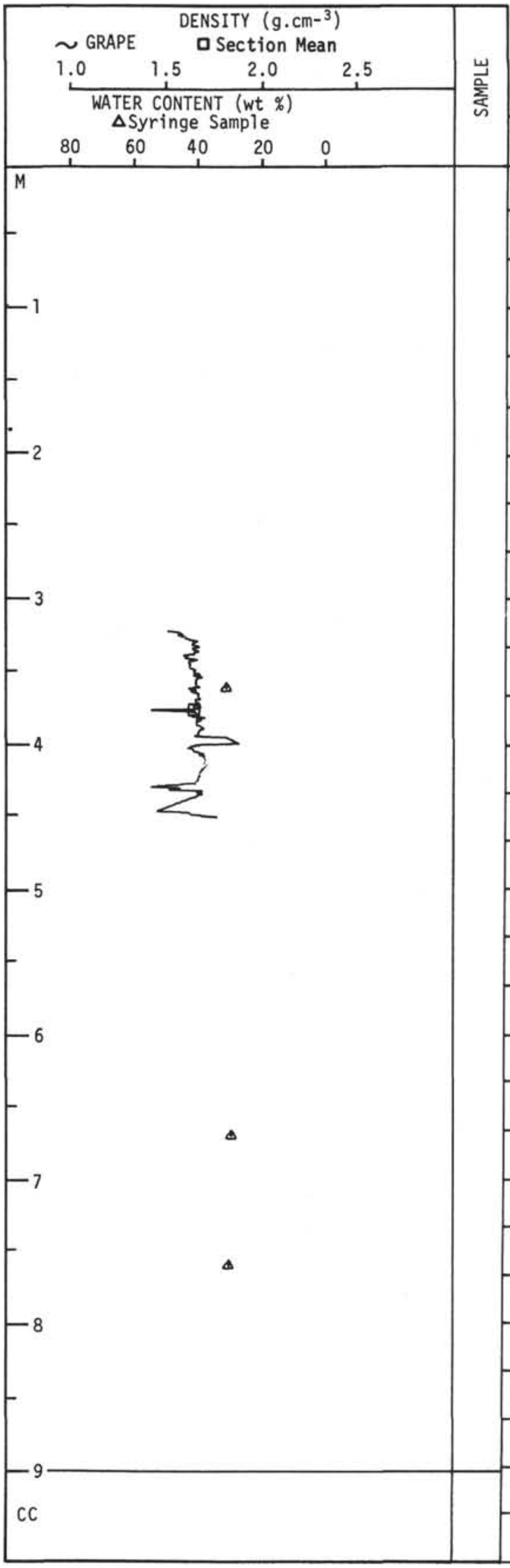

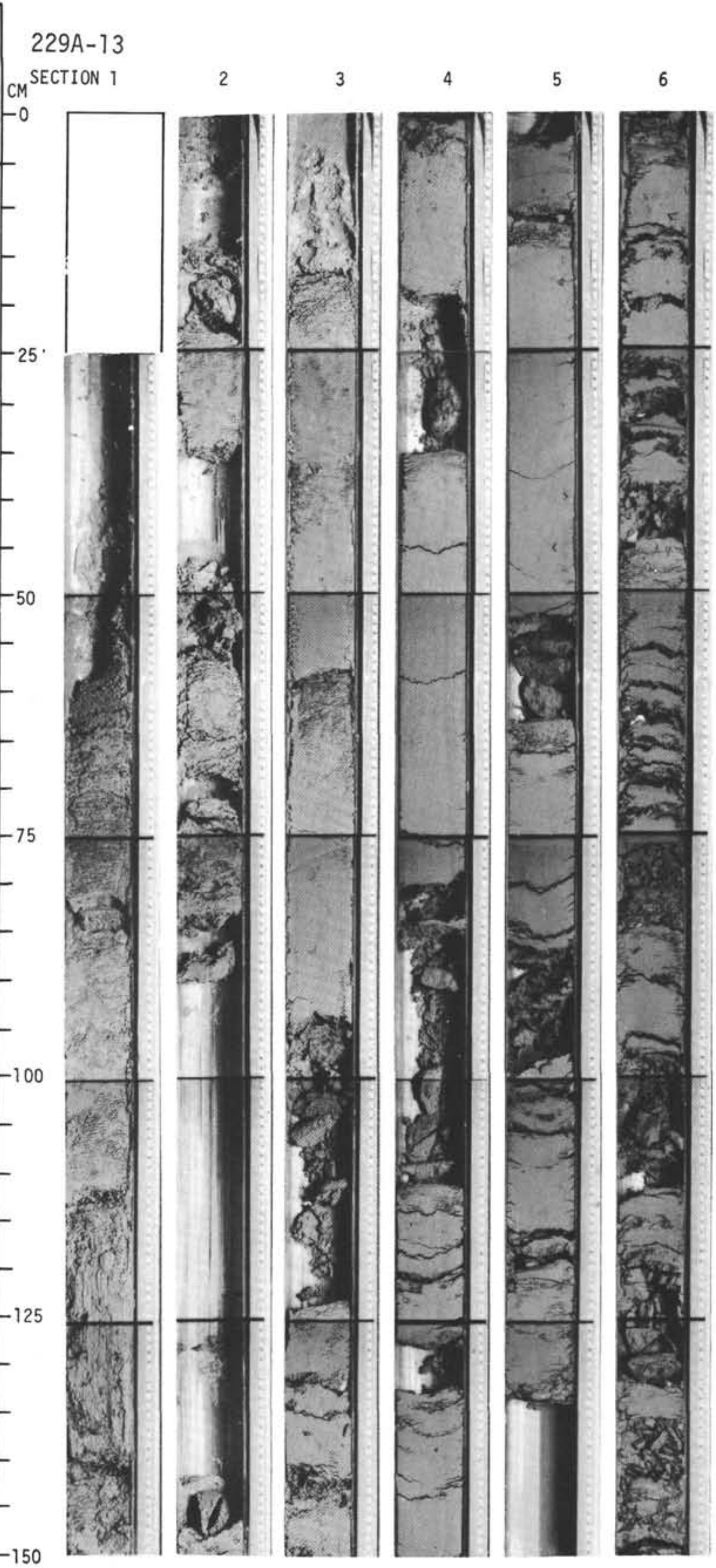

For Explanatory Notes, see Chapter 2

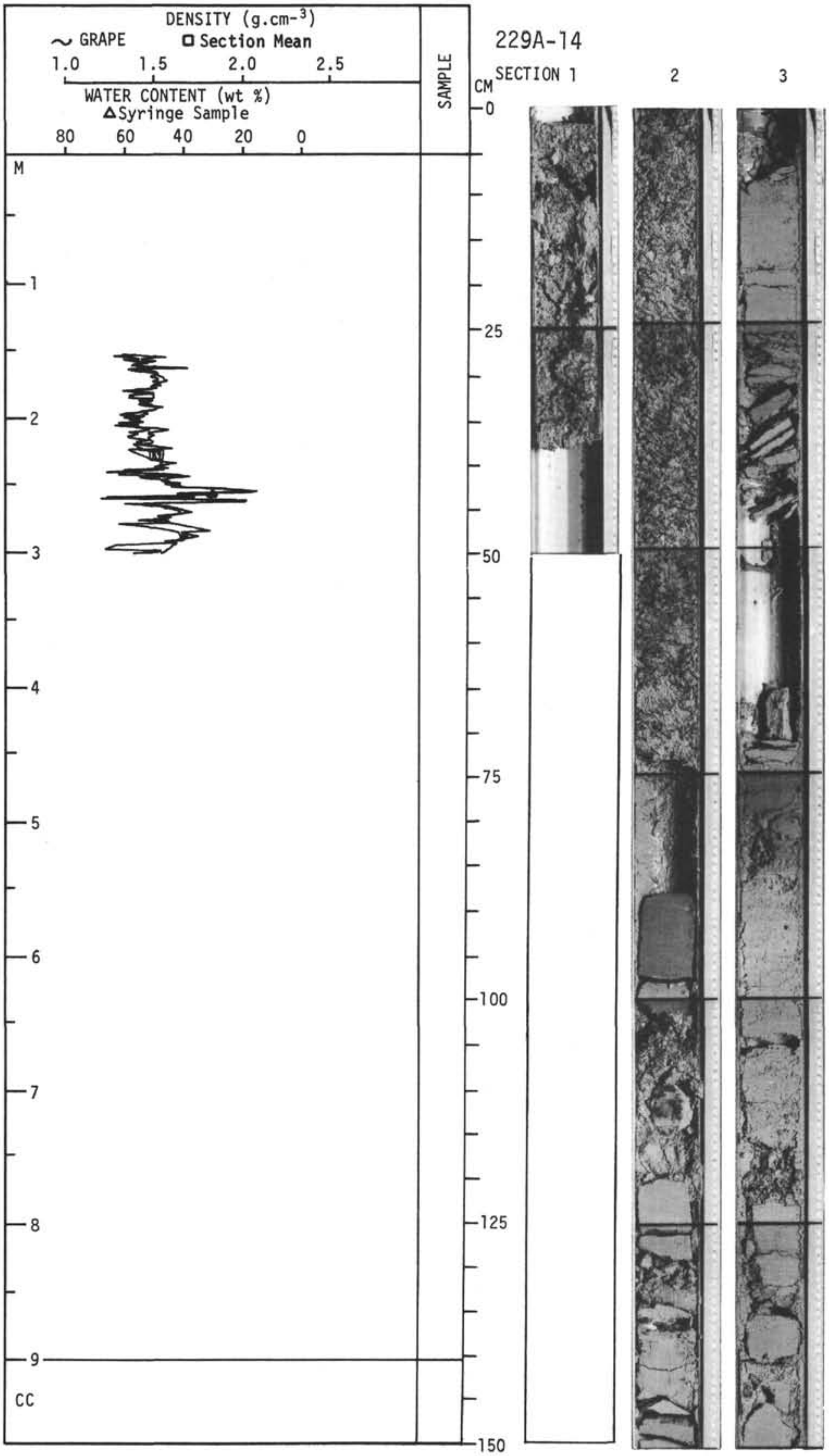

For Explanatory Notes, see Chapter 2

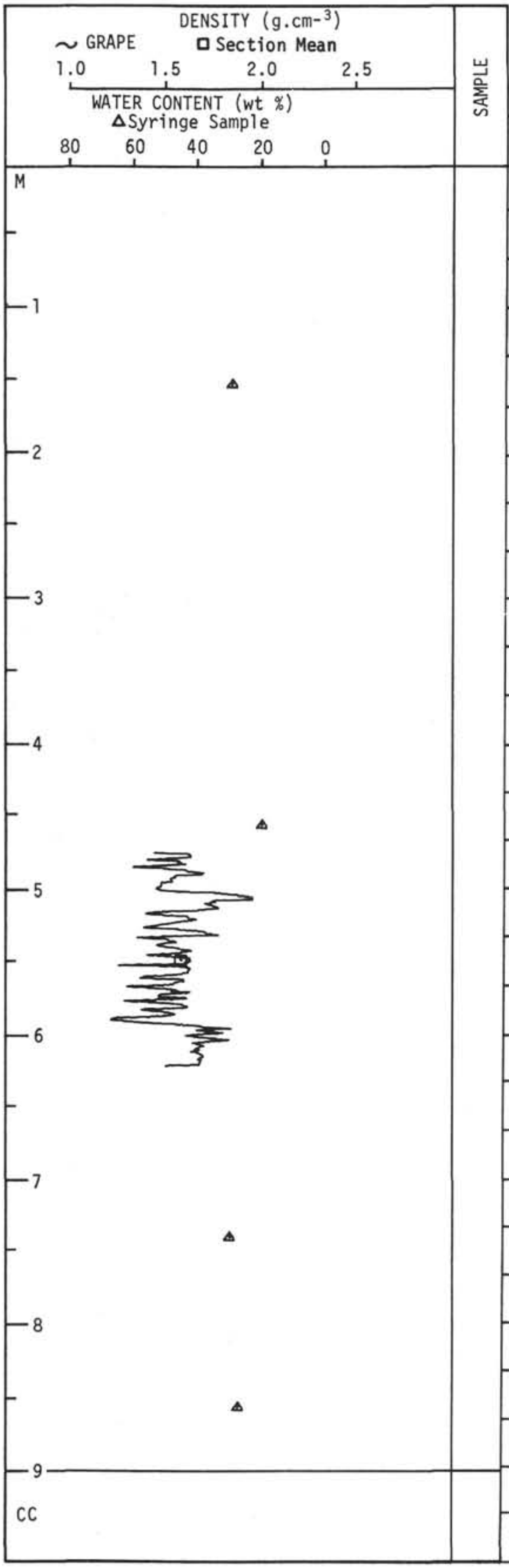

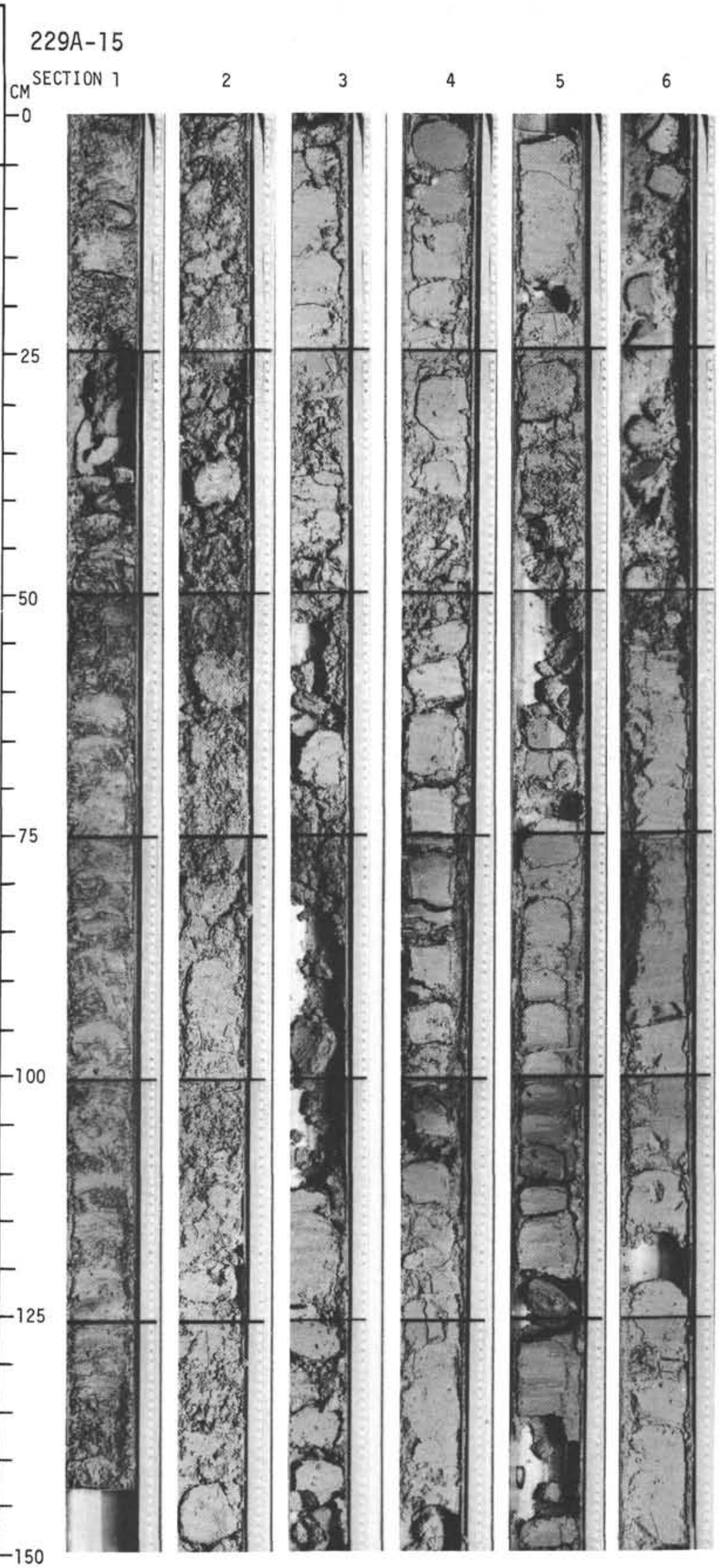

For Explanatory Notes, see Chapter 2

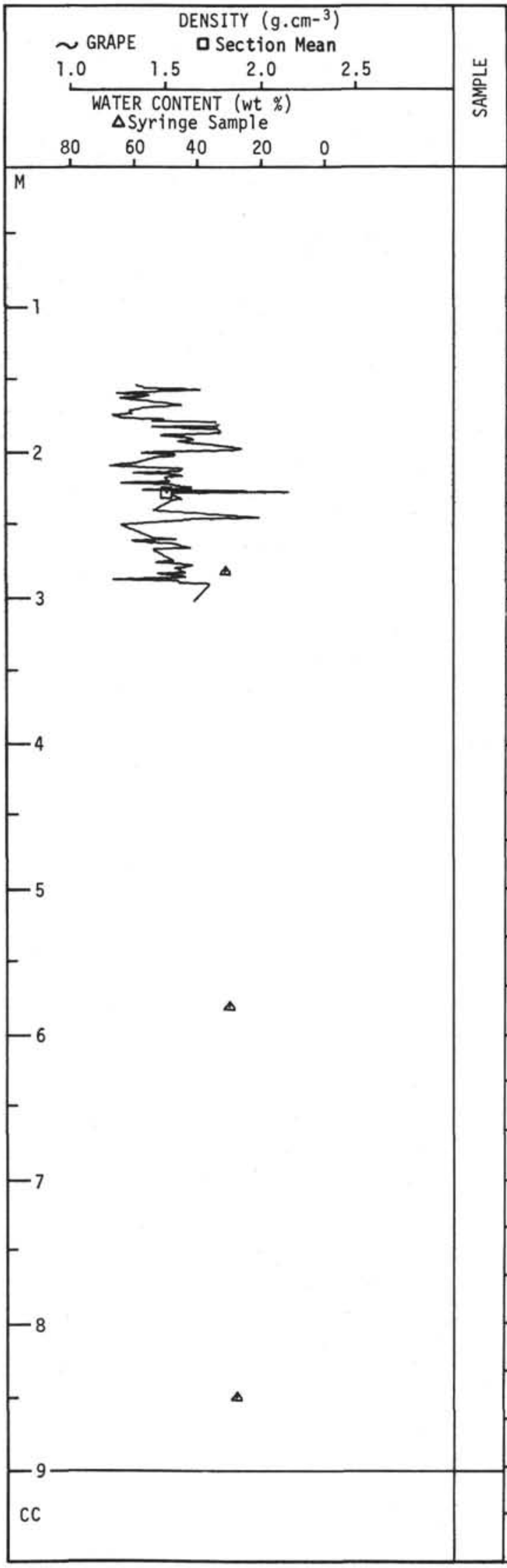

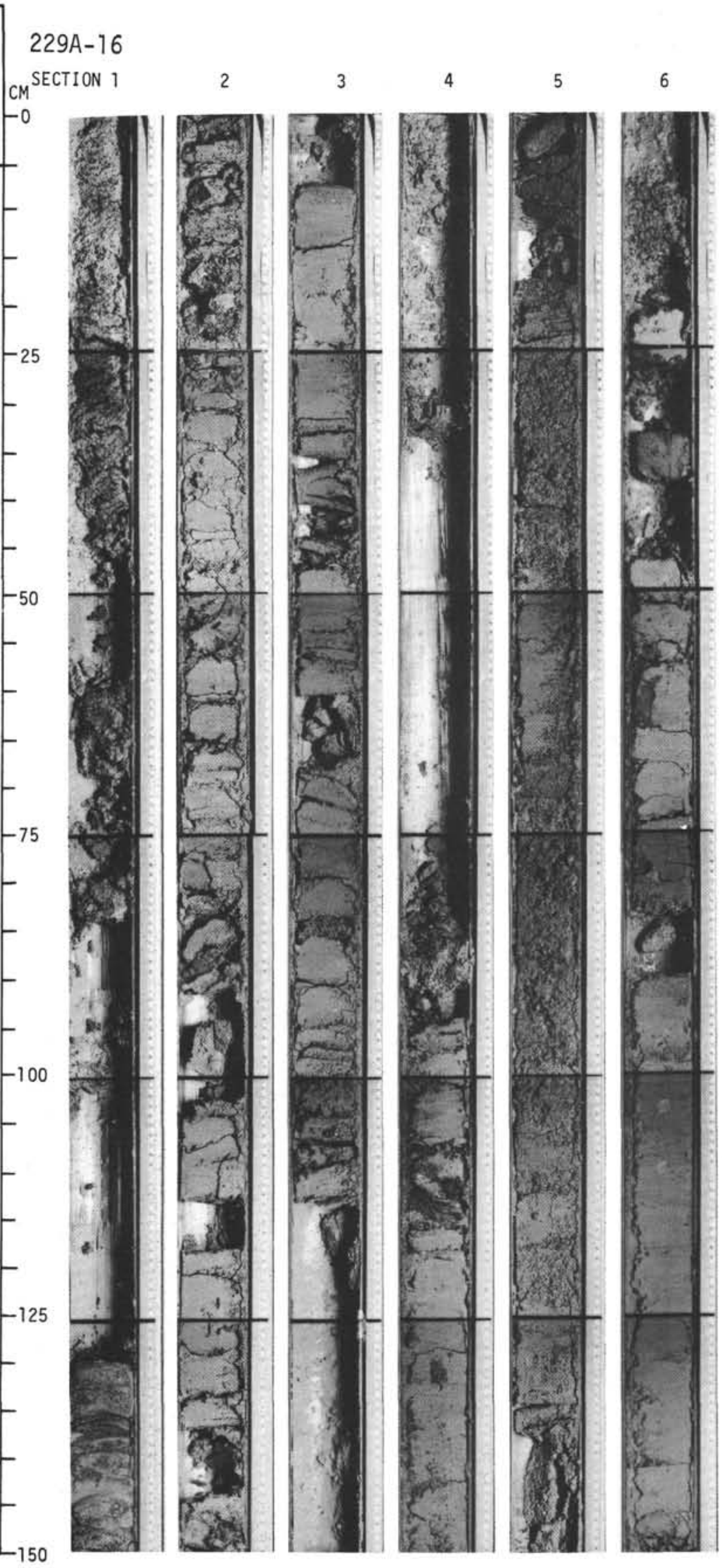

For Explanatory Notes, see Chapter 2

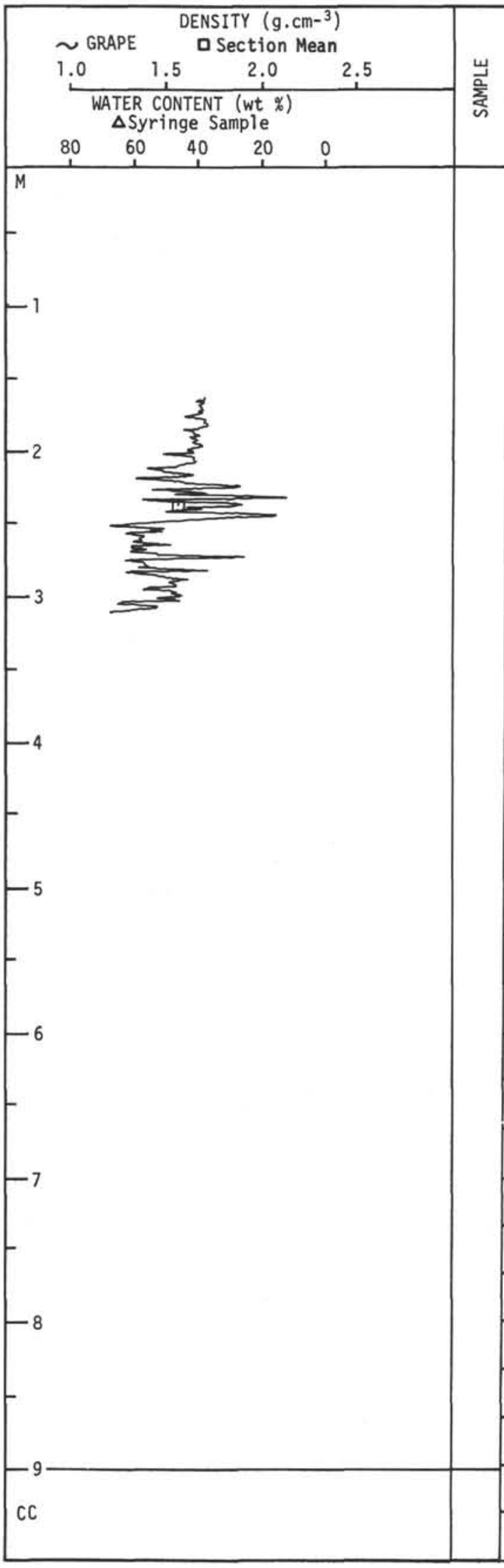

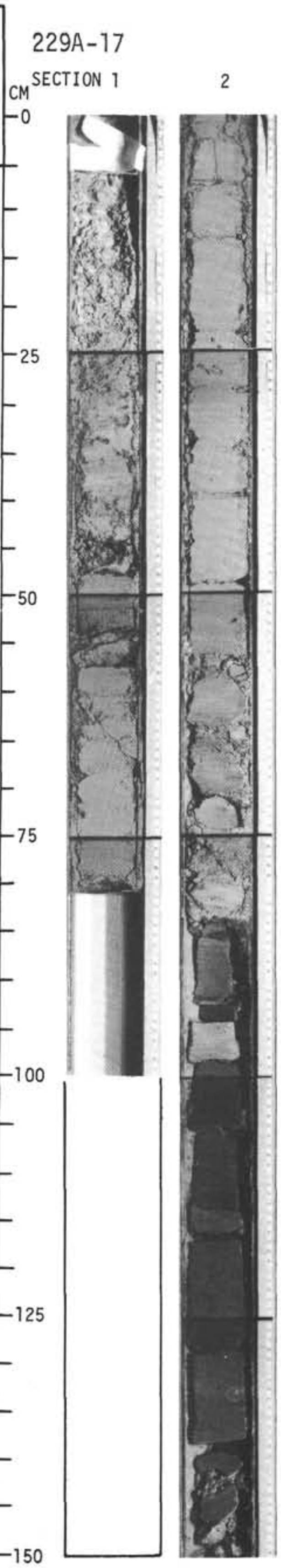

For Explanatory Notes, see Chapter 2

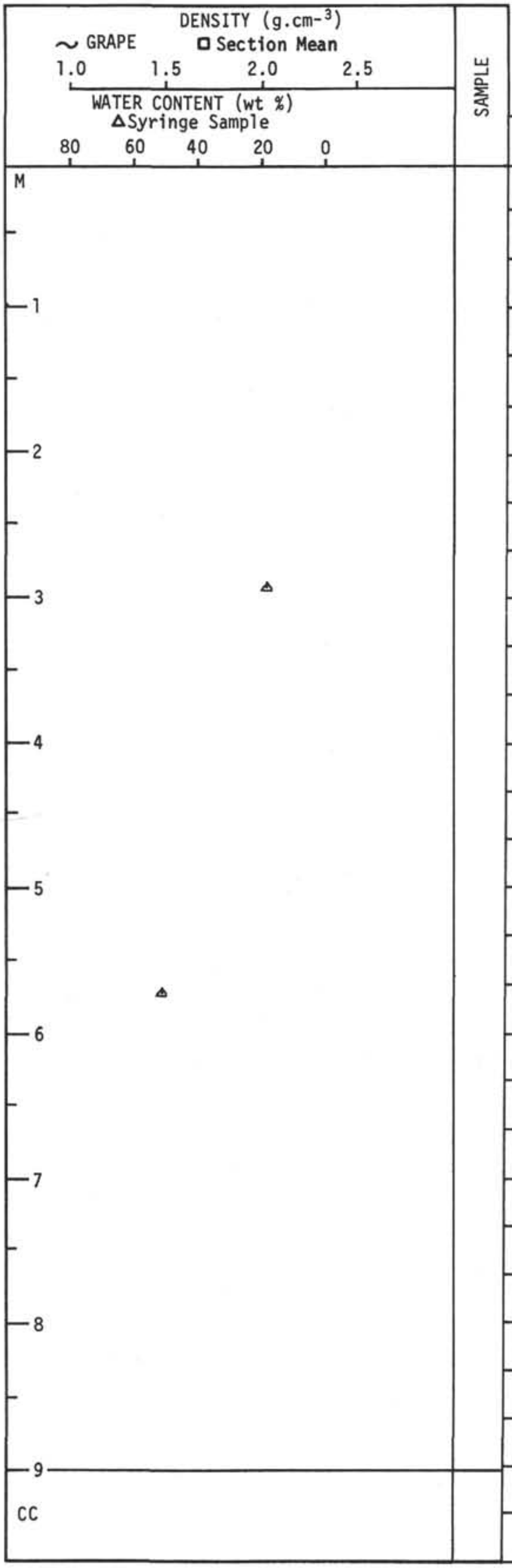

229A-18

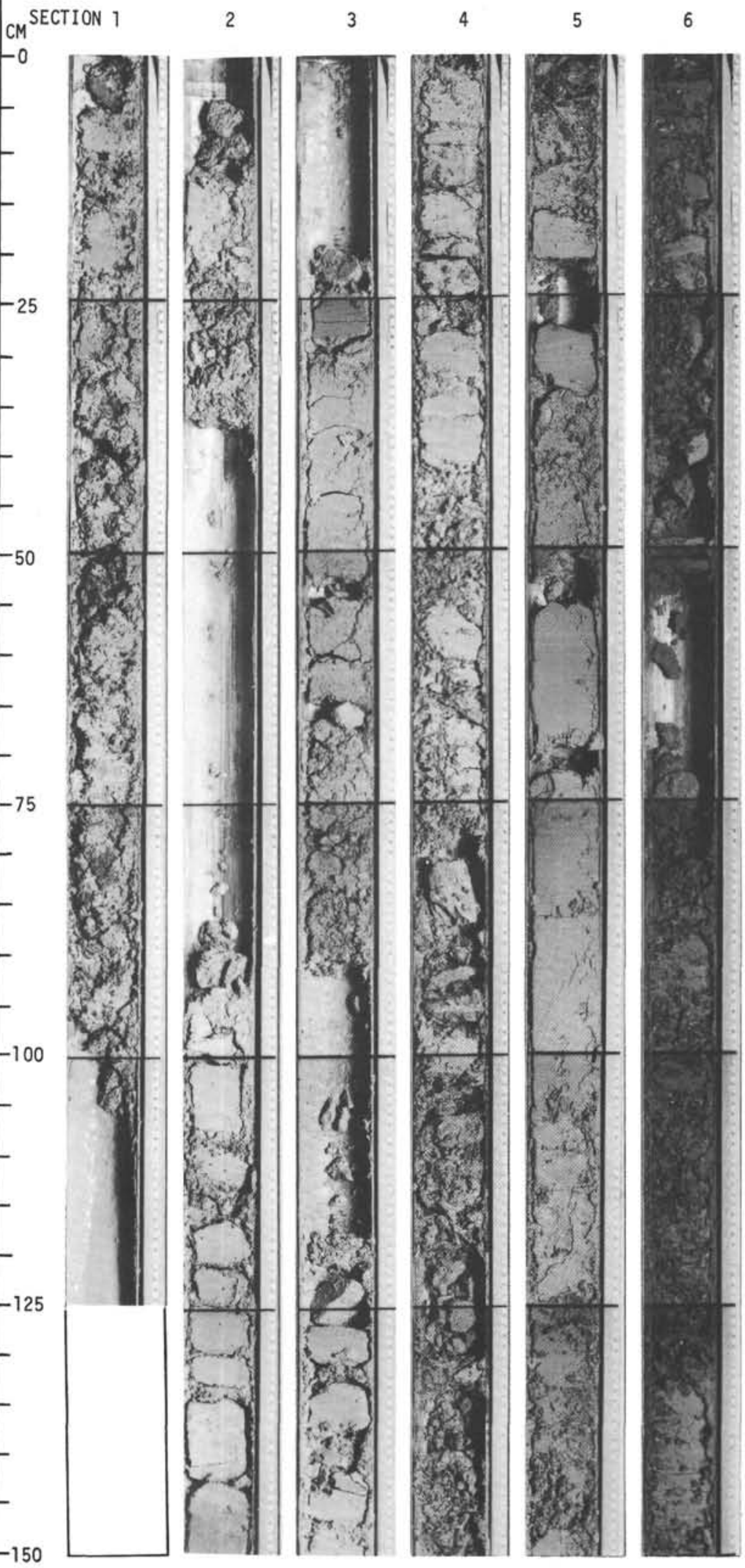

For Explanatory Notes, see Chapter 2